

**ANALYTICAL STUDY OF
NON-DIMENSIONAL PARAMETERS GOVERNING
SUPERCRITICAL FLOW INSTABILITIES**

BY

Venkata Anil Voodi

A Thesis
Submitted to the Faculty of Graduate Studies
In Partial Fulfillment of the Requirements for the Degree of

**Master of Science
In
Mechanical Engineering**

Department of Mechanical and Manufacturing Engineering
University of Manitoba
Winnipeg, Manitoba
Canada

©Copyright, Venkata Anil Voodi, 2004. All rights reserved.

THE UNIVERSITY OF MANITOBA
FACULTY OF GRADUATE STUDIES

COPYRIGHT PERMISSION

**ANALYTICAL STUDY OF
NON-DIMENSIONAL PARAMETERS GOVERNING
SUPERCRITICAL FLOW INSTABILITIES**

BY

Venkata Anil Voodi

**A Thesis/Practicum submitted to the Faculty of Graduate Studies of The University of
Manitoba in partial fulfillment of the requirement of the degree
Of
MASTER OF SCIENCE**

Venkata Anil Voodi © 2004

Permission has been granted to the Library of the University of Manitoba to lend or sell copies of this thesis/practicum, to the National Library of Canada to microfilm this thesis and to lend or sell copies of the film, and to University Microfilms Inc. to publish an abstract of this thesis/practicum.

This reproduction or copy of this thesis has been made available by authority of the copyright owner solely for the purpose of private study and research, and may only be reproduced and copied as permitted by copyright laws or with express written authorization from the copyright owner.

ABSTRACT

The present study is a stability analysis of a supercritical flow in single channel distributed heated systems using the SPORTS code. The intent of this study is to validate the non-dimensional parameters defining the stability boundary. The aim of this research work is to broaden the limited understanding of instabilities in supercritical flows using the SPORTS code, which is a non-linear code developed to obtain steady state and stability transients. Numerical experiments are conducted for water, carbon-dioxide and hydrogen. SPORTS was modified to model these fluids by incorporating the new NIST Refprop 7 package. Many parameters that affect flow stability, such as height of the loop, inlet temperature, inlet and outlet flow resistance coefficient (K-factors), and length of the heated section, were studied. These non dimensional numbers could play a vital role in the design of supercritical systems, such as a nuclear reactor's primary cooling system. From this study it can be concluded that one can accurately predict the boundary flow rate and approximately the boundary power using a steady-state analysis.

ACKNOWLEDGEMENTS

I would like to express my sincere acknowledgments and gratitude to my advisor Dr. Chatoorgoon for giving me the opportunity to work in this challenging field of research. He provided invaluable help in all aspects. He was patient and strenuous to get the best out of me. In addition, I would also like to thank Dr. Ormiston for helping me in SPORTS code modification and Dr. Eric Lemmon for his helpful tips on NIST package.

Also I would like to thank my parents and sisters who gave me a lot of moral support, making me come out with flying colors and finally I would like to thank all my friends all through my life who have been supportive and given me a helping hand at hard times.

DEDICATION

I whole heartedly dedicate my thesis to my beloved parents Sri Vasudeva Rao Voodi,
Smt Geetha Voodi, and to the Lord of Seven Hills (Lord Venkateswara).

TABLE OF CONTENTS

PERMISSION TO USE	i
ABSTRACT	iii
ACKNOWLEDGEMENTS	iv
DEDICATION	v
TABLE OF CONTENTS	vi
LIST OF FIGURES	ix
LIST OF TABLES	x
NOMENCLATURE	xi
CHAPTER 1	1
Introduction	
1.1 Thermohydraulic Instabilities in Boiling Two-phase Flow Systems	5
1.2 Types of Two-Phase Instabilities	8
1.3 Factors Affecting Two-Phase Instabilities:	10
1.3.1 Effect of Channel Length on Flow Instability	10
1.3.2 Effect of Inlet and Exit Restrictions on Flow Instability	10
1.3.3 Effect of Pressure on Instability	10
1.3.4 Effect of Mass Velocity and Power	11
1.4 Objectives of this study	11
CHAPTER 2	12
Literature Review	

2.1	Studies on Natural-circulation Loops	12
2.2	Experimental Studies on Two-Phase Instabilities	17
2.3	Studies on Single-Phase Instabilities	18
2.4	Studies on Two-Phase Instabilities	19
2.5	Studies on Linear Analysis of Instabilities	20
2.6	Studies on Non-linear Analysis of Instabilities	21
2.7	Supercritical Instability Studies	22
CHAPTER 3		23
Theoretical Background		
3.1	Analytical Model of Flow Instability	23
3.2	Formulation of New Approximation	26
3.3	SPORTS Code	27
3.3.1	Stability and Transient Simulations	28
3.3.2	Boundary Conditions	28
3.3.3	Input Files	29
3.4	Modification of SPORTS Code	31
3.4.1	WINDOWS Version	31
3.4.2	Sample Test	33
3.4.3	UNIX Version	35
CHAPTER 4		36
Numerical Experiments		
4.1	Loop Set-up for Simulation	36
4.2	Calculation of the constants	37

4.3	Numerical Simulations	40
4.3.1	Numerical Experiments for Water	41
4.3.2	Discussion of Results for Water with 1 m Heated Length	47
4.3.3	Discussion of Results for Water with 2 m Heated Length	52
4.3.4	Numerical Experiments for Carbon-Dioxide and Hydrogen	54
4.3.5	Discussion of Results for Carbon-dioxide and Hydrogen	65
4.3.6	Summary from all the Results	68
CHAPTER 5		70
Conclusions and Recommendations		
5.1	Conclusions	70
5.2	Recommendations	73
References		74
APPENDIX A: Make File for SPORTS Code		84
APPENDIX B: Sample Input Files		99
APPENDIX C: Subroutines CONVHIN.F and STPROP.F		106
APPENDIX D: Summary of Tables		111
APPENDIX E: Sample Cases: Transient and Steady-state profiles		137

LIST OF FIGURES

Figure 1.1: Schematics of the Various Natural-circulation Loops	3
Figure 2.1: Pressurized Water Reactor	14
Figure 2.2: Boiling Water Reactor	14
Figure 3.1: Schematic of the Loop Setup	23
Figure 3.2: Comparison of Plots for Old and Modified SPORTS Code	34
Figure 4.1: Schematic of the Loop Setup	36
Figure 4.2: Density Versus Enthalpy (Water)	38
Figure 4.3: Density Versus Enthalpy (Carbon-dioxide)	39
Figure 4.4: Density Versus Enthalpy (Hydrogen)	39
Figure 4.5: Steady-State Profile	43
Figure 4.6: Water with Heated Length of 1 m	45
Figure 4.7: Water with Heated Length of 2 m	50
Figure 4.8: Carbon-Dioxide with Heated Length of 1 m	57
Figure 4.9: Carbon-Dioxide with Heated Length of 2 m	59
Figure 4.10: Hydrogen with Heated Length of 1 m	61
Figure 4.11: Hydrogen with Heated Length of 2 m	63
Figure 4.12: Steady-State Profile Showing Different Regions	68
Appendix E: Transient Plots for Water	137

LIST OF TABLES

Table 1.1: Types of Instabilities in Two-Phase Flow	5
Table 4.1: Constants for Different Fluids	38
Table 4.2: Numerical Experiments for Water	41
Table 4.3: Numerical Experiments for Carbon-Dioxide	54
Table 4.4: Numerical Experiments for Hydrogen	55
Tables D1-D5: Results Table for 1 m Water	112
Tables D6-D10: Results Table for 2 m Water	118
Tables D11-D14: Results Table for 1 m Carbon-Dioxide	122
Tables D15-D18: Results Table for 2 m Carbon-Dioxide	125
Tables D19-D22: Results Table for 1 m Hydrogen	129
Tables D23-D26: Results Table for 2 m Hydrogen	133

NOMENCLATURE

A	-	Flow area (m^2)
D	-	Hydraulic diameter (m)
f	-	Friction factor
G	-	Mass flux ($kg/m^2/s$)
G_m	-	Maximum mass flux ($kg/m^2/s$)
G_s	-	Maximum mass flux from SPORTS ($kg/m^2/s$)
g	-	Gravitation constant (m/s^2)
h	-	Fluid enthalpy (kJ/kg)
h_1	-	Cold-side enthalpy (kJ/kg)
h_2	-	Hot-side enthalpy (kJ/kg)
h_{2b}	-	Hot-side enthalpy at the maximum mass flux (kJ/kg)
h_t	-	Height of the loop (m)
K	-	K-factor
p	-	Static pressure (N/m^2)
Q	-	Total channel power (kW)
Q_b	-	Power at the maximum mass flux (kW)
L_{TS}	-	Length of Test Section (m)
K_1	-	Inlet K-factor
K_2	-	Outlet K-factor
T_{IN}	-	Inlet Temperature ($^{\circ}C$)
z_1	-	Length from inlet to the critical point in the heater section (m)

z_2 - Length from the critical point in the heater section to the critical point in the heat exchanger (m)

z_3 - Length critical point in the heat exchanger to the outlet (m)

Non-dimensional variables:

G^* - Non-dimensional mass flux

G_m^* - Non-dimensional maximum mass flux

Q^* - Non-dimensional bounding power

R^* - Non-dimensional density

\tilde{Q}_b^* - Non-dimensional power when $G=0.95G_m$

Greek symbols:

α - $\frac{G}{G_m}$

β - Inclination to horizontal

θ - $\frac{C_{k_2} z_2}{C_{k_1} z_1 + C_{k_3} z_3}$

Φ - $-\theta + \sqrt{\theta^2 + \theta}$

ρ_1 - Fluid density (kg/m³)

ρ_2 - Cold-density upstream of heater (kg/m³)

ρ_3 - Fluid density downstream of heat sink (kg/m³)

ρ_{2b} - Hot-side density when $G=G_m$ (kg/m³)

ξ - $\sqrt{\frac{2gDh_t}{f_2 z_2}}$ (m/s)

CHAPTER 1

Introduction

Nuclear power plants use a working fluid to flow through a volume and which is heated using nuclear fission chain reaction. For a nuclear reactor, operating at the higher supercritical conditions can lead to improved thermodynamic efficiency of the plant. Hence new reactors are designed for high temperature and high pressure primary coolant conditions. Water is normally used in boiling water reactors and is circulated in the core reactor close to saturation temperatures, and it partially vaporizes while circulating inside fuel channels. Water plays a dual role in this type of boiling reactors: dissipating heat from fission reaction and acting to moderate fast fission-neutrons. Boiling Water Reactors (BWRs) may be considered to have two distinctive processes: neutronic process which is in the core region of the reactor that regulates the way heat is generated, and a thermal-hydraulics loop which is generally a natural-circulation loop that controls the dissipation of heat from the core through the difference in coolant density, heat transfer rate, and flow. In these two loops fluids heated at elevated temperatures can exhibit numerous instabilities under certain reactor operating conditions. Large changes in the density can cause the reactor power to oscillate through reactivity feedback. Usually at low flow and high power reactivity feedback can become so large that the power oscillations diverge and thus the reactor is said to become unstable.

The thermo-hydraulics loop controls the dissipation of heat from the core by natural-circulation loops or thermosyphons. Natural-circulation loops have been

extensively studied by Mertol [1] and Greif [1]. There are several types of natural-circulation loop available. Many factors come into play in design of a natural-circulation loop like robustness, geometry and configurations etc. The following figures depict different natural-circulation loops most commonly used and studied.

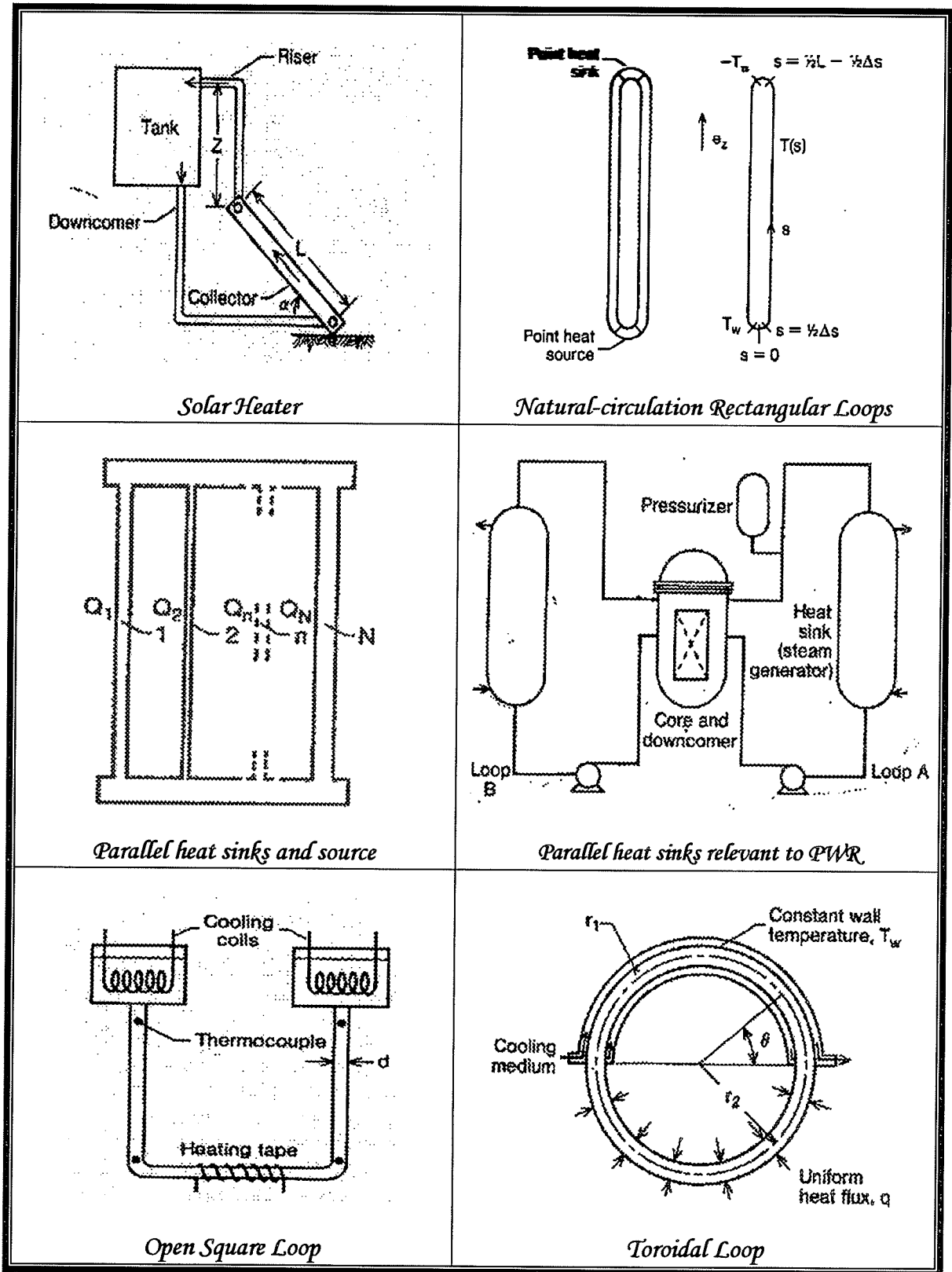


Figure 1.1: Schematics of the Various Natural-circulation Loops [2]

Figure 1.1 depicts various natural-circulation loops available. The toroidal and the rectangular loops are the most popular. Several investigators have performed intense studies on these natural-circulation loops. Many have proved that there is a point where the instabilities occur in these systems. These instabilities are of several types and are characterized by flow rate and temperature variations. Instabilities are highly undesirable and should be avoided for safety concerns. Hence care should be taken and design factors must be taken into consideration when designing nuclear reactors.

The reasons being [3]

- continuous and simultaneous occurring pressure and temperature oscillations induce mechanical and vibration and thermal fatigue in the heat exchangers and thus lead to their rupture or internal damage,
- flow oscillation might cause system control problems,
- local heat transfer characteristics are affected by flow oscillations, and this is characterized by a sudden drop in the heat transfer coefficient due to change of boiling mechanism,
- flow oscillation affects the local heat transfer characteristic and may induce boiling crisis namely dry out and burnout,
- sustained flow oscillations cause forced mechanical vibration of components.

Instabilities are observed in applications namely steam generators, boiling systems, liquid propellant rocket engines, and nuclear reactors etc. Investigations have shown that the most important instabilities in a BWR are basically of two categories: pure

thermohydraulic and coupled neutronic-thermohydraulic instabilities. The vital difference between the two instabilities is that in thermohydraulic there is flow feedback and in neutronic-thermohydraulic instabilities there is power feedback in addition to flow feedback.

1.1 Thermohydraulic Instabilities in Boiling Two-phase Flow Systems

Thermohydraulic instabilities in two-phase flow systems have been studied by many authors. Boure et al. [4] summarized the studies of several authors in two-phase flow.

They tabulated several types of instabilities which are shown Table 1.1

Table 1.1: Types of Instabilities in Two-Phase Flow [5]

Class	Type	Cause	Characteristics
I Static Instabilities			
1.1 Fundamental Static instability	1. Flow excursion or Ledinegg instability	Attempt to operate in the negative slope region of pressure drop versus flow rate curve	Flow undergoes excursion to a new steady state which may itself be stable or unstable
	2. Boiling crisis	Ineffective removal of heat from heated surface	Wall temperature excursion and flow oscillation
1.2 Fundamental relaxation instability	1. Flow pattern transition instability	Bubbly flow has less void but higher pressure drop than that of annular flow	Cyclic flow pattern transitions and flow rate variations
1.3 Compound	1. Bumping, geysering	Periodic adjustment	Periodic process of

relaxation instability	and clogging	of metastable condition, usually due to lack of nucleation sites	superheat and violent evaporation with possible expulsion and refilling
II Dynamic Instabilities			
2.1 Fundamental dynamic instability	1. Acoustic oscillations	Resonance or pressure waves	High frequencies(10-100 Hz) related to time required for pressure wave propagation in system
	2. Density wave oscillations	Delay and feedback effects in relationship between flow rate, density and pressure drop	Low frequencies (1 Hz) related to transit time of a continuity wave
2.2 Compound dynamic instability	1. Thermal Oscillations	Interaction of variable heat transfer coefficient with flow dynamics	Occurs in film boiling
	2. Boiling water instability	Interaction of void reactivity coupling with flow dynamics and heat transfer	Strong only for small fuel time under low pressures
	3. Parallel Channel Instability	Interaction among small number of parallel channels	Various modes of flow redistribution
2.3 Compound dynamic	1. Pressure drop oscillations	Flow excursion initiates dynamic	Very low frequency periodic process

instability as secondary phenomenon		interaction between channel and compressible volume	(0.1 Hz)
---	--	--	----------

1.2 Types of Two-Phase Instabilities

Steady state laws governing the system cause the *static instability* phenomenon [5]. Hence by using the steady state laws, the onset of this instability can be predicted. The primary or the static instability can be explained as the change of flow conditions by small step from steady state condition, a steady state value cannot be reached in the vicinity of the original steady state. *Density wave oscillations* are mostly encountered by the instability in a BWR and this might occur from the start up to the rated operating conditions and may induce power oscillations through the void reactivity coupling. The main cause of occurrence of this type of instability was described in detail by Yadigaroglu and Bergles [6]. They considered an oscillatory subcooled inlet flow entering a heated boiling channel. Enthalpy perturbations in the single-phase were created by inlet flow fluctuations and the amplitude and phase of the enthalpy perturbations at the point where the flow reached saturation. Boiling boundary at the inlet flow fluctuated [5]. Vijayan et al. [7] explained these basic types of instabilities and further mentioned the possible causes for these instabilities.

In the dynamic instability factors like inertia plays a vital role in the process [7]. In dynamic instability one can notice oscillation in temperature, pressure or flow rate. There is another instability which is also known as the compound instability; in this type many elementary mechanisms can be involved so that this instability cannot be studied as a separate issue.

These two types of instabilities can be initiated by small fluctuations or variations in the system caused by turbulence and nucleation. The start for any instability such as static could be predicted using steady state laws, but in the case of dynamic instability we cannot conclude density wave oscillation using a steady state laws. Density wave instabilities are influenced by low frequency flow oscillations in which the period is approximately equal to the order of magnitude of the time required for a density wave to travel through the channel. They are also called density wave oscillations, flow void feedback oscillations, time delay oscillations, and pressure drop oscillations [3].

1.3 Factors Affecting Two-Phase Instabilities:

Boure et al. [4] discussed the density wave instabilities in detail and studied factors that affect the instabilities:

1.3.1 Effect of Channel Length on Flow Instability

The effect of channel length with a constant power density was studied in a Freon loop by Crawley et al. [8]. They concluded that the reduction of the heated length increases the flow stability in the forced circulation and they also proved that the change in the heated length did not affect the period of oscillation because the flow rate was kept constant.

1.3.2 Effect of Inlet and Exit Restrictions on Flow Instability

According to authors [9, 10, 11] an inlet restriction increases single-phase flow friction and thus it provides a damping effect on the increasing flow. Therefore, the inlet restriction increases the flow stability. The exit restriction of a boiling channel increases two-phase friction, which is out of phase with the change of inlet flow [4]. A low inlet flow in single-phase increases void generation and exit pressure drop.

1.3.3 Effect of Pressure on Instability

The effect of pressure on instability was studied by Boure et al. [4]. They found that the increase in system pressure at a given power input reduces the void fraction and thus the two-phase flow friction and momentum pressure drops. The increase of pressure decreases the amplitude of the void response to disturbances. Still it does not affect the frequency of oscillation significantly [4].

1.3.4 Effect of Mass Velocity and Power

Collins and Gacesa [12] studied the effects of mass velocity and power. They found that the oscillation frequency increases with mass velocity and also with power input into the channel.

1.4 Objectives of this study

The following are the objectives of this study,

- The aim of the study was to validate the non-dimensional parameters using the SPORTS code
- The original version of SPORTS can run only for water hence in this study the first task was to modify SPORTS code by incorporating new NIST package which works for different fluids.
- Conduct numerical experiments using the modified SPORTS code by varying several parameters
- Analyze the numerical results
- Validate the non-dimensional parameters which govern the stability boundary in supercritical flow conditions

CHAPTER 2

Literature Review

There are many publications in the area of instabilities. A general review of instabilities and related topics has been performed by many authors, and it is not the intention of this literature review to repeat them. However the previous publications considered more relevant to the present study are reviewed.

2.1 Studies on Natural-circulation Loops

Before getting into details of the instabilities, a study on the concept and understanding of natural-circulation loops is required. Greif [1] reviewed the studies on natural-circulation loops. He defined “natural-circulation loop systems as the flow driven by thermally generated density gradients so that pumping is not required. These loops are often heated from below and cooled from above, which then establishes an unstable density gradient in the fluid. Under the influence of gravity the lighter fluid rises and the heavier fluid falls and the fluid is said to flow due to natural convection” [1].

Review on natural-circulation loops was done by Mertol and Greif [13]. Grief [14] studied the circular toroidal loop. Experimental studies on the instabilities in a circular loop with water at one atmosphere pressure and at moderate temperatures were studied by Crevling et al. [15], and they confirmed that there exist three distinctive regions of operation: namely stable flow at low power, oscillatory flow at

intermediate power, and stable flow again at high power and flow reversals.

Applications of the natural-circulation loops were summarized by Mertol [13] as follows:

- emergency cooling of nuclear reactor cores,
- solar energy heating and cooling systems,
- geothermal power production,
- greenhouses,
- permafrost protection,
- turbine blade cooling, and
- engine and computer cooling applications,

Figures 2.1 and 2.2 are schematics for a pressurized water reactor and a boiling water reactor and show the natural-circulation loop for cooling.

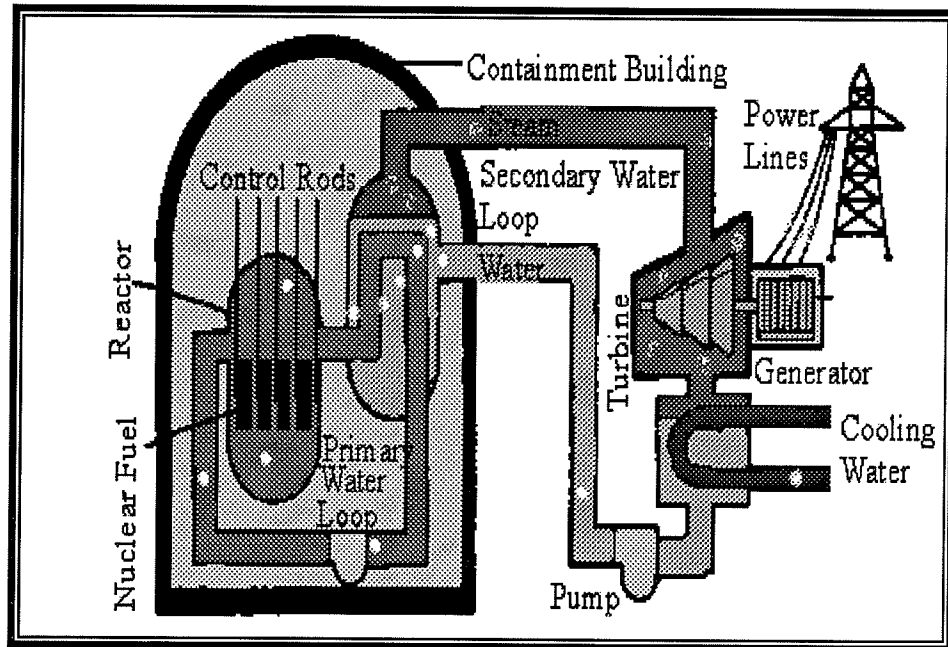


Figure 2.1: Pressurized Water Reactor [16]

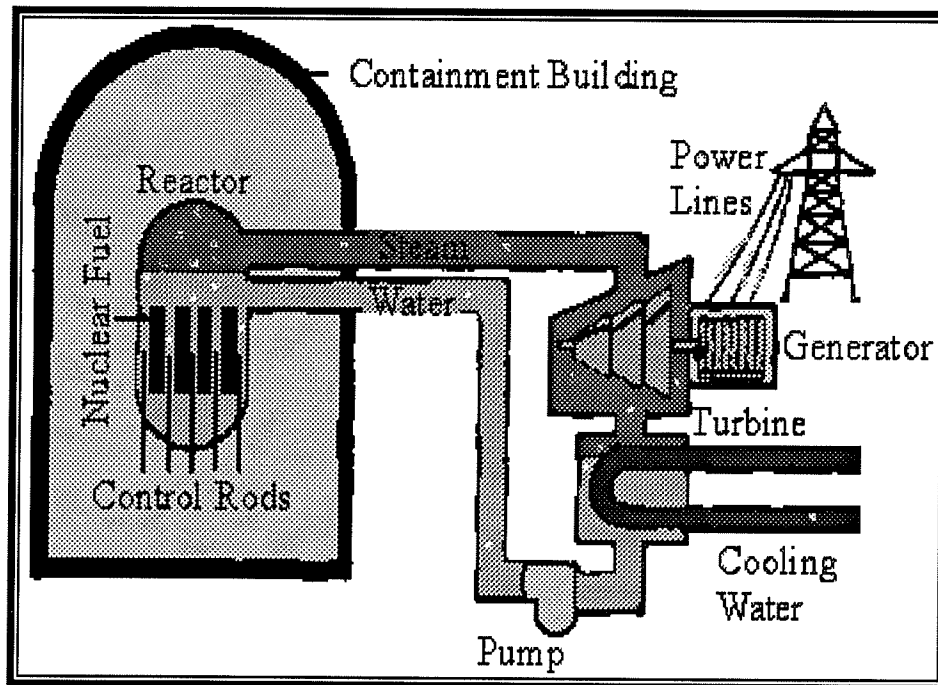


Figure 2.2: Boiling Water Reactor [16]

Zvirin [17] analytically studied the effect of through flow of a natural-circulation loop. He reported that in a certain range of the system parameters, the loop flow rate reaches a maximum when the through flow is evaluated. He extended his work in [18] and studied the effects of a through flow on the steady-state and stability of a natural-circulation loop. In addition to he reviewed natural-circulation loops in pressurized water reactors and other related systems. Later, Zvirin and Rabinoviz [19] studied the behavior of natural-circulation loops with parallel channels. A theoretical one-dimensional approach was adopted. They found that significant deviations between the branches appear only when the secondary flows rates are small. Mertol et al. [13] studied transient heat transfer, fluid flow, and pressure drop in a natural-circulation loop under laminar flow conditions. Ishii and Kataoka [20] formulated the scaling laws for single-phase and two-phase natural-circulation. Similarly Krishnan et al. [21] studied the stability of natural-circulation flow for various channel powers, system pressures and inlet flow subcooling levels. Huang and Zelaya [22] carried out stability analysis for rectangular loops, they concluded that reducing the loop friction and increasing the distance between the heated and cooled sections would improve the system efficiency but would also get system to become unstable which will ultimately reduce the system efficiency.

Auria et al. [23] discussed the problem of scaling in complex thermohydraulic scenarios measured in experimental facilities which simulate pressurized water reactor systems. Van Bragt et al. [24] formulated a theoretical model describing coupled neutronic thermohydraulic power oscillations in natural-circulation boiling

water reactors. They concluded from their study that using dimensionless stability maps was an efficient way to determine the dynamic characteristics of natural-circulation BWRs. Nayak et al. [26] analytically studied the stability behavior of a natural-circulation pressure tube type boiling water reactor. Their results indicated that both Type-I and Type-II density wave instabilities could occur in the reactor in both in-phase and out-of-phase mode of oscillations in the boiling channels of the reactor. Dimmick et al. [27] studied natural convection for advanced CANDU reactor. They showed that, by experiments and code simulations, flashing-driven system was feasible at normal operating powers. Jiang et al. [9] studied the change of the flow stability due to variation of the tube wall thermal conductivity. The stability of supercritical fluids in natural-circulation is of particular importance for the nuclear and power generation industry, as nuclear power has become an important source for energy. In order to optimize the efficiency of nuclear power plants, designers need reliable and accurate information when designing the loops. Hence, research on the instabilities of natural-circulation becomes important.

The literature review on instabilities is segregated into:

- experimental studies in instabilities,
- studies on single-phase instabilities,
- studies on two-phase instabilities,
- studies on linear analysis of instabilities,
- studies on non-linear of instabilities analysis, and
- studies on supercritical flow instabilities.

2.2 Experimental Studies on Two-Phase Instabilities

The first experiment was conducted by Anderson et al. [10] in 1962 and followed by Jain et al. [28]. They conducted experiments and observed density wave instability. They found instability increased with an increase in channel exit restriction, inlet subcooling, decrease in pressure, channel inlet restriction, and downcomer level. Similar observations were also noticed in parallel heated channels of a two-phase natural-circulation loop by Mathisen [29]. Nejat Veziroglu et al. [30] studied the boiling flow instabilities in a cross connected parallel channel upflow systems. Goichi Matsui [31] conducted an experimental study of flow instability in boiling channel systems. Chexal and Bergles [32] observed four unsteady flow regimes when their loop was heated from a cold condition. Aritomi et al. [33] conducted experiments in parallel channel for forced convection boiling upflow systems. Fukuda and Kobori [34] observed two modes of oscillation in parallel heated natural circulated channels. Cumo M., et al. [35] conducted experiments on parallel channels with different heat flux profiles. Ishii and Hsu [36] studies in two-phase natural-circulation and flow termination in a loop experimentally. Lee et al. [37] found that the non equilibrium between the phases, such as flashing, created flow instability in the loop. Aritomi et al. [38] studied thermohydraulics during start up in natural-circulation boiling water reactors. The flow characteristics in an open two-phase natural-circulation loop using Freon-113 was done by Kyung and Lee [39]; they observed three different modes of oscillation with increase heat flux. Jiang et al. [40] observed three kinds of instabilities during the power rising process of a two-phase natural-circulation loop with twin boiling channels, such as geysering, in-phase oscillation and out of phase

density wave oscillations. Furoya et al. [41] performed experimental estimation of instability regions with a test facility which facilitated scaling law.

2.3 Studies on Single-Phase Instabilities

Creveling and De Paz [42] studied the stability characteristics of a single-phase free convection loop. Jeuck III et al. [43] had conducted experiments on single-phase natural-circulation on heat removal. The natural convection facility was composed of four loops with U tube heat exchanger in each loop. These natural-circulation loops were used in the cooling section of the nuclear reactors. Processes for the removal of residual heat from a PWR (pressure water reactor) were single-phase natural-circulation and two-phase natural-circulation. The main purpose of their work was to understand the basic physical processes in natural-circulation and to provide data for benchmarking of computer codes. Viskanta et al. [44] studied a dynamic one-dimensional model of a simple, rectangular natural-circulation loop with tube bundles in the two vertical legs. At steady-state conditions they predicted and measured temperatures within 5%. Misale and Tagliafico [45] performed transient and stability analysis of single-phase natural-circulation loops. They formulated a numerical finite difference scheme for the simulation of the one-dimensional transient behavior of a simple loop comprised of two parallel vertical braches with point heat source and sink. Numerical and theoretical results proposed showed satisfactory agreement. Acosta et al. [46] studied single-phase natural-circulation loops in a tilted square loop. The existence of multiple steady state convective flows in natural-circulation loops was proved experimentally. Vijayan et al. [47] investigated the stability of natural-

circulation with through flow in a figure eight loop, a configuration that is employed in the pressure tube type heavy water reactors. They also carried out a linear stability analysis and finite difference analysis. They found sound agreement between theory and experiment. Another investigation was carried out by Michael and Peter [48]. They examined the dynamic and numerical stability of a one-dimensional, single-phase flow. The stability limits formulated were verified numerically using single-phase flow equations under natural-circulation conditions. Recently, Vijayan [49] reported experimental observations on the general trends of the steady state and stability behavior of single-phase natural-circulation loops.

2.4 Studies on Two-Phase Instabilities

Becker et al. [3] presented a theoretical model for predicting the threshold of instability for two-phase flow in a natural-circulation loop. They solved numerically using finite difference approximation code on a digital computer. Ishii and Zuber [50] reported thermally induced flow oscillations in two-phase mixtures. Boure et al. [4] summarized the instabilities in the two-phase flows. They classified these instabilities and discussed the cause for these various categories. Saga et al. [51] investigated experimentally thermally induced flow oscillations in two-phase systems. Nakanishi [52] reviewed all the existing reports in two-phase flow instabilities and discussed all the existing numerical models. Fukuda and Kobori [35] classified all the existing two-phase flow instabilities. They summarized that instabilities could be categorized into eight types, three of them, the static or the Ledinegg instability, and other five into dynamic and density wave instability. They observed two types of instability in their

experiment. Podowski et al. [53] studied the modeling and analysis of channel to channel instabilities in boiling channels. Rizwann-Uddin et al. [54] discussed the nonlinear periodic, quasi periodic and chaotic dynamics of a two-phase flow system and later they studied the nonlinear dynamics of two-phase flow in multiple parallel heated channels. Wang et al. 1994 [55] studied experimentally the thermal and stability analysis of a two-phase natural-circulation loop. A linear stability analysis is performed in the frequency domain to establish the stability map of a natural-circulation loop.

2.5 Studies on Linear Analysis of Instabilities

Many authors have analyzed the instabilities by linear and non-linear approaches. Nyquist criterion was used to analyze the stability of single channel and multi-channel systems. Gross and See [56] analyzed the density-wave phenomena by the equation of continuity. Sumida and Kawai [57] emphasized the theory of hydraulic stability in boiling channels. Park et al. [58] studied the one-dimensional thermal-hydraulic model which can be used for the linear analysis of boiling water reactor stability. Their model accounted for slip, heated wall dynamics, distributed spacers and detailed model of the loop. The final form included the coupled neutron-kinetics/thermal-hydraulics model which constitutes a multi-input/multi-output linear system of a boiling water reactor. Lahey [59] gave the advances in analytical modeling of linear and nonlinear density wave oscillation modes. Furutera [60] considered seven different homogeneous flow models based on linear approximation. Auria et al. [61] presented a linear model to study fluid dynamic instabilities in

boiling channels due to density oscillations. Marco et al. [62] studied the nodal analysis of instabilities in boiling channels. Won Lee and Yang Lee [63] formulated the linear analysis of flow stabilities in an open two-phase natural-circulation loop. Hashimoto [64] gave the linear modal analyses for out of phase instability in boiling water reactor cores. Ambrosini et al. [65] studied the density wave oscillations in a boiling channel with uniform and constant heat flux and analyzed by linear and nonlinear analytical tools. Zboray et al. [66] performed linear stability analysis of a natural-circulation boiling water reactor. The root locus method was to examine the stability of the system.

2.6 Studies on Non-linear Analysis of Instabilities

Dijkman and Slutter [67] developed a numerical model based on conservation of mass, energy and momentum. The main use of the model was to support a number of experiments performed to study the phase relationship between void fraction and inlet flow rate in a natural-circulation boiling water channel and the effect of sine shaped heat flux on the stability of the system. Non-linear analyses based on numerical technique have been carried by Gurugenci et al. [68]. They developed a numerical code to generate limit cycles of pressure drop and density wave oscillations in a boiling upflow system in a channel. Chatoorgoon [69] developed SPORTS which solves the conservation equations numerically with minimum approximations, avoiding the use of property derivatives and matrix inversions. Marco et al. [70] conducted the non-linear analysis of density-wave and excursive instability phenomenon in a boiling channel. Rizwan-Uddin and Dorning [71] have studied the

basic dynamic bifurcation and stability of adding unheated riser sections above the channels. Nigmatulin et al. [72] have done the non-linear numerical analysis of boiling flow instability in parallel heated channels and a computer program was implemented to predict the effect of technical steps towards providing stability. Lin and Pan [73] studied the non-linear dynamics of a two-phase natural-circulation boiling channel by employing galerkin nodal approximation method based on homogeneous flow model. The developed model was also used to generate transient behavior of the channel for step change in power.

2.7 Supercritical Instability Studies

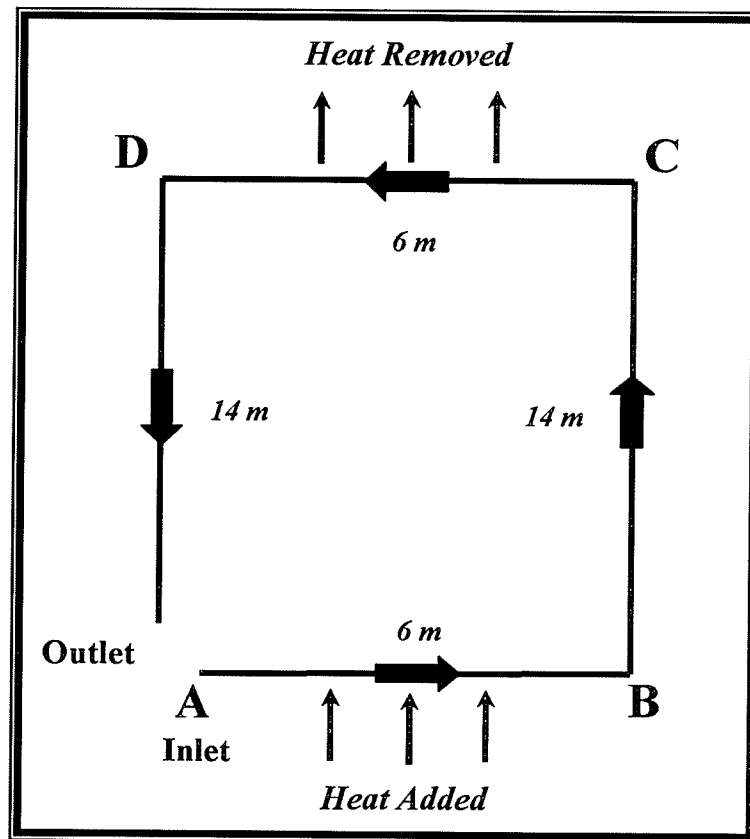
In the early 1960's Harden and Boggs [74] and Walker and Harden [75] reported an analytical and experimental study of a closed natural-circulation system with Freon 114 near the critical temperature. The exit heated temperature was at times near the critical temperature but did not exceed the critical temperature. Walker and Harden [76] also presented the results of an experiment which produced fluctuations in that portion of the single-phase supercritical-pressure region characterized by a maximum in the density-enthalpy product versus density, enthalpy and pressure. Cornelius and Parker [77] studied the instabilities, which result in a periodic variation of flow pressure during heat transfer to a fluid near its thermodynamic critical point. A recent study by Lomperski et al. [78] reported experiments of supercritical carbon-dioxide in a natural circulation loop. No flow instabilities were obtained in their experiment. At these conditions this work of an experiment is first published and therefore, it is regarded as important and relevant.

CHAPTER 3

Theoretical Background

3.1 Analytical Model of Flow Instability

Chatoorgoon [79] developed an analytical model for a single channel natural-circulation loop of a simple configuration which is shown in Figure 3.1, in his approach he assumed point heat source and sink in the middle of AB and CD.



D	=	0.07485 m
z_1	=	3.0 m
z_2	=	20.0 m
z_3	=	17.0 m

Figure 3.1: Schematic of the Loop Setup

According to the theory instability boundary for a single channel, natural-circulation loop at supercritical conditions could be approximated by the criterion

$$\frac{\partial(\text{flow})}{\partial(Q)} = 0, \quad (3.1)$$

where Q is the channel power. The complete analytical method is discussed by Chatoorgoon [79]. The following equations are obtained from the analytical method,

$$\left(\frac{G_m}{\rho_{2b}}\right)^2 = \frac{2gDh_t}{f_2 z_2} = \xi^2, \quad (3.2)$$

$$G_m = \rho_{2b}\xi, \text{ where } \xi^2 = \frac{2gDh_t}{f_2 z_2},$$

$$\xi^2 = \frac{2gh_t}{f_2 z_2 / D}$$

$$C_k = \frac{1}{2} \left(\frac{K}{\Delta Z} + \frac{f}{D} \right) \quad (3.3)$$

$$\begin{aligned} \int \left(\frac{K}{\Delta Z} + \frac{f}{D} \right) dz &= \int 2C_k dz \\ &= 2 \sum C_k dz \end{aligned}$$

$$\xi^2 = \frac{2gh_t}{2 \sum C_k \Delta z} = \frac{2gh_t}{2 \Delta z \sum C_k} = \frac{2gh_t}{2 \Delta z C_{k2}} \quad (3.4)$$

G_m is the maximum value of the mass is flux for a given geometry and ρ_{2b} is the corresponding hot side density at that mass flux. To derive the corresponding power at the stability boundary Q_b , the following simplified state relation is introduced for the hot side

$$\rho_2 = \frac{B}{h_2^{\eta_2}}. \quad (3.5)$$

The constants B and η_2 can be deduced by plotting h_2 versus ρ_2 on log log plots and determining the slope and ordinate intersection. These constants are different for different fluids and these log plots are shown and constants deduced for water, carbon-dioxide and hydrogen are in subsequent chapters.

$$Q_b = G_m A (h_2 - h_1). \quad (3.6)$$

$$Q_b = G_m A \left[\left(\frac{B}{\rho_{2b}} \right)^{\frac{1}{\eta_2}} - h_1 \right] \quad (3.7)$$

$$\theta = \frac{C_{k_2} z_2}{C_{k_1} z_1 + C_{k_3} z_3} \quad (3.8)$$

$$\Phi = -\theta + \sqrt{\theta^2 + \theta}, \quad (3.9)$$

$$G_m = \xi \rho_{2b} = \xi \rho_1 \Phi, \quad (3.10)$$

$$\rho_{2b} = \rho_1 \Phi$$

$$h_{2b} = \left(\frac{B}{\rho_1 \Phi} \right)^{1/\eta_2} - h_1. \quad (3.11)$$

$$Q_b = A \rho_1 \xi \Phi \left[\left(\frac{B}{\rho_1 \Phi} \right)^{1/\eta_2} - h_1 \right]. \quad (3.12)$$

Equation 3.12 defines the approximate power at the stability boundary Q_s as a function of inlet conditions and loop geometry for a single channel, natural-circulation system under supercritical flow.

For convenience the additional non-dimensional parameters are introduced, where

$$G^* = \frac{G}{\rho_1 \xi},$$

$$G_m^* = \frac{G_m}{\rho_1 \xi} \quad (3.13)$$

$$Q_b^* = \frac{Q_b}{AG_m h_1} = \frac{Q_b}{A \rho_1 h_1 \xi G_m^*} \quad (3.14)$$

$$R_b^* = \rho_2 / \rho_1. \quad (3.15)$$

The study is based on the following plots between the parameters:

$$Q_s^* \text{ vs } \left(\frac{B^*}{\Phi} \right)^{1/n_2} - 1 \quad (3.16)$$

$$Q_s^* \text{ vs } Q_b^* \quad (3.17)$$

$$R_s^* \text{ vs } \Phi \quad (3.18)$$

$$G_s^* \text{ vs } G_m^* \quad (3.19)$$

the aim of this study is to assess the validity of the non-dimensional parameters Q_b^* , G_m^* and R_b^* on the stability boundary by numerically simulating a large number of numerical cases.

3.2 Formulation of New Approximation

The analytical method formulated by Chatoorgoon [79] is extended by Chatoorgoon [83] using improved method. In this method the various non-dimensional parameters in the previous model were formulated using the approximation, that the stability boundary lies in the region $\alpha G_m \leq G_s \leq G_m$ where $\alpha = 0.95$. G_m is the peak flow

obtained from the steady-state profile, and is approximated to αG_m . All the parameters are derived taking the new value for G_m . The new approximation method is presented below,

Define Q_b to be Q at αG_m or $\alpha = G/G_m$, where $\alpha < 1$

equation 3.6 becomes

$$Q_b = \alpha G_m A (h_2 - h_1) \quad (3.20)$$

hence replacing G_m by αG_m

$$\tilde{Q}_b = \alpha A \rho_1 \xi \tilde{\Phi} \left[\left(\frac{B}{\tilde{\rho}_2} \right)^{1/n_2} - h_1 \right] \quad (3.21)$$

$$\tilde{Q}_b^* = \alpha \left[\left(\frac{B}{\rho_1 h_1^{n_2} \tilde{\Phi}} \right)^{1/n_2} - 1 \right] \quad (3.22)$$

$$\tilde{\Phi} = \frac{1}{2} + \alpha^2 \left(\Phi - \frac{1}{2} \right) \pm \frac{1}{2} \sqrt{(1 - \alpha^2) \{ (1 - \alpha^2) + 4\alpha^2 \Phi (1 - \Phi) \}} \quad (3.23)$$

Therefore from the improved theory Φ can be approximated by $\tilde{\Phi}$ and Q_b with \tilde{Q}_b^* .

In this study the above expression is used to validate the non-dimensional parameters by plotting the points obtained by taking α of the peak flow rate.

3.3 SPORTS Code

SPORTS (Special Predictions of Reactor Thermalhydraulics and Stability)

SPORTS code has proven suitable for supercritical studies. A unique method of solution of finite difference equations was devised and incorporated. Many complex procedures and approximations as in many other stability codes were avoided. In

supercritical flow applications there are large changes in some property derivatives across the critical point. The large variation in specific heat is mitigated in SPORTS by expressing the energy equation in terms of the fluid enthalpy. Therefore, SPORTS numerical procedures perform well for computations through the critical and into the supercritical regions.

3.3.1 Stability and Transient Simulations

SPORTS code is used for running transient and steady-state. For the steady-state runs ITR=0 (iteration factor), while for transient and stability run by the value of FPOW, the final power. If the entered value of FPOW (final power) is the same as POW (power) a stability simulation is performed by SPORTS. An inlet flow perturbation is introduced by introducing an error in the outlet pressure boundary condition for one time-step, after which the error is removed. SPORTS solve the basic equations that are the mass, momentum, energy and state equations using the finite-difference scheme. The detail theory behind the formulation of SPORTS code is in [69]

3.3.2 Boundary Conditions

SPORTS can take variety of possible boundary conditions, which are controlled by the input data as PIN, the inlet pressure, and PEX, the external reference pressure. If the flow rate FLOW is known, the user must specify PEX equal to zero in the input data and the known FLOW [80]. If PIN and/or PEX are known, the correct value must be specified in the data. If PIN and /or PEX is not known, but must be

calculated from a static head of water, as in a surge tank or pool, PIN and/or PEX must be set equal to one, and a value of ZIN must be specified, where ZIN is the height of the static head of water in meters. It is assumed that the static head of water is open to atmosphere. This type is appropriate for natural-circulation systems and pool-type reactors.

Power: The user must specify an average applied power and also the heat flux profile. If the entered value of FPOW is different from POW, no perturbation in inlet flow is introduced and SPORTS performs a simulation run.

The SPORTS code is formulated in such a way that it can run for both stability and transient runs. For a stability run the user inputs zero power change and the code automatically inputs a zero power change and the code automatically inputs a perturbation in the outlet pressure for duration of one time step. This in effect causes a temporary perturbation in the inlet flow velocity. After the first time step the correct outlet pressure is reinstated and the systems transients is followed in time to determine if the perturbations grow or decay. The results of stability analyses are very sensitive to assumptions made in the modeling of the loop, e.g. linear temperature distributions.

3.3.3 Input Files

The input files for water, carbon-dioxide and hydrogen are provided in APPENDIX-B these files give an idea of the input parameters and the parameters which are obtained from the SPORTS code. In these input files it could be noticed that the loops dimensions are specified. The ITR factor which allows us to do different runs, if

ITR=0 then its a steady-state run and if it is run for ITR=1 then it is transient run. There are other input parameters like the time step. The FLOW is the inlet flow rate. PIN and PEX are the inlet and outlet pressures respectively. POW and the FPOW are the initial and the final power. For a transient run this factor is increased for the run until the system gets unstable. There are other parameters like the RHOFLG and PRFLG these are the flags for density and pressure.

3.4 Modification of SPORTS Code

3.4.1 WINDOWS Version

The SPORTS [80] code originally incorporated with a steam package from NIST which can run only for water as fluid. Hence, for this study SPORTS code must be modified in order to run for different fluids. New NIST Refprop 7 [83], which works for fluids like water, carbon-dioxide and hydrogen is used to replace the old property package. Hence to make the necessary modification one should get well versed with the code. Primary task was to locate the places where the SPORTS code calls for NIST files and then identify the new the NIST files which could replace them. The old NIST files were recognized as auxpk.F, propk.F, intpk.F and solvpk.F. The next task was to find suitable files in the new NIST package that could replace the old files.

SPORTS code calls for NIST files in subroutines CONVHIN.F and STPROP.F, hence the new NIST files should replace at these entry points. Minor initialization has to be done while using the new NIST package, that is specifying the fluid name and should be done in SETUP.FOR subroutine. The parameters in this subroutine are nc, hfiles, hfmix, hrf, ierr, herr. The following lines explains how set-up is done

Inputs:

nc--number of components (1 for pure fluid) [integer]

hfiles--array of file names specifying fluid/mixture components

[character*255 variable] for each of the nc components;

e.g., fluids:R134a.fld (Mac) or fluids\R134a.fld (DOS) or

[full_path]/fluids/R134a.fld (UNIX)

hfmix--mixture coefficients [character*255]

File name containing coefficients for mixture model,

e.g., :fluids:HMX.bnc

hrf--reference state for thermodynamic calculations [character*3]

'DEF': default reference state as specified in fluid file

is applied to each pure component

'NBP': $h, s = 0$ at pure component normal boiling point(s)

'ASH': $h, s = 0$ for sat liquid at -40 C (ASHRAE convention)

'IIR': $h = 200, s = 1.0$ for sat liq at 0 C (IIR convention)

other choices are possible, but these require a separate

call to SETREF

outputs:

ierr--error flag: 0 = successful

101 = error in opening file

102 = error in file or premature end of file

103 = unknown model encountered in file

104 = error in setup of model

105 = specified model not found

111 = error in opening mixture file

112 = mixture file of wrong type

herr--error string (character*255 variable if ierr \neq 0)

[fluid parameters, etc. returned via various common blocks]

There are minor changes between the old NIST and new NIST files that have to be overcome. The old NIST package calculates the properties in the SI units, but for the new NIST package the units are not. To overcome this properties obtained from the NIST was changed to SI units by making necessary changes by multiplying with molecular weight. The two subroutines in SPORTS code that are modified are presented in APPENDIX-C

After making the above changes in the code, the next step was to compile the files and form an executable and then to verify the results. Hence the results from modified code and the code with old NIST package were compared.

3.4.2 Sample Test

The modified SPORTS code was tested for accuracy. A numerical experiment was conducted using both the versions of SPORTS code, codes were run for the same input files. The results obtained from both the codes were plotted presented in Figure 5.1, the results showed good agreement. Modified SPORTS code could run for different fluids by making the necessary changes in the code by specifying the fluid names. Thus the major task was achieved by modifying the code. Now the UNIX-version of the SPORTS code was to be formulated which allows doing simultaneous runs.

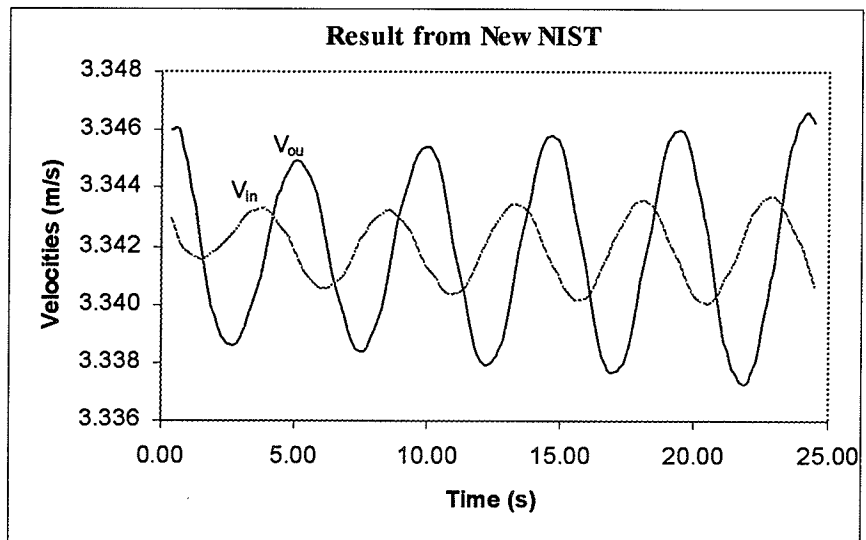
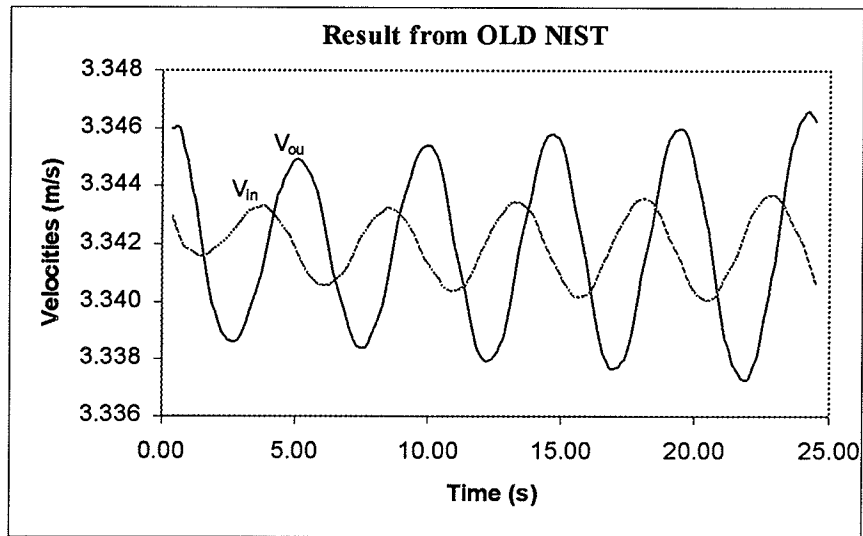


Figure 3.2: Comparison of Plots for Old and Modified SPORTS Code

3.4.3 UNIX Version

After the successful completion of the Windows version of the SPORTS code, there was a need for a UNIX version. Hence the next task was to make the UNIX version of the SPORTS code. For UNIX version the SPORTS code requires make file. The old SPORTS code had a make file which was modified by replacing the old with new NIST files. SPORTS make file is presented in APPENDIX-A. After formulation of the make file the task was to compile and check the code. Initially it showed up an error opening a file 101 while executing. The problem was solved by hit and trail method by making the changes in cases of the file names. Since UNIX machines are highly case sensitive, uniform cases for file names should be used. The new version of the UNIX was tested for accuracy; this was done by running a test case and comparing with the old code. The results matched exactly.

Once the SPORTS code was modified and tested numerical experiments for various fluids water, carbon-dioxide and hydrogen were conducted and the non-dimensional parameters were validated. This is presented in detail in the following chapters.

CHAPTER 4

Numerical Experiments

4.1 Loop Set-up for Simulation

In this study, SPORTS code is used to conduct a host of numerical experiments to better understand supercritical flow instability and non-dimensional parameters. Numerical simulations were conducted for various fluids to validate the non-dimensional parameters. The schematic of the loop for which the study is done is shown in Figure 4.1

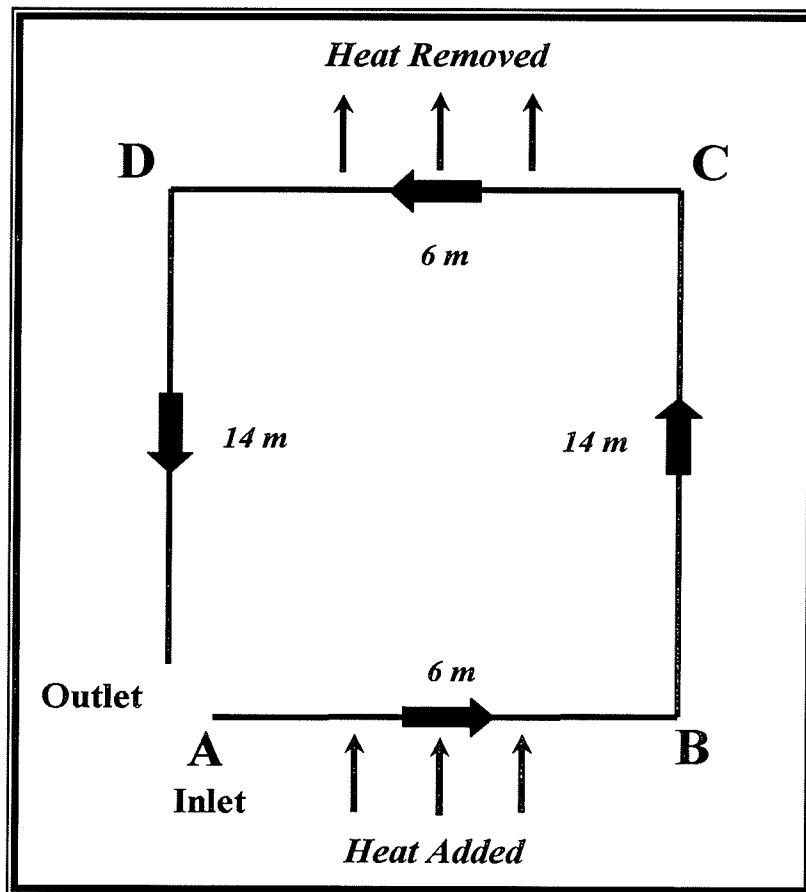


Figure 4.1: Schematic of the Loop Setup

It is a simple, constant area, single channel flow loop oriented vertically with relevant dimensions. The flow is driven by natural convection. Heat is being supplied from the central portion of the lower horizontal segment and removed from the central portion of the upper horizontal segment. The heat removal was always fixed to 1 m. The entire loop is of the diameter 0.07485m. A constant and axially uniformly heat flux was assumed, hence any thermal dependency on the wall thermal conductivity is ignored.

4.2 Calculation of the constants

The following is the state equation from the analytical method in chapter 3

$$\rho_2 = \frac{B}{h_2^{\eta_2}}. \quad (4.1)$$

From this equation constants B and η_2 are different for different fluids and hence they have to be calculated for each fluid studied. Constants can be deduced by plotting h_2 versus ρ_2 on log log plots and determining the slope and ordinate intersection. In Figure 4.2 ρ_2 versus h_2 at 25 MPa and for the temperature range 376⁰-500⁰ C is plotted for water. To a very good approximation, log ρ versus log h is linear in the temperature range of interest. Similarly B and η_2 are also calculated for carbon-dioxide and hydrogen. ρ_2 versus h_2 at 8 MPa and for the temperature range 30⁰-50⁰ C for carbon-dioxide is shown in Figure 4.3 and ρ_2 versus h_2 at 1.31 MPa for carbon-dioxide and for the temperature range -238^{0.5} to -223⁰ C for hydrogen is shown in Figure 4.4

Table 4.1: Constants for Different Fluids

Fluids	B	η_2
H ₂ O	1.7418×10^{23}	3.277
CO ₂	1.32×10^{18}	2.7966
H ₂	8.3849×10^{10}	1.7189

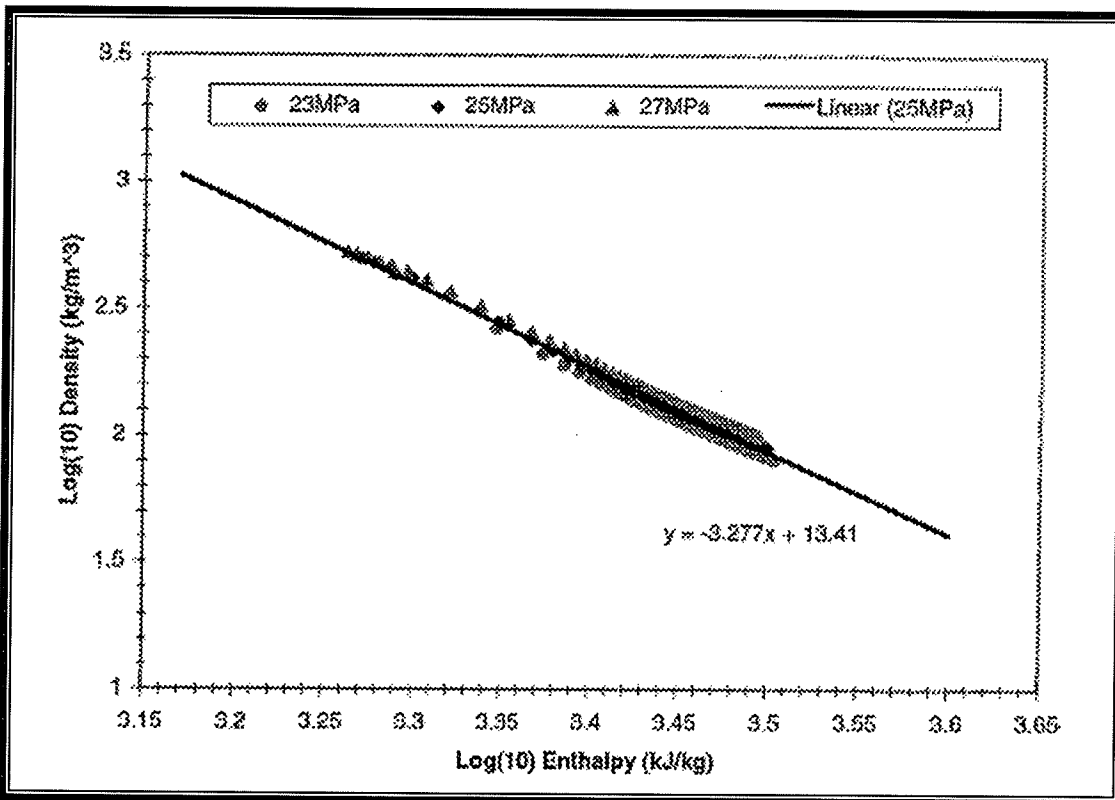


Figure 4.2: Density Versus Enthalpy (Water)

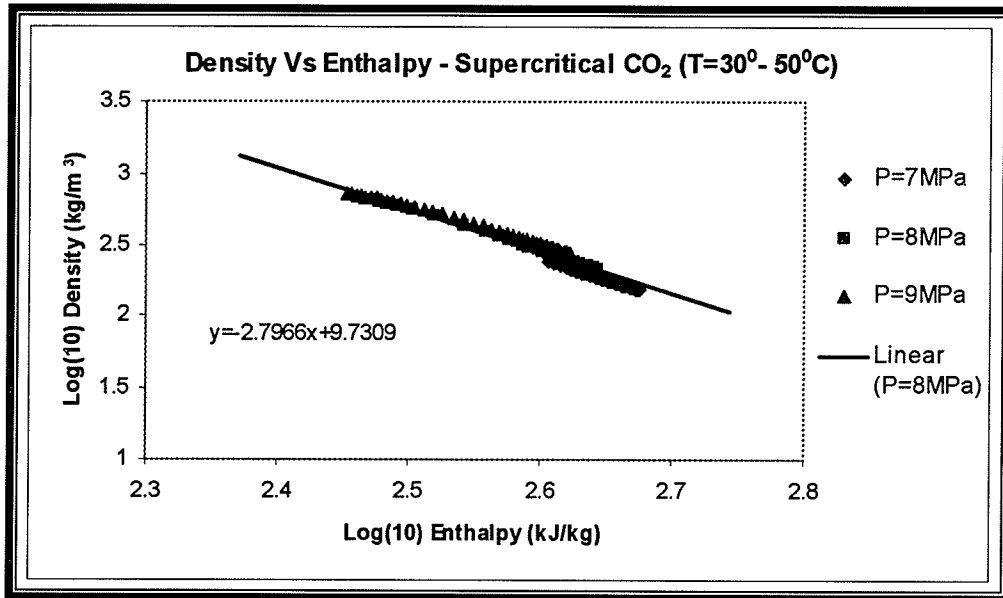


Figure 4.3: Density Versus Enthalpy (Carbon-dioxide)

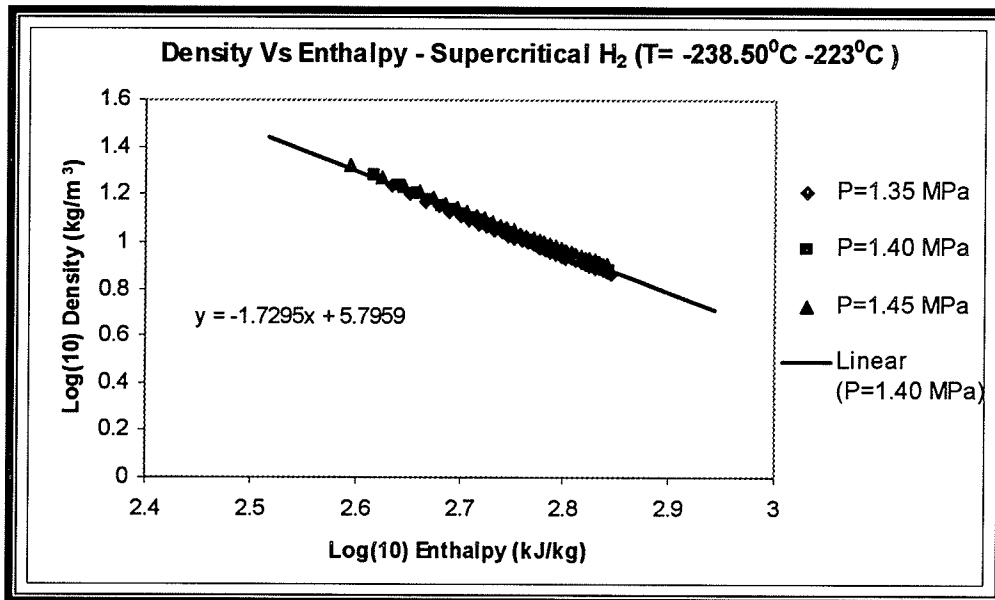


Figure 4.4: Density Versus Enthalpy (Hydrogen)

4.3 Numerical Simulations

The aim of this research is to validate non-dimensional parameters defining instability by conducting numerical experiments using SPORTS code. These non-dimensional parameters are originally formulated for point source and are extended to the distributed heated source. Numerical simulations were conducted by changing various parameters one at a time while keeping the remaining parameters constant.

The parameters that are varied in this study are:

- length of the heated section
- height of the loop
- friction factors at the inlet and outlet of the heated length
- inlet temperatures

Numerical simulations that are conducted for water, carbon-dioxide and hydrogen are tabulated in the following sections.

Table 4.2: Numerical Experiments for Water

<i>Table for Water Runs</i>					
L_{TS}	T_{IN}	h_t	R_{K1}	R_{K2}	No of Runs
(m)	($^{\circ}C$)	(m)			
1	350	10	1.0 – 10.0	1.0	10
1	350	14	1.0 – 10.0	0.5	10
1	350	17	0.5 - 3.0	0.5	4
1	340	14	1.0 – 10.0	1.0	10
			5.0	8.0	1
1	360	14	1.0 - 6.0	1.0	6
			8.0-9.0	10.0	2
L_{TS}	T_{IN}	h_t	R_{K1}	R_{K2}	No of Runs
(m)	($^{\circ}C$)	(m)			
2	350	10	1.0 – 10.0	0.5	10
2	350	14	1.0 – 10.0	1.0	10
2	350	17	1.0 – 10.0	1.0	10
2	340	14	1.0 - 4.0	5.0	4
			1.0 - 5.0	4.0	5
2	360	14	1.0 – 10.0	1.0	10
			8.0-9.0	8.0	2

4.3.1 Numerical Experiments for Water

Table 4.2 gives the summary of numerical simulations conducted for water. SPORTS determine system stability through a non-linear solution governing equations. Initially a perturbation is introduced into the inlet flow velocity and a system transient simulated, which determines the system is stable or not. In a transient case all the parameters are held constant and power was steadily increased until the system becomes unstable. The stability of the system is determined by plotting the velocity

profiles against time obtained from the output file of the SPORTS code. The system is considered stable for a converging velocity profile and unstable if it is diverging and stability of the system is determined. The boundary is power the threshold power at which the system becomes unstable or the velocity profile starts diverging. It is always recommended that the time step is usually one twentieth of the time period of the velocity profile.

From the SPORTS output file various parameters like converged flow rate, outlet temperature and hot side density are also noted and tabulated. C_{k1} , C_{k2} , C_{k3} are calculated. C_{k1} is obtained by summing the friction factor in the loop from the starting node to the node where the temperature becomes in supercritical range and C_{k2} is the sum of friction factors where the temperature stays supercritical and C_{k3} is the sum of friction factors for the remaining part of the loop. K-factors are values are kept lower than 10 as they are reasonable and more practical.

Steady-state runs were performed for all the transient cases done. From steady-state profile, peak power and peak flow are calculated and tabulated. From the all the values obtained for flow rate at different powers, steady-state profile of flow rate vs power is plotted. The plot of the steady-state profile shows the pattern that flow increases with power and after reaching maximum starts decreasing, the maximum value of the flow rate reached is taken as peak flow rate. Figure 4.5 shows how the flow rate increases and decreases with an increase in power. The peak power and peak flow rate are also shown

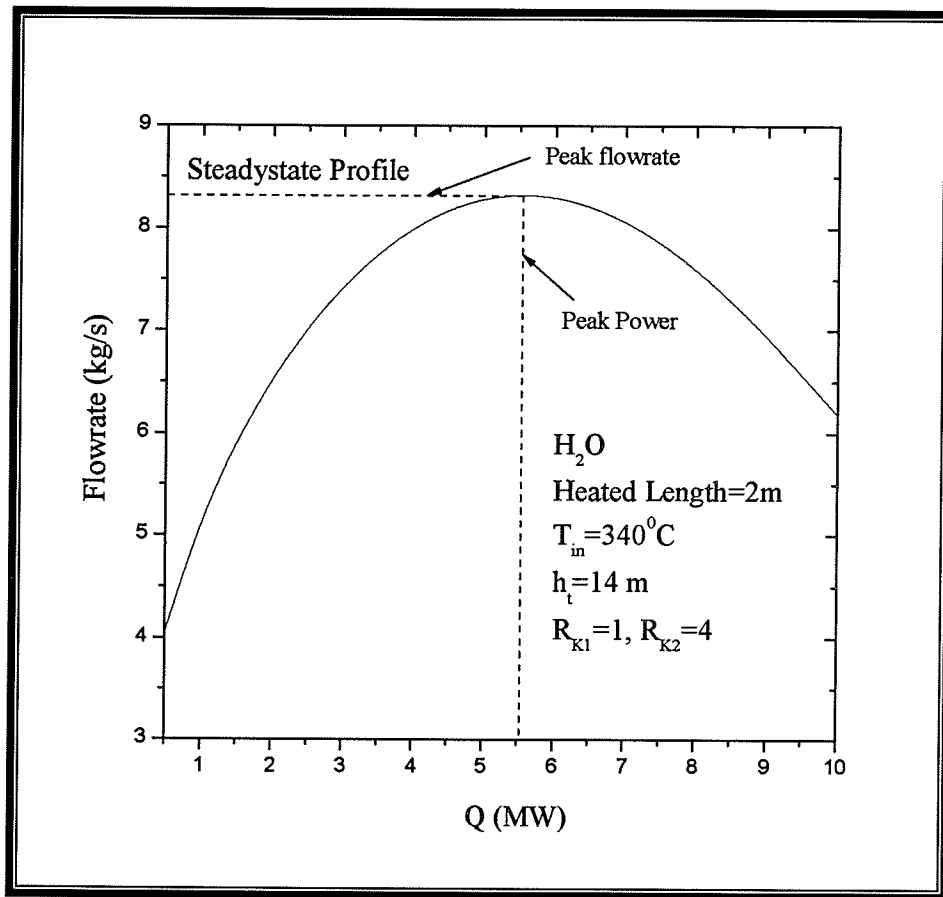


Figure 4.5: Steady-State Profile

According to the theory postulated by Chatoorgoon [79] the boundary lies on the peak of the steady-state profile. The system is stable for the power on the positive slope of the steady-state profile and unstable on the negative slope of the profile. The runs were tested for validation of this theory and studied for any discrepancies of the results.

The numerical simulations for different fluids are shown in Tables [4.2], [4.3], and [4.4]. Transient runs are conducted for every case and steady state runs are also conducted. Sample set of transient runs and steady-state profiles are provided in Appendix-E. From the results obtained from the transient runs and steady-state profiles various parameters which are derived from the analytical model and non-

dimensional parameters were calculated and tabulated. The following non-dimensional numbers which were discussed in chapter 3 are calculated and plotted for there validation.

- G_s^* Non-dimensional mass flux from SPORTS code
- G_m^* Non-dimensional maximum mass flux from steady-state profile
- Q_b^* Non-dimensional peak power from steady-state profile
- Q_s^* Non-dimensional boundary power from SPORTS code
- R_s^* Non-dimensional density

Figures 4.6 summarize various plots for the above set of non-dimensionalized parameters for 1 m heated length for water.

$$Q_s^* \text{ vs } \left(\frac{B^*}{\Phi} \right)^{1/2} - 1 \quad (4.2)$$

$$G_s^* \text{ vs } G_m^* \quad (4.3)$$

$$Q_s^* \text{ vs } Q_b^* \quad (4.4)$$

$$G_s^* \text{ vs } \Phi \quad (4.5)$$

$$R_s^* \text{ vs } \Phi \quad (4.6)$$

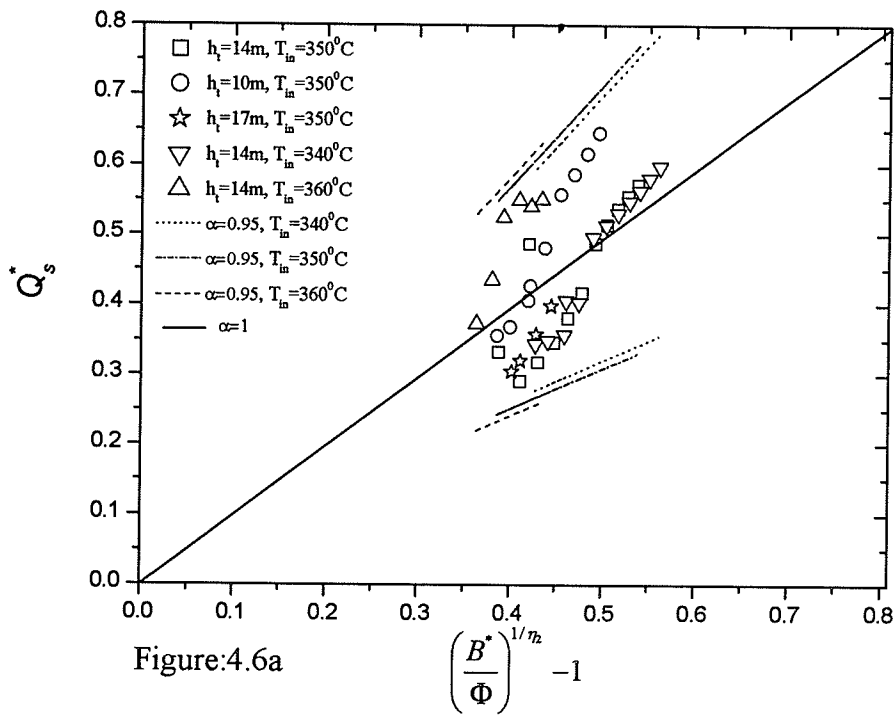


Figure:4.6a

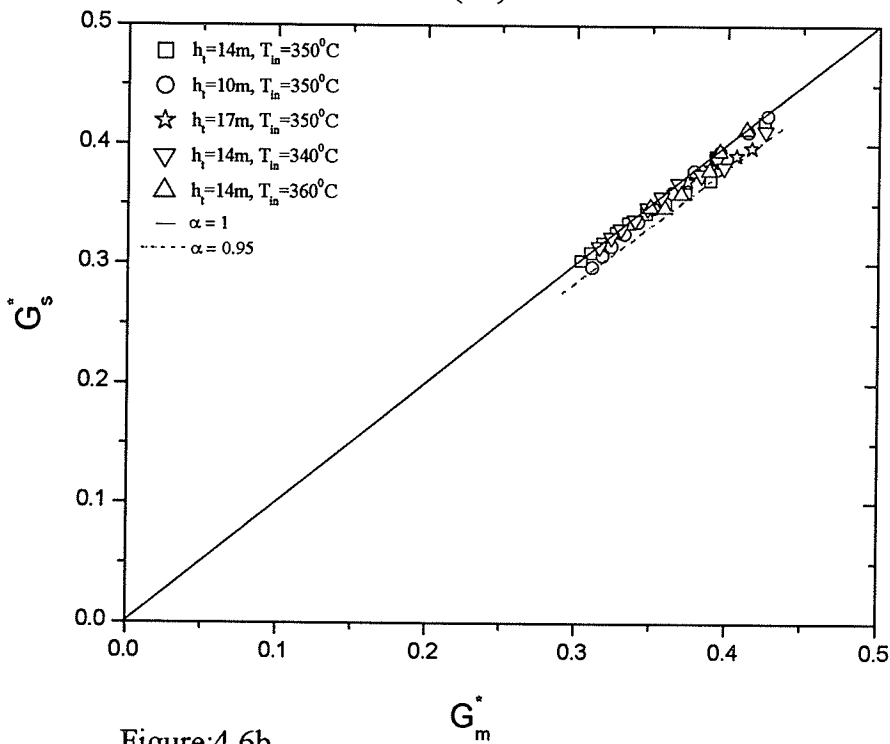
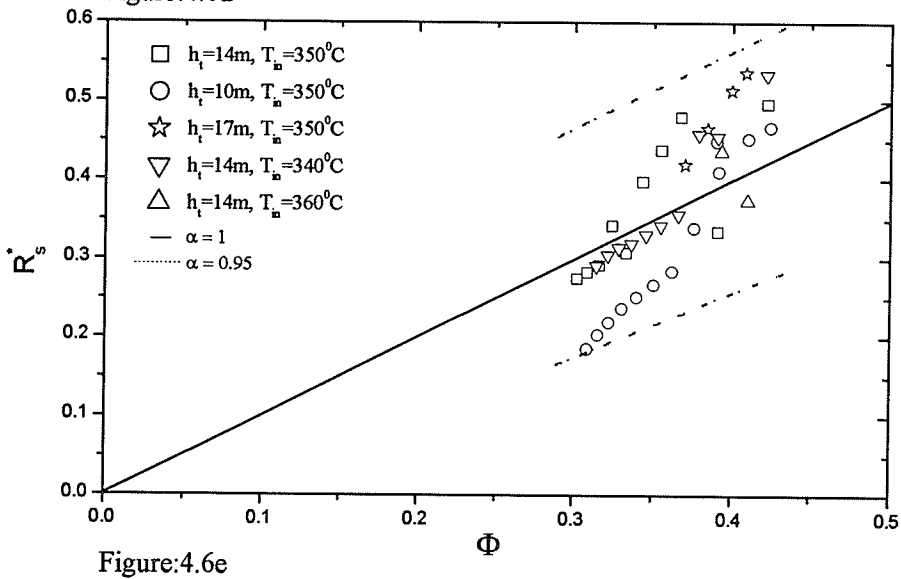
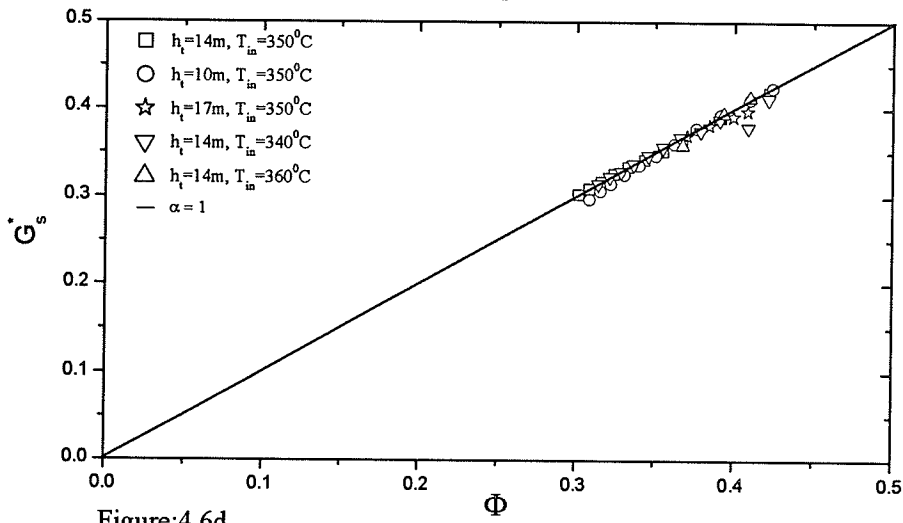
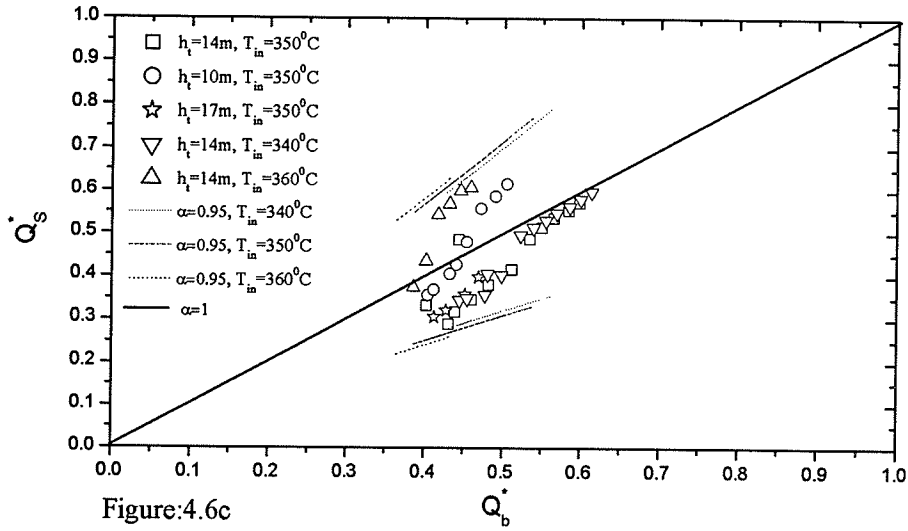


Figure:4.6b

Figure 4.6: Water with Heated Length of 1 m



4.3.2 Discussion of Results for Water with 1 m Heated Length

The validity of the non-dimensional parameters Q_b^* , G_m^* and R_b^* as stable boundary parameters is now assessed by finding how well the numerically produced results correlate with these non-dimensional parameters. Appendix-E summarizes the transient and steady-state results for water of heated length 1 m. Transient cases near the stability boundary are submitted and also the steady-state profile is included with these transient plots. The results and the parameters obtained from these transient and the steady-state solution are tabulated and presented in Appendix-D, Tables D1-D5. All the parameters from the analytical method and all the non-dimensional parameters formulated in chapter-3 are calculated. In this summary of results various parameters like non-dimensional mass flux obtained from the SPORTS code and non-dimensional mass flux obtained from the peak flow from the steady-state profile are calculated. Maximum temperature in the loop is also tabulated to study its variation. From the velocity profiles obtained from the transient run the time-period is also calculated and tabulated. Time-period plays a significant role in determining the stability of a system. It is seen from the results that time-period of the system is steadily decreasing with an increase in the inlet K-factor as the inlet K-factor stabilizes the system and outlet K-factor acts as an destabilizing factor. For high values of inlet restriction the time-period is very small, 1.7 s, and for cases where the inlet and the outlet K-factors are kept reasonably small the time period is relatively high, 8 s. It can also be concluded from results that as the inlet K-factor, increases the system become stable and adversely increases the bounding power and vice-versa with the outlet K-factor as destabilizes the system as its value increases. In each set of

conditions a particular parameter is varied keeping the other constant. Several parameters like the converged flow rate, boundary power, hot side density, C_{k1} , C_{k2} , and C_{k3} are obtained from the SPORTS output file. Peak power and peak flow rate are obtained and tabulated from steady-state profile.

Figure 4.6a is the plot for $\left(\frac{B^*}{\Phi}\right)^{1/\eta_2} - 1$ vs Q_s^* . It is seen that in each condition studied are given different legends and different types of lines which encompasses the entire points are the lines obtained from the approximation theory by taking $\alpha = 0.95$. There are three types of dotted lines for each of three temperature runs done. The solid line that passes through the centre is the theoretical line for $\alpha = 1$, that is obtained from the theory. It could be seen that all the points are well within the dotted lines obtained from ninety five percent of the flow rate approximation. This is a good approximation as it holds the theory.

Figure 4.6b is plotted of G_s^* vs G_m^* . Where G_s^* non-dimensional mass-flux which is obtained from the SPORTS code and G_m^* is the non-dimensional peak steady-state mass flux determined from the steady-state analysis. In the plot the lower dotted line is ninety five percent is the line corresponding to 95% G_m^* . This line brackets all the stability predictions. It is seen that all the points lie close to the solid centre line which is a very good approximation. Therefore, the stability boundary flow rate can be predicted to within 95% accuracy by using the peak steady-state flow rate as the stability flow rate.

Figure 4.6c is the plot of Q_s^* vs Q_b^* . Here Q_s^* is non-dimensional bounding power obtained from the stability analysis from the SPORTS code. Q_b^* is non-dimensional

power obtained from a steady-state analysis and is obtained from the power corresponding to the peak steady-state flow rate. Different legends are used to represent different set of conditions. The two types of lines that are used the straight line for $\alpha = 1$ and dotted lines are for $\alpha = 0.95$. We can notice each dotted line represents each set of different temperature runs. The data is scattered around $\alpha = 1$ line and is bracketed by the $\alpha = 0.95$ dotted lines. Thus, the data is reasonably correlated. These findings suggest that the stability boundary power can lie anywhere in the stability boundary region denoted in Figure 4.6c the edges of the region are defined by the pair of steady-state powers corresponding to $G = 0.95 G_m$.

Figure 4.6d is the plot of G_s^* vs Φ . This plot also correlated well. Here it can be noted that Φ is mainly a geometrical parameter and it solely governs G_s^* . These non-dimensional parameters are also validated as it can be vividly seen that fall close to $\alpha = 1$ line. Hence these non-dimensional parameters are also validated.

Figure 4.6e is plots of R_s^* vs Φ . Where R_s^* is the ratio of hot side density to the cold side density upstream of water $\left(R_s^* \equiv \frac{\rho_{2_s}}{\rho_1} \right)$, ρ_{2_s} is the hot side density when the system is at the stability boundary. Φ is approximated from the equation 3.22 in chapter 3 with $\alpha = 1$ and $\alpha = 0.95$ or $G = 0.95 G_m$ and shown as straight and dotted types respectively. It is evident that the non-dimensional hot-side density at the stability boundary correlates well with Φ as predicted. Here the trend continues, all points fall within $\alpha = 0.95$ dotted lines which is a very good approximation.

The present study is extended to 2 m heated length water. The following Figure 4.7 summarizes the plots for 2 m heated length water.

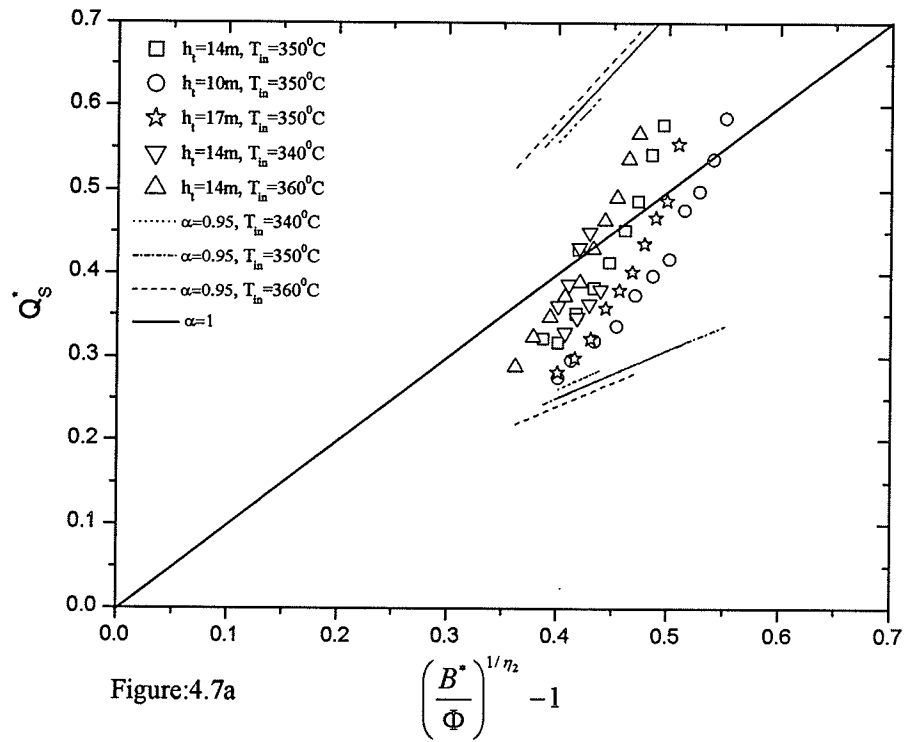


Figure:4.7a

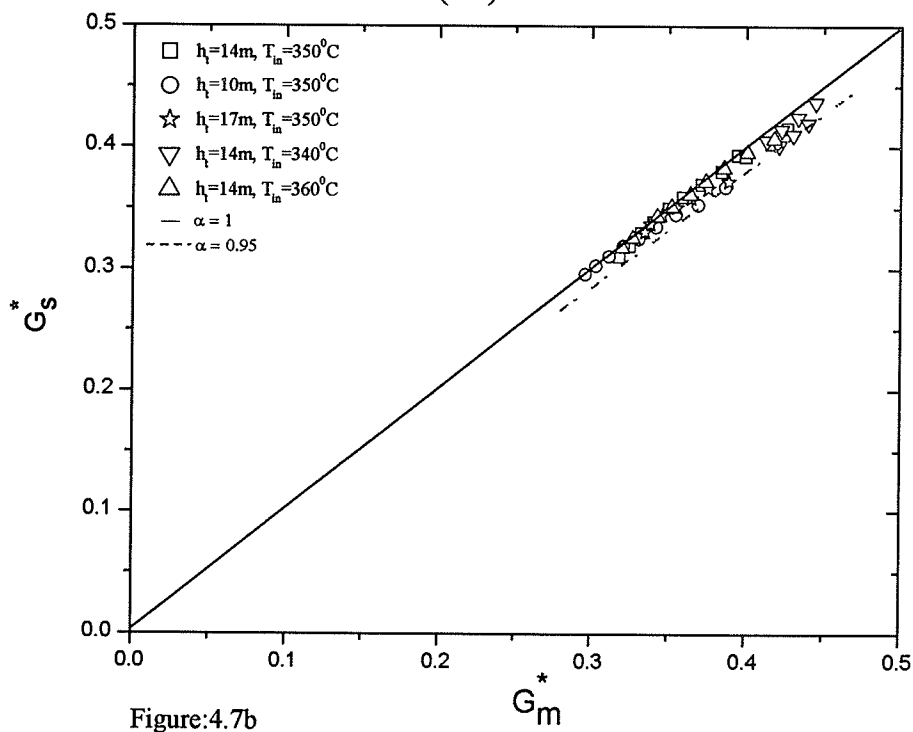
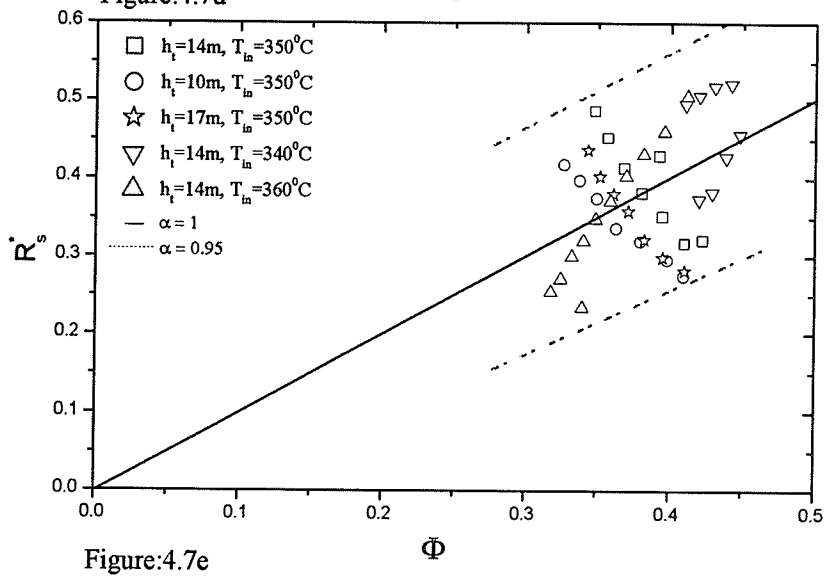
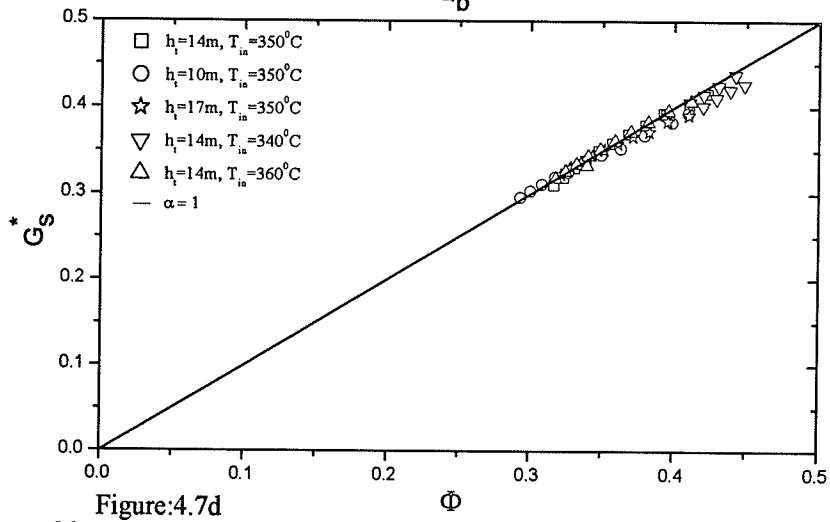
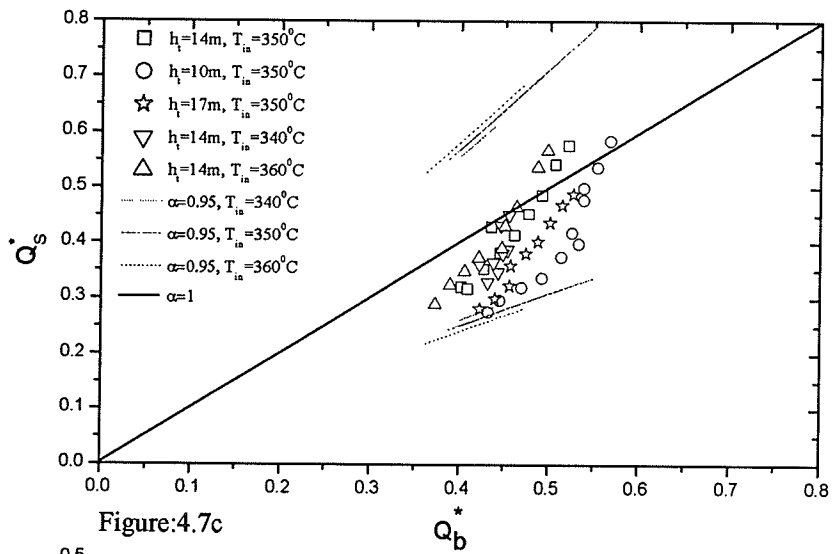


Figure:4.7b

Figure 4.7: Water with Heated Length of 2 m



4.3.3 Discussion of Results for Water with 2 m Heated Length

Summary of results for 2 m heated length cases are presented in Appendix-D, Tables D5-D10. In this study inlet and outlet K-factors, height of the loop and the inlet temperature are the varying parameters. Time-step and the time-period are also recorded and tabulated in the results. From the results it is noticed that inlet K-factor stabilizes and the outlet K-factor destabilizes the system. Time-period is seen to follow a similar trend as in the case of water 1 m heated length. Maximum temperatures in the heated section are tabulated and found to be above critical temperatures. Non-dimensional parameters obtained from the tables are plotted for their validity. The trend remains similar as that of 1 m results.

It can be seen from Figure 4.7a $\left(\frac{B^*}{\Phi}\right)^{1/\eta_2} - 1$ vs Q_s^* , It is seen that points obtained from different set of conditions fall well within the solid and the dotted lines. We can conclude that all the points fall within the ninety five percent of the peak flow which is a very good approximation from the theory. Comparison of Figure 4.6a and Figure 4.7a shows the similarity except that there is more scatter in the 2 m case. This shows that as we increase the heated length or move away from the point source the theory does not hold well and we can notice considerable scatter.

Figure 4.7b shows the relationship of G_s^* vs G_m^* , it can be seen that the lines $G_s^* = G_m^*$ and $G_s^* = 0.95 G_m^*$ bracket all the stability predictions. It could be inferred that the points fall close to the straight line and also fall within the ninety five percent which is a very good approximation. Hence this validates the theory that boundary flow rate

obtained from the SPORTS code is equal to the peak flow rate obtained from steady-state profile.

Figure 4.7c is the Q_s^* vs Q_b^* . It could be seen that all the points fall within the ninety five approximations, but the scatter of the points are relatively more to the plot from figure 4.7b which is for bounding flow rate. Hence it could be stated that one could approximate the bounding flow rate but the bounding power can be approximated ninety five percent.

Figure 4.7d is the plot between G_s^* vs Φ . In this plot which is similar to Figure 4.7c, where all the points are close to the centre line. Hence these non-dimensional parameters are validated. Figure 4.7e is the plot of the R_s^* vs Φ . This plot also contains the dotted lines for Φ calculated from $\alpha = 0.95$ and solid line for $\alpha = 1$. This plot also follow similar trend as all the points fall within the dotted lines.

Therefore from the plots for 2 m heated length water, it can be concluded that the results are similar to that of the 1 m heated length water. Also there is more scatter in the 2 m heated length than the 1 m which follows the theory. From these results obtained for different heated length for water, it can be concluded that one could approximate the bounding flow rate and also bounding power in a system. This study also allows us to approximate the bounding power without conducting a transient analysis which is a time consuming process. The study is extended to other fluids i.e. for carbon-dioxide and hydrogen in the following sections.

4.3.4 Numerical Experiments for Carbon-Dioxide and Hydrogen

The study for validation of non-dimensional parameters was extended to carbon-dioxide and hydrogen. Numerical experiments were conducted for carbon-dioxide and hydrogen using the modified code. The following Tables 4.3 and 4.4 summarize the numerical runs done for carbon-dioxide and hydrogen respectively.

Table 4.3: Numerical Experiments for Carbon-Dioxide

<i>Table for Carbon-dioxide Runs</i>					
L_{TS} (m)	T_{IN} ($^{\circ}C$)	h_t (m)	R_{K1}	R_{K2}	No of Runs
1	25	10	1.0 - 7.0	1	7
1	25	14	1.0 - 5.0	1.0	5
1	25	17	1.0 - 5.0	0.5	5
1	27	14	1.0 - 3.0	1	3
			1.0 - 3.0	3	3
L_{TS} (m)	T_{IN} ($^{\circ}C$)	h_t (m)	R_{K1}	R_{K2}	No of Runs
2	25	10	1.0 - 6.0	1	6
			0.1 - 0.9	0.5	5
2	25	14	1.0 - 8.0	1	8
2	25	17	1.0 - 5.0	0.5	5
2	27	14	1.0 - 5.0	1	5
			1.0 - 6.0	0.5	6

Table 4.4: Numerical Experiments for Hydrogen

<i>Table for Hydrogen Runs</i>					
L_{TS} (m)	T_{IN} (°C)	h_t (m)	R_{K1}	R_{K2}	No of Runs
1	-243	10	1.0 - 10.0	3	10
1	-243	14	1.0 - 10.0	1	10
			1.0 - 5.0	0.5	5
1	-243	17	1.0 - 10.0	1	10
1	-245	14	1.0 - 10.0	5	10
L_{TS} (m)	T_{IN} (°C)	h_t (m)	R_{K1}	R_{K2}	No of Runs
2	-243	10	1.0 - 10.0	1	10
2	-243	14	1.0 - 10.0	1	10
2	-243	17	1.0 - 10.0	5	10
2	-245	14	5.0 - 10.0	10	5
			1.0 - 5.0	5	5

Appendix-D, Tables D11-D28 summarizes all the results obtained for carbon-dioxide and hydrogen for different heated lengths. From these tables, the non-dimensional parameters are calculated for plotting the following set of plots

$$\left(\frac{B^*}{\Phi}\right)^{1/\eta_2} - 1 \text{ vs } Q_s^*$$

$$G_s^* \text{ vs } G_m^*$$

$$Q_s^* \text{ vs } Q_b^*$$

$$G_s^* \text{ vs } \Phi$$

$$R_s^* \text{ vs } \Phi$$

Figures 4.8 to 4.11 summarize the plots for the above non-dimensional parameters.

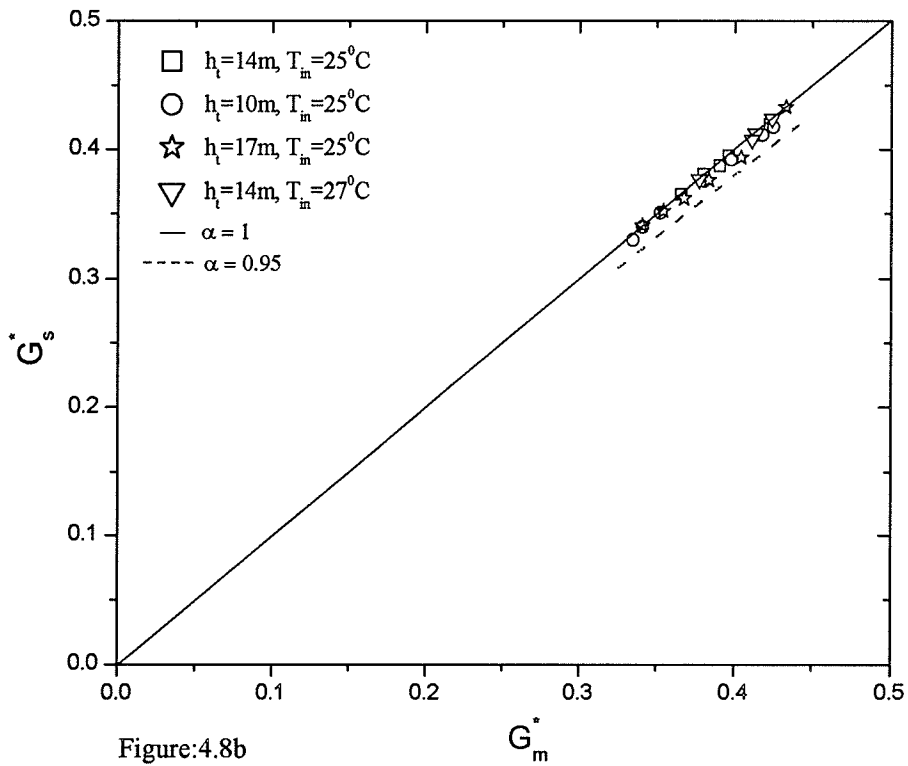
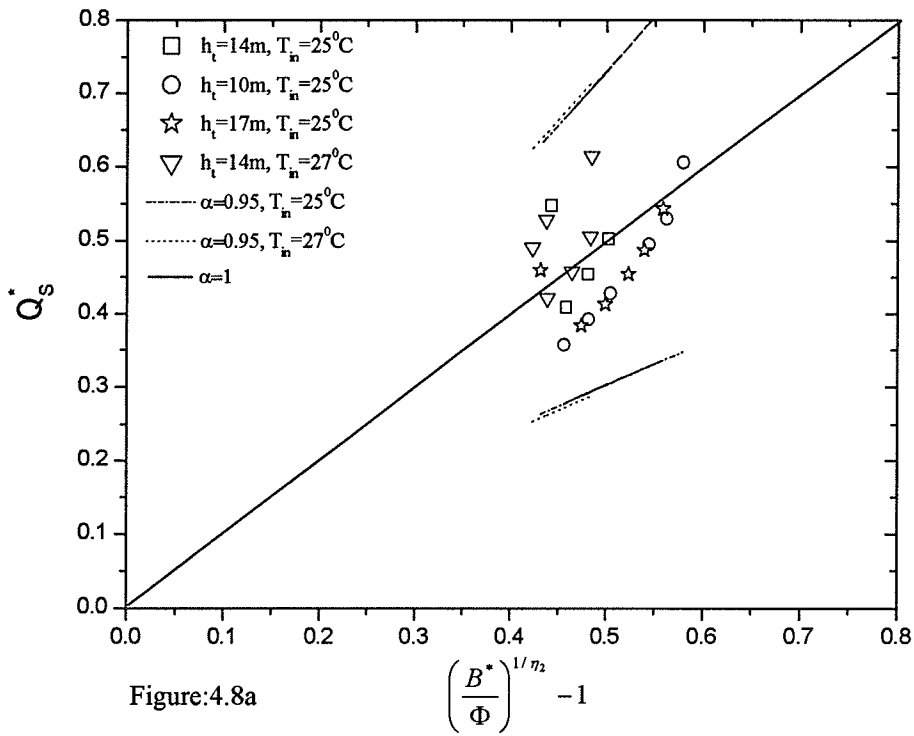


Figure 4.8: Carbon-Dioxide with Heated Length of 1 m

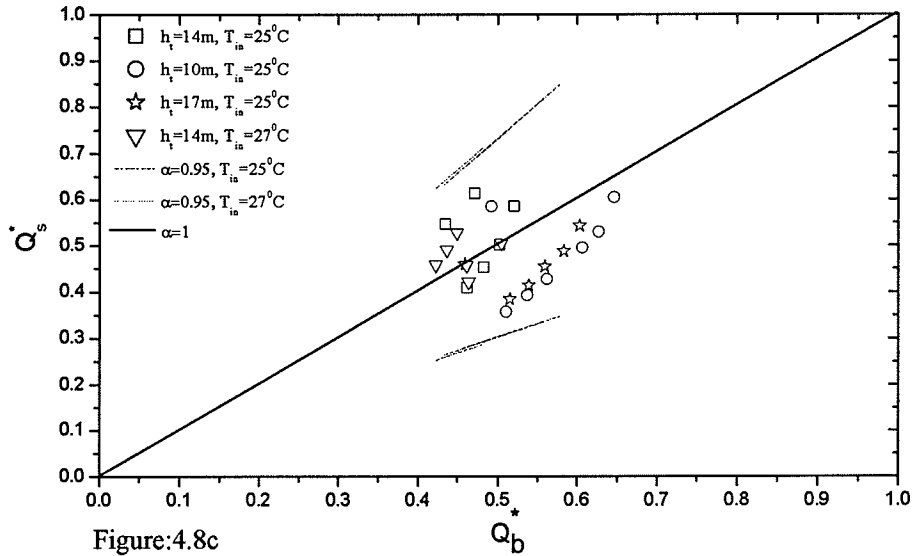


Figure:4.8c

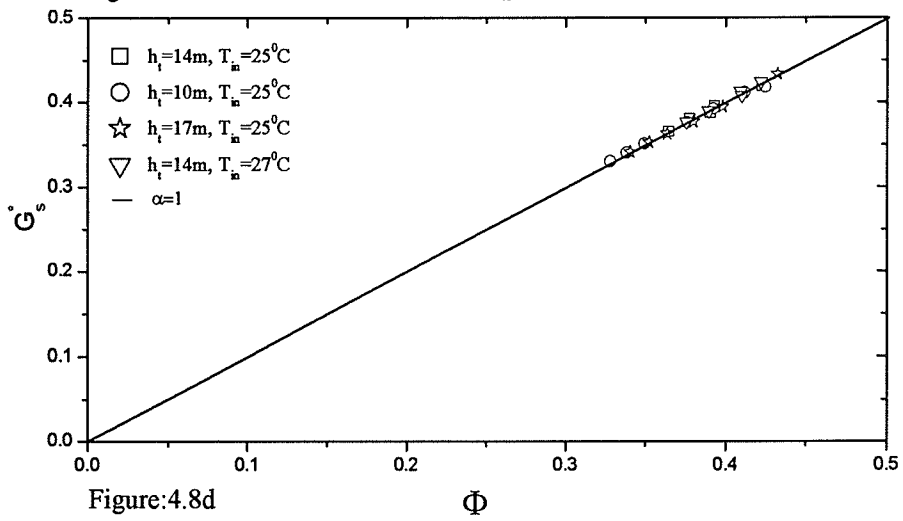


Figure:4.8d

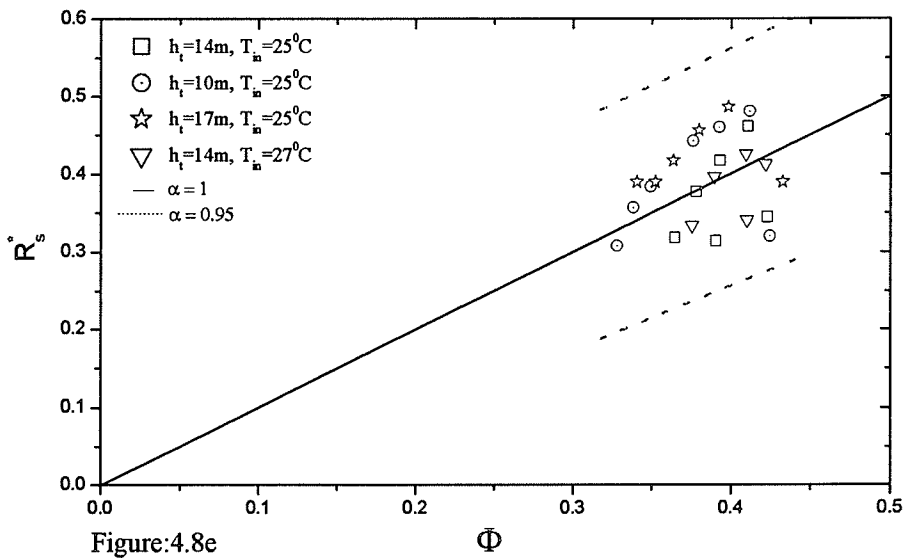


Figure:4.8e

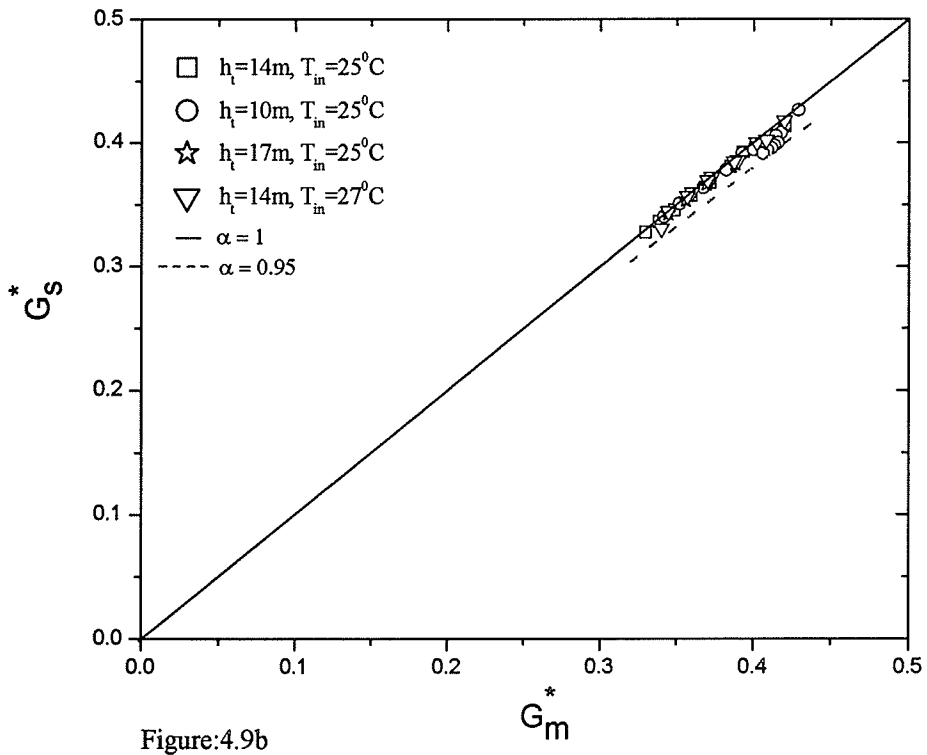
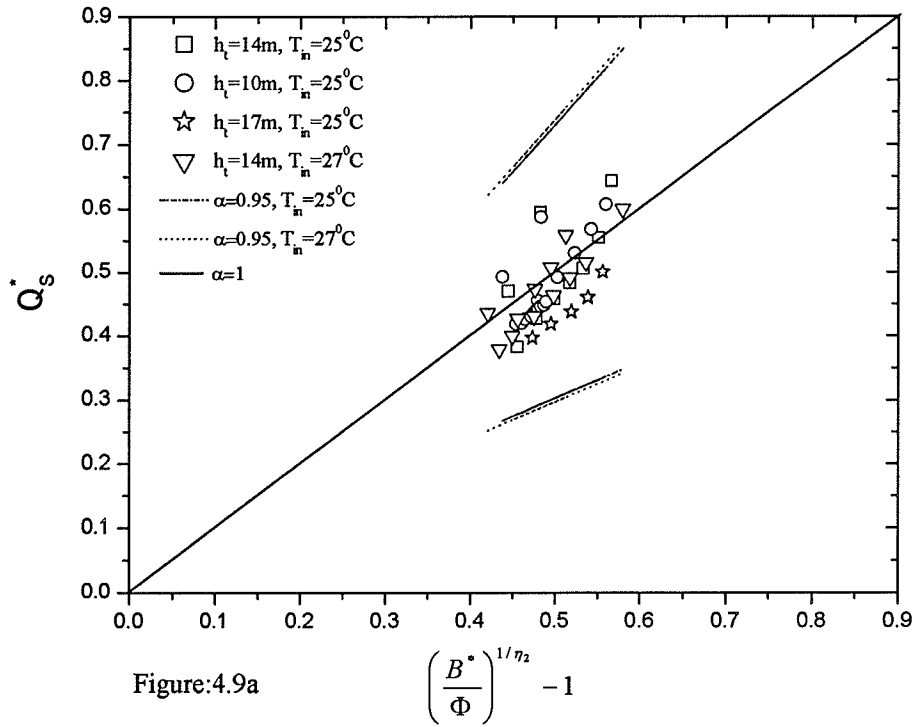
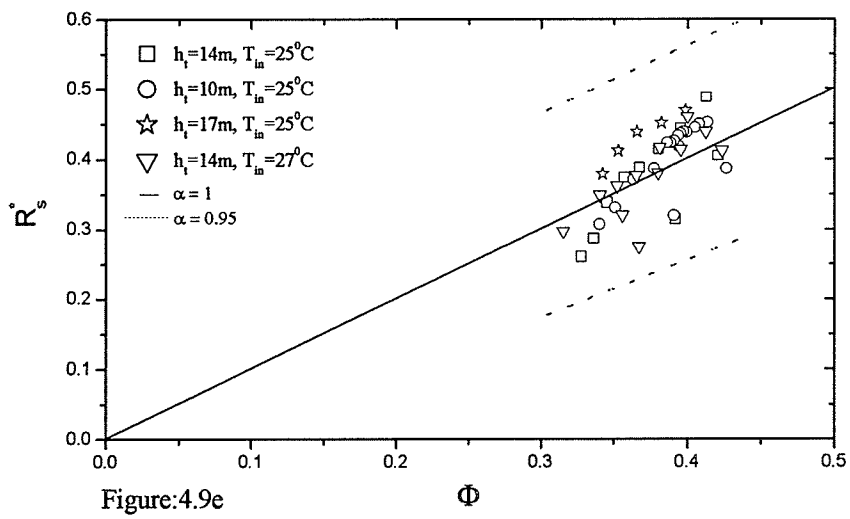
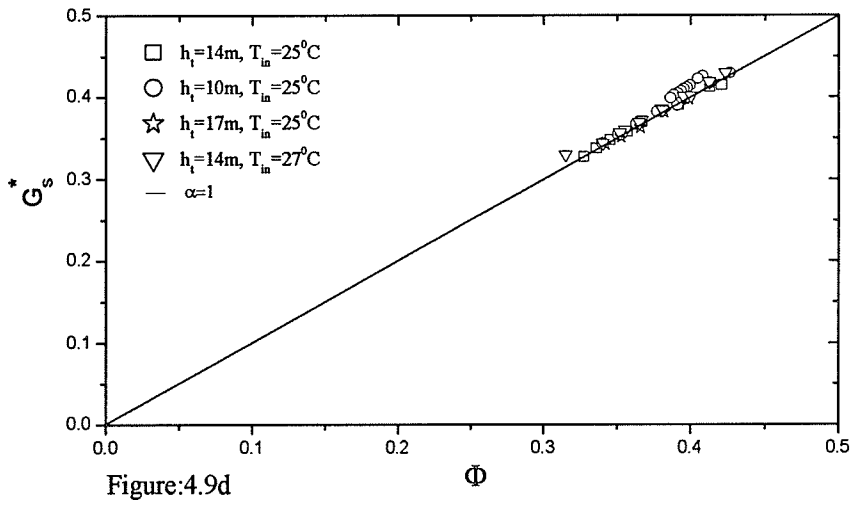
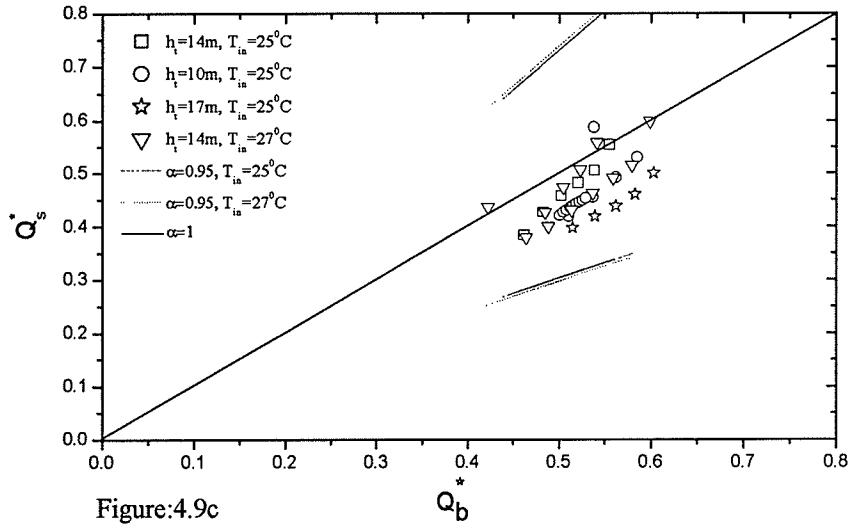


Figure 4.9: Carbon-Dioxide with Heated Length of 2 m



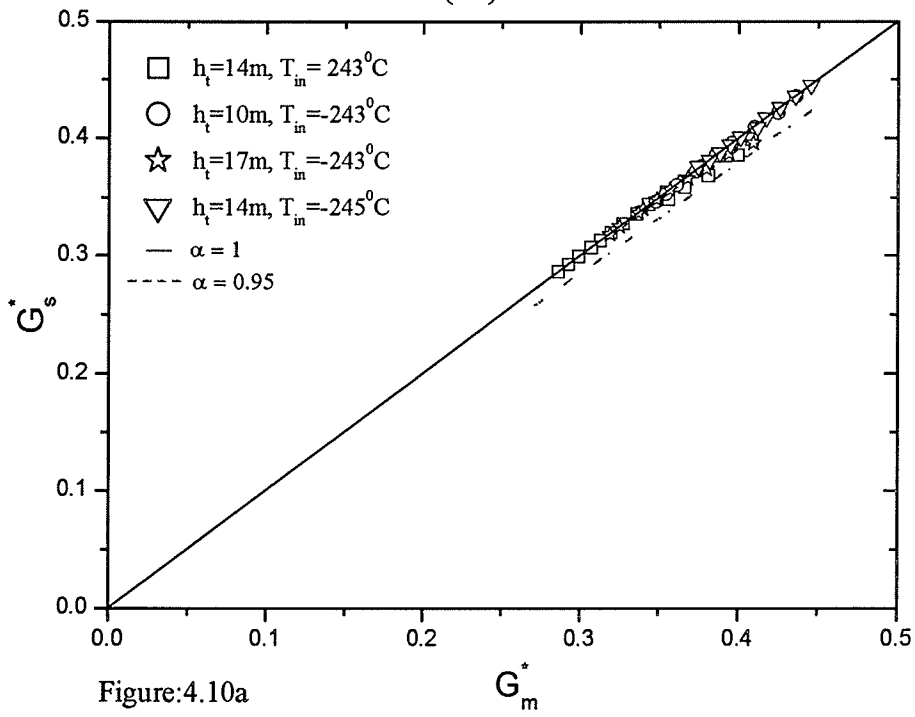
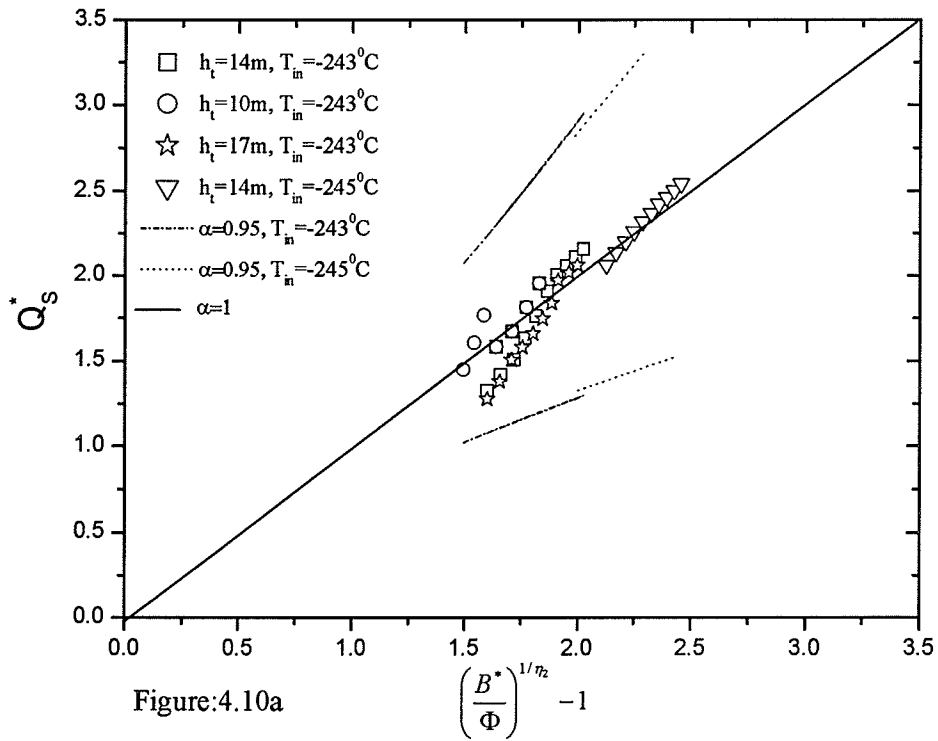
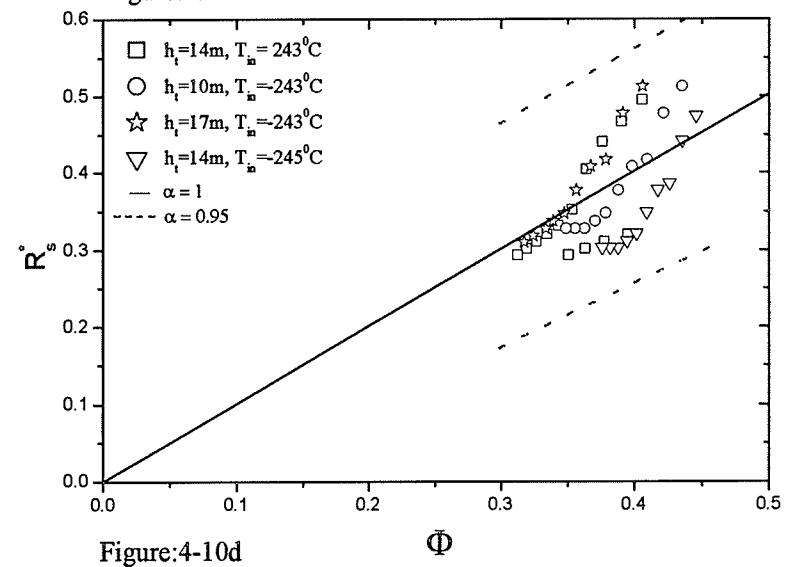
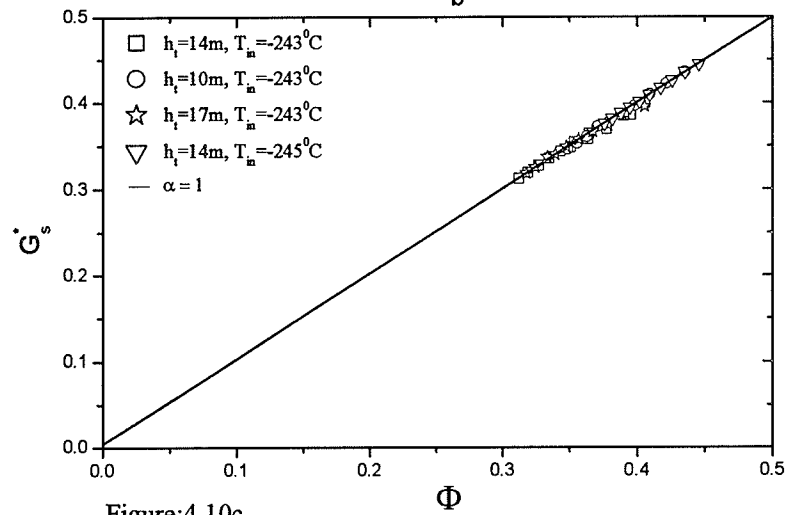
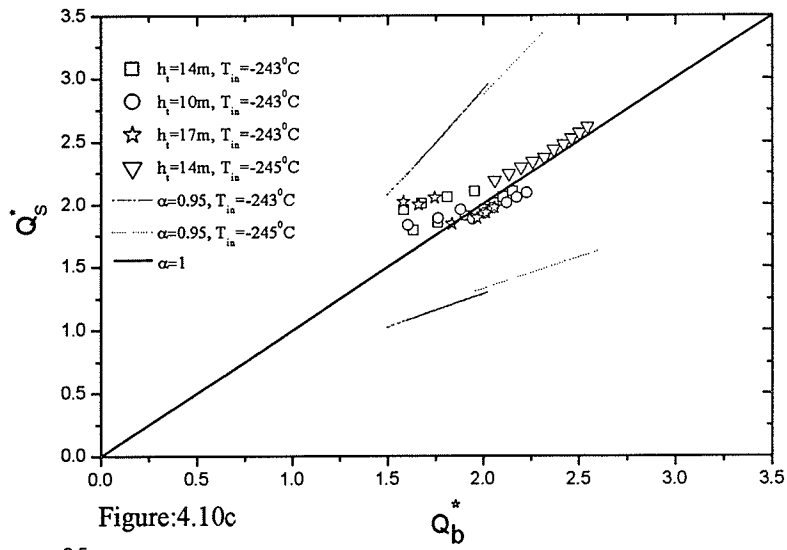


Figure 4.10: Hydrogen with Heated Length of 1 m



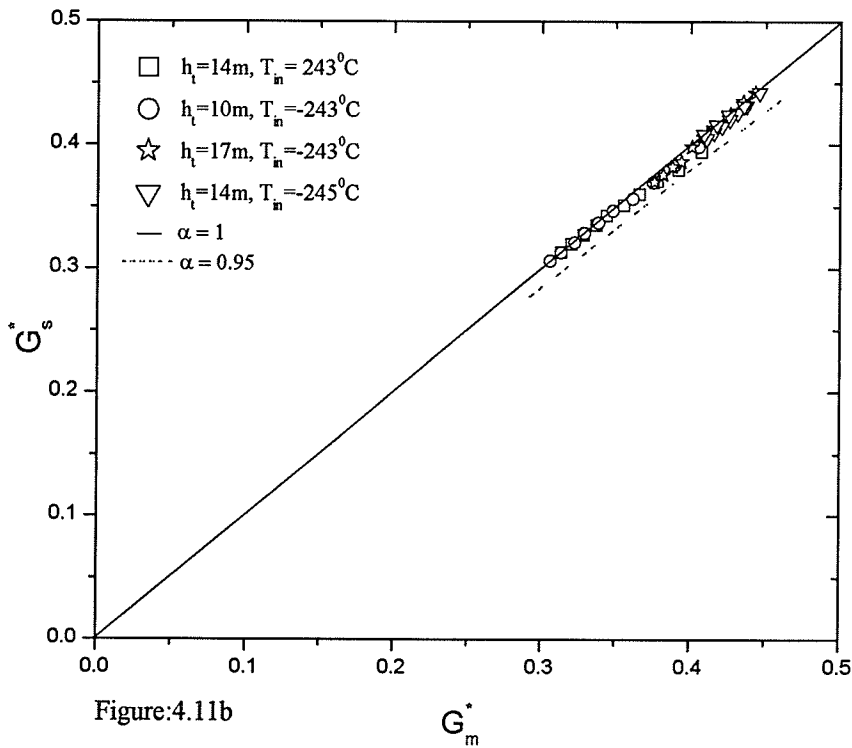
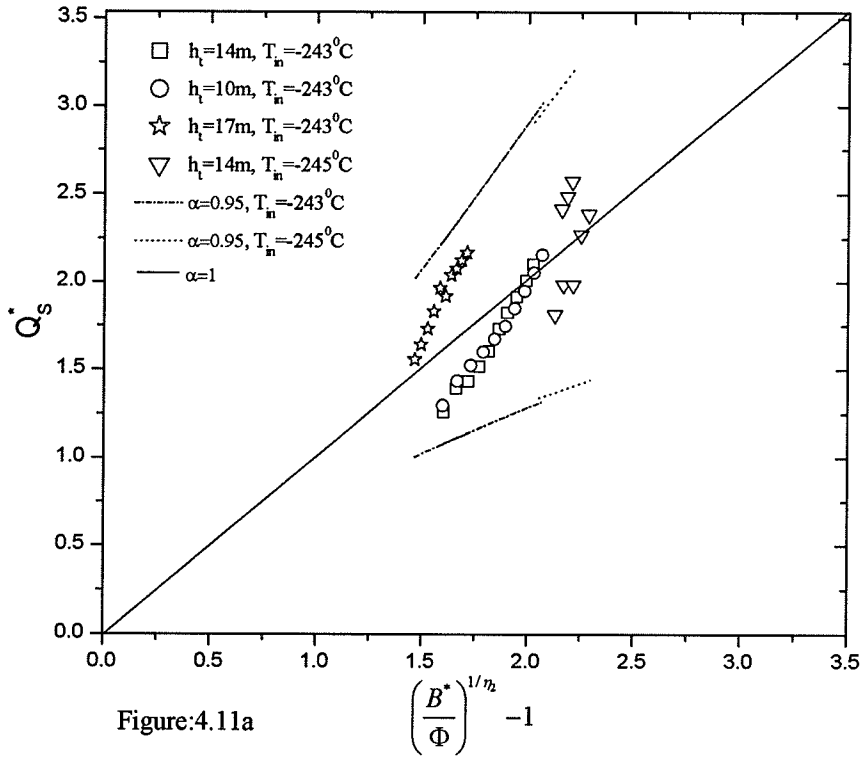
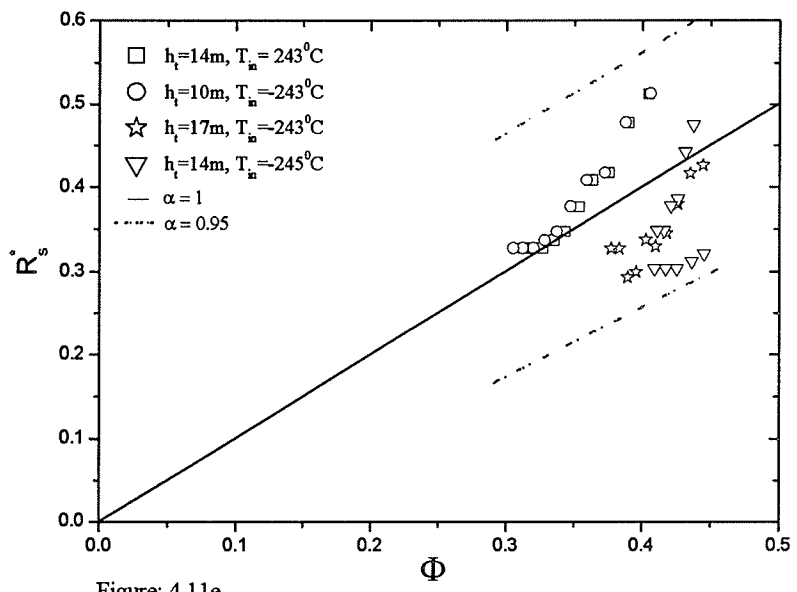
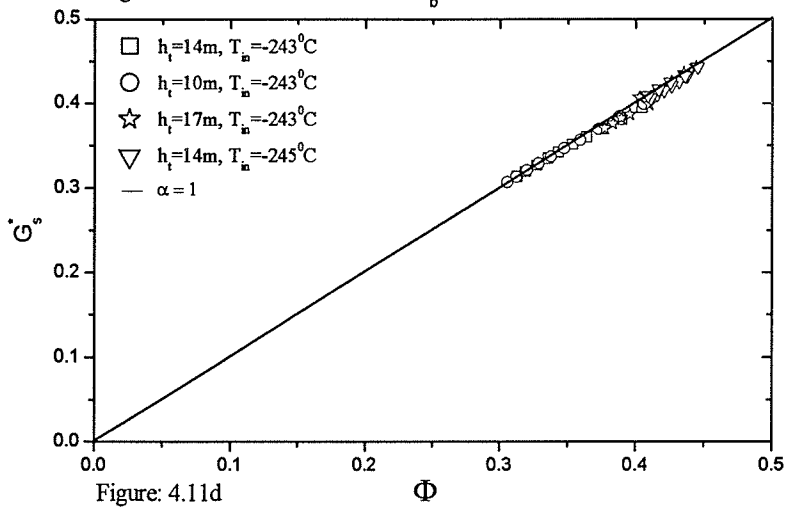
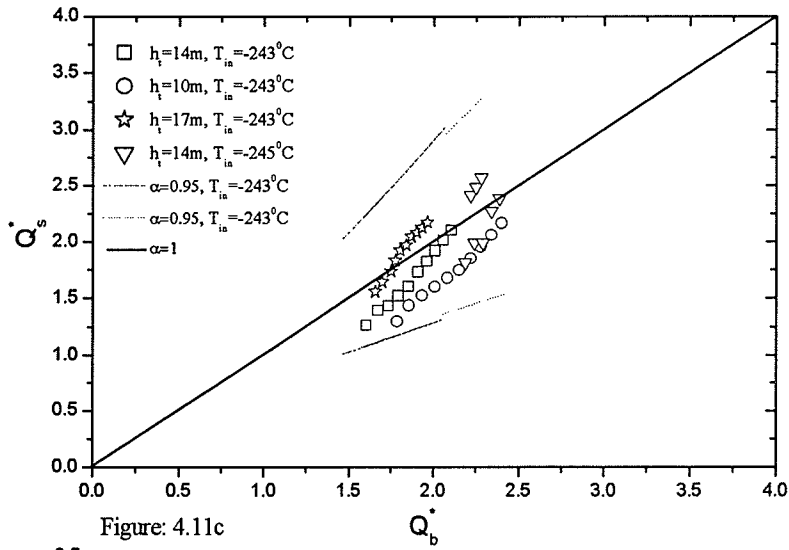


Figure 4.11: Hydrogen with Heated Length of 2 m



4.3.5 Discussion of Results for Carbon-dioxide and Hydrogen

Summary of tabulated results for numerical experiments conducted for carbon-dioxide and hydrogen are presented in Appendix D11-D26. From the tables the following can be inferred, as the inlet K-factor increases the system becomes stable and as the outlet K-factor increases the system destabilizes. The temperatures noted from the core section were above the critical temperatures. There is a decrease in time-period as the inlet K-factor increases, i.e. as the system becomes more stable. There is a decrease in boundary flow rate obtained from the SPORTS code as the inlet K-factor increases as inlet K-factor increases it restricts the flow resulting in the decrease in the flow rate. Figures 4.8 to 4.11 give the summary of all plots of the non-dimensional parameters 1 m and 2 m heated length carbon-dioxide and hydrogen respectively. As studied before each set of conditions are given separate legend.

Figure 4.8a, Figure 4.9a, Figure 4.10a and Figure 4.11a are the plots for $\left(\frac{B^*}{\Phi}\right)^{1/\eta_2} - 1$ vs Q_s^* between carbon-dioxide and hydrogen having different heated lengths. It is seen that all the points fall well within the dotted lines which is approximated with α percentage of the peak flow rate. Even though the data is centered on the theoretical line, there is a large scatter in Q_s^* . The reason for the large scattering in Q_s^* is that the almost insensitive variations of flow-rate with power near the peak of the flow-rate versus power steady-state profile. This can be attributed to the roundedness of the profile near the peak flow-rate.

Figure 4.8b, Figure 4.9b, Figure 4.10b and Figure 4.11b are the plots between G_s^* vs G_m^* . It is obvious that G_m^* is a very good approximation of G_s^* , the non-dimensional mass flux at the stability boundary. Hence it can be concluded that bounding flow rate could be easily approximated without doing the transient runs using SPORTS code.

The third set of plots Figure 4.8c, Figure 4.9c, Figure 4.10c and Figure 4.11c are for Q_s^* vs Q_b^* . From the plots, we could conclude that the trend continues that the points fall within the approximated lines validating the theory. Therefore, one could approximate the bounding power from the ninety five percent of the peak flow rate from steady-state analysis.

Figure 4.8d, Figure 4.9d, Figure 4.10d and Figure 4.11d plots for G_s^* vs Φ , in these plots it is noticed that points fall close to the straight line approximated from theory $\alpha = 1$. The plots look similar for the case of carbon-dioxide and hydrogen different heated lengths. This validates the theory.

Figure 4.8e, Figure 4.9e, Figure 4.10e and Figure 4.11e plots for R_s^* vs Φ , in these plots also similar trend is observed as previously observed. It is evident that the non-dimensional hot-side density at the stability boundary correlated well with Φ which is geometrical factor. It is encouraging to see that all the numerical data fall within the dotted lines.

Therefore, from the results obtained for different heated length of carbon-dioxide and hydrogen, it can be seen that the trend is similar to that of water. It can be concluded that the theory postulated for point source and sink single channel natural-circulation loop holds good for the distributed heated length. Also the bounding power could be approximated from the ninety five percent of peak power and

bounding flow rate could also be approximated. Hence the non-dimensional parameters are validated successfully using the SPORTS code. It is noticed that there is some scattering of points in the plots for all three fluids. This could be explained below

- According to the theory, the bounding power is approximated as the peak power obtained from the steady-state profile. But in some cases steady-state profile appears to be more rounded. This can also be interpreted as there is small amount of variation in flow rate with large margin of power variation. This makes the bounding power lie scattered over the peak. Thus making the results look more scattered. This could be one of the reasons for the scatter seen in the plots.
- The other vital reason for this scatter could be attributed to the presence of two or more modes of instability. However this is not yet been corroborated and further study is under review.

4.3.6 Summary from all the Results

In this numerical study conducted for water, carbon-dioxide and hydrogen using SPORTS code, results were obtained and various non-dimensional parameters were plotted for their validity. The non-dimensional plots show similar trend for different heated lengths and different fluids having different heated lengths. From the results it could be noticed that the points lie between the ninety five percent approximation lines and the theoretical line which is a good approximation for these non-dimensional parameters.

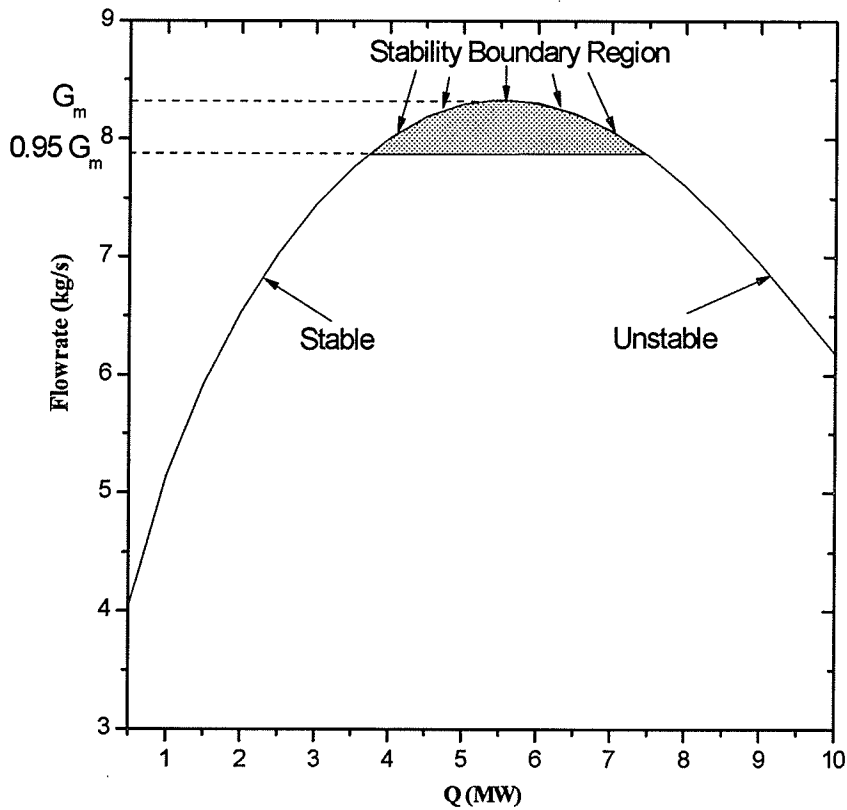


Figure 4.12: Steady-State Profile Showing Different Regions

Figure 4.12 summarizes the entire study in one plot. From this study it can be concluded that the stability boundary region lies within the peak and 0.95 of the peak G_m . The stable points lie to the positive slope or the left hand side of the profile and unstable points lie on the negative slope of the steady-state profile or the right hand side. From this study it can also be concluded that the non-dimensional parameters which are formulated for single channel point heated systems are valid for single channel distributed heated systems.

CHAPTER 5

Conclusions and Recommendations

5.1 Conclusions

In this study 230 numerical experiments were performed to better understand the non-dimensional parameters defining the flow stability boundary in natural-convection loops. This is done for a range of inlet and outlet K-factors, various inlet temperatures, heated lengths and vertical loop heights. The following conclusions can be drawn from this study:

- According to the theory the boundary flow rate could be approximated and boundary power could be approximated from steady-state analysis without transient analysis. G_m^* is a very good approximation of G_s^* . The accuracy is 95%.
- The non-dimensional parameters formulated are good approximation as the plots shows that the points lie within the lines approximated from the theory for $\alpha = 1$ and $\alpha = 0.95$
- Q_s^* can be approximated by Q_b^* which can also be approximated by
$$\left(\frac{B^*}{\Phi}\right)^{1/\eta_2} - 1.$$
- G_s^* is well approximated by the geometric parameter Φ , with an accuracy of 95%.
- R_s^* is also well approximated by Φ , with an accuracy of about 95%.

- The non-dimensional parameters are significant in designing the nuclear reactor's primary cooling system. This study helps in approximating the boundary flow rate and power and avoids instability.
- SPORTS code initially run for water was modified to run for different fluids of interest. In this study fluids like water, carbon-dioxide and hydrogen are studied
- In some plots there is some scattering of points around the $\alpha = 1$ line which could be explained as
 - In some cases, the shape of steady-state profile obtained is more round at the peak and this makes peak power scatters in this region.
 - There might be two or modes of instability. On this topic, further study is needed.
- Fluids that have extreme supercritical conditions are hard to conduct experimental studies and could be simulated easily with the help of the SPORTS code. The prediction of the stability boundary power without conducting experiment.
- The non-dimensional parameters originally formulated for a point heat source and sink situation, appear to be valid for a supercritical natural-convection flow system with distributed heating and cooling.
- The non-dimensional parameters validated are first of its kind in stability studies in supercritical flows and hence plays a very vital role in design of primary cooling systems of a future nuclear reactors.

- For a nuclear reactor, operating at the higher supercritical conditions can lead to improved thermodynamic efficiency of the plant. Hence this study helps in designing a safe primary cooling systems for nuclear reactors.

5.2 Recommendations

From this study many new points have been observed and yet lots to be still studied.

The following are the list of places where further studies should carried out.

- Studies on the validation of the non-dimensional parameters could be extended using a linear method.
- Results should be validated using experimental study.
- Study should be extended to parallel channels, which are also of significant importance to nuclear reactors.
- This study three particular fluids were concentrated, other fluids that are of particular interest should be considered in future studies.
- There might be several trends or more modes of instability from the presented results, hence further study analyses should be conducted thoroughly.
- Supercritical Helium is also considered as coolant in nuclear reactors due to its significant properties like the high specific heat and also it can also work at low pressure, with significant safety advantage.

References

1. Mertol A., Grief R, "A review of natural-circulation loops," Natural-Convection: Fundamentals and Applications.
2. Zvirin Y., "A review of natural-circulation loops in pressurized water reactors and other systems," Nuclear Engineering and Design, Vol 67, 1981, p 203-225.
3. Becker K.M., Jahnberg S., Haga and Mathison R.P. "Hydrodynamic instability and dynamic burnout in natural-circulation two-phase flow, an experimental and theoretical study," AE 1964.
4. Boure J.A., Bergles T, "Review of two-phase flow stability," Nuclear Engineering and Design, Vol 25, 1973, p 165-192.
5. Krishnan V., "Non-linear density-wave flow oscillations in subcritical and supercritical heat exchanger systems," Masters Thesis 1971, Department of Chemical Engineering, The University of Rochester.
6. Yadigaroglu G., Bergles A.F., "Fundamental and higher mode density wave oscillation in two-phase flow: the importance of the single-phase region," Journal of Heat Transfer, Vol 94. 1972, p 189-195.
7. Nayak A.K., Vijayan P.K., Saha D., "Analytical modeling and study of the stability characteristics of the advanced heavy water reactor," Bhabha atomic research centre, BARC/2000/E/011.
8. Crowley J.D., Deane C. and Gouse S.W., "Two-phase flow oscillation in vertical, parallel heated channels," EURATOM Report, Proceedings Symposium on two-phase flow dynamics, Eindhoven, 1967, 1131.

9. Yjiang Y., Shoji M., "Flow stability in a natural-circulation loop: Influences of wall thermal conductivity," Nuclear Engineering and Design, Vol 202, 2003, p 16-28.
10. Anderson R.P., Bryant L.T., Carter J.C., Marchatterree J.F., "Transient analysis of two-phase natural-circulation systems," Argonne national laboratory 1962.
11. Wallis C.G. and Heasley J.H., "Oscillations in two-phase flow system," Transactions, ASME, 83, 1961, p 363-369.
12. Collins D.B. and Gacesa M., "Hydrodynamic instability in a full-scale simulated reactor channel," Proceedings Instn. Mechanical Engineers, 1969.
13. Mertol A., Greif R., Zvirin Y., "Two dimensional analysis of transient flow and heat transfer in a natural-circulation loop," Warme Und Stoffubertragung, Vol 18, 1984, p 89-98.
14. Greif R., "Natural-circulation loops," Journal of Heat Transfer, Vol 110, 1988, p 1243-1258.
15. Crevling H.F, De Paz J.F, Baladi J.Y, Schoenhals R.J., " Stability characteristics of a single-phase free convection loop," Journal of fluid Mechanics, Vol 67, 1975, p 65-84.
16. <http://www.echoscaninc.com/product.cgi?code=U1VSLTAwMQ> viewed on June 24, 2004.
17. Zvirin Y., "On the behavior of a natural-circulation loop with a through flow," 14th Intersociety Energy Conversion Engineering Conference, Boston, Masschusettes, 1979, p 1974-1978.

18. Zvirin Y., "The effects of a throughflow on the steady state and stability of a natural-circulation loop," 19th National heat transfer conference, Orlando, Florida.1980.
19. Zvirin Y. and Rabunoviz Y, "On the behavior of natural-circulation loops with parallel channels," 7th International Heat Transfer Conference, Munich, Federal Republic Germany, Vol 2, 1982, p 299-304.
20. Ishii M., Kataoka I., "Scaling laws for thermal hydraulic system under single-phase and two-phase natural-circulation," Nuclear Engineering and Design, Vol 81, 1984, p 411-425.
21. Krishnan V.S. and Gulshani P., "Stability of natural-circulation flow in a CANDU Type fuel channel," Nuclear Engineering and Design, Vol 99, 1987, p 403-412.
22. Huang, Zelaya, "Heat transfer behavior of rectangular thermosyphon loop," ASME Journal of Heat Transfer, 1987.
23. Auria F.D., Galasi G.M., Vigni P., Calastri A. "Scaling of natural-circulation in PWR systems," Nuclear Engineering and Design, Vol 132, 1991, p 187-205.
24. David, Van Bragt and Tim Vander hagen, , "Stability of natural-circulation boiling water reactors:partii parametric study of coupled neutronic thermohydraulic stability," Nuclear Technology, Vol 121, 1998, p 40-51.
25. David, Van Bragt and Tim Vander hagen., "Stability of natural-circulation boiling water reactors: part II parametric study of coupled neutronic thermohydraulic stability," Vol 121, 1998, p 52-62.

26. Nayak A.K., Vijayan P.K., Saha D., Venkat Raj V and Aritomi M., "Study on the stability behavior of a natural-circulation pressure tube type boiling water reactor," Nuclear Engineering and Design, Vol 215, 2002, p 127-137.
27. Dimmick G.R., Chatoorgoon V., Khartabil H.F., Duffey R.B., "Natural convection studies for advanced CANDU reactor concepts," Nuclear Engineering and Design, Vol 215, 2002, p 27-38.
28. Jain K.C., Petric M., Miller D and Bankoff S.G., "Self sustained hydrodynamic oscillations in a natural-circulation boiling water loop," Nuclear Engineering and Design, Vol 4 ,1966, p 233-252.
29. Mathisen, R.P "Out of pile instability in the loop skalvan," Symposium on two-phase flow dynamics , EURATON 1, 1967, p 19-64.
30. Veziroglu T., Lee Sameul S., "Boiling flow instabilities in a cross connected parallel channel upflow system," ASME 71-HT-12, 1971.
31. Matsui G., "An experimental study of flow instability in boiling channel systems," Heat transfer-Japanese Research, Vol 1, 1972, p 46-52.
32. Chexal V.K. and Bergles A.E, "Two-phase instabilities in a low pressure natural-circulation loop," AIChE Symposium Series, 1972, p 37-45.
33. Aritomi, Aoki, Inoue, "Instabilities in parallel channel of forced convection boiling upflow system," Journal of Nuclear Science and Technology, Vol 4, 1977, p 88-96.
34. Fukuda and Kobori "Classification of two-phase flow stability by density wave oscillation model," Journal of Nuclear Science and Technology, Vol 16, 1979, p 95-103.

35. Cumo M., Palazzi G., Rinaldi L., "An experimental study on two-phase flow instability in parallel channels with different heat flux profile," CNEN-RT/ING, 1981.
36. Hsu Juiei Tsuen, Ishii Mamoru "Experimental study in two-phase natural-circulation and flow termination in a loop," NUREG/CR 4682, ANL 86-32, 1986.
37. Lee Sang Yong, Ishii Mamoru "Characteristics of two-phase natural-circulation in FREON-113 Boiling loop," Nuclear Engineering and Design Vol 121, 1990, p 69-81.
38. Aritomi Masanori, Chiang Jing Hsien, Nakahashi Tohru "Fundamental study on thermo hydraulics during start up in natural-circulation boiling water reactors," Journal of Nuclear Science and Technology, Vol 29, 1992, p 631-641.
39. Kyung Ick Soo, Lee Sang Yong "Experimental observations on flow characteristics in an open two-phase natural-circulation loop," Nuclear engineering and Design, Vol 159, 1994, p 163-176.
40. Jiang S.Y., Yao M.S., Bo J.H., Wu S.R., "Experimental simulation study on start up of the 5MW nuclear heating sector," Nuclear Engineering and Design, Vol 158, 1996, p 111-123.
41. Inada F., Furuya M., Yasuo A., Tabata H., Yoshioka Y., and Kim H.T. "Thermo hydraulic instability of natural-circulation BWR at low pressure start up; Experimental estimation of instability region with test facility considering

- scaling law,” 3rd International Conference Nuclear Engineering, 1995, p 173-178.
42. Creveling H.F., De J.F. “Stability characteristics of a single-phase free convection loop,” *Journal of Fluid Mechanics*, Vol 67, 1975, p 65-85.
 43. Jeuck P., Lennert L., King R.L. “Single-phase natural-circulation experiments on small break accident heat removal,” Report, NP 2006, 1981.
 44. Hallinan K.P., Viskanta R. “Dynamics of a natural-circulation loop: analysis and experiments,” *Heat Transfer Engineering*, Vol 7, 1986, p 45-51.
 45. Misale M., Tagliafico L., “The transient and stability behavior of single-phase natural-circulation loops,” *Heat and Technology*, Vol 5, 1987, p 101-113.
 46. Acosta E., Msen, Ramos E., “Single-phase natural-circulation in a tilted square loop,” *Thermo and Fluid Dynamics*, Vol 21, 2987, p 269-275.
 47. Vijayan P.K and Date A.W., “The limits of conditional stability for single-phase natural-circulation with throughflow in a figure of eight loop,” *Nuclear Engineering and Design*, Vol 136, 1991, p 361-380.
 48. Doster Michael, Kendal Peter K, “Stability of one dimensional natural-circulation flows,” *Nuclear Science and Engineering*, Vol 132, 1999, p 105-117.
 49. Vijayan P.K., “Experimental observations on the general trends of the steady state and stability behavior of single-phase natural-circulation loops,” *Nuclear Engineering and Design*, Vol 215, 2002, p 139-152.
 50. Ishii, M., Zuber, N., “Thermally induced flow instabilities in two-phase mixtures,” 4th International Conference, Paris, 1970.

51. Saha, Ishii, Zuber, "An experimental investigation of the thermally induced flow oscillations in two-phase systems", ASME, 1976.
52. Nakanishi S., "Recent Japanese research on two-phase flow instabilities," Japan-US seminar on two-phase flow dynamics lecture series, 1979, p 311-351.
53. Podowski M.Z., Lahey R.T., Clause A. "Modeling and analysis of channel to channel instabilities in a boiling systems," Chemical engineering commerce, Vol 93, 1990, p 75-92.
54. Rizwan-Uddin, Dorning J.J., "Chaotic dynamics of a triply forced two-phase flow system," Nuclear Science and Engineering, Vol 105, 1990, p 123-135.
55. Wang Fu-Shin, Hu Lin-Wen, Pan Chin, "Thermal and stability analysis of a two-phase natural-circulation loop," Nuclear Science and Engineering, Vol 117, 1994, p 33-46.
56. Gross R.J., See F.T., "A contribution to thermal hydraulic stability analysis," ASME, 73-WA/HT-23, 1973.
57. Sumida, Kawai, "Theory of hydraulic stability of boiling channels," Journal of Nuclear Science and Technology, Vol 15, 1978, p 323-337.
58. Park G.C., Podowski M., Becker M., Lahey R.T, "The modeling of density wave oscillations in boiling water nuclear reactors," Rensseler polytechnic institute, USA, 1984.
59. Lahey R.T., "Advances in the analytical modeling of linear and nonlinear density wave instability modes," Nuclear Engineering and Design, Vol 95, 1986, p 5 -34.

60. Furutera, "Validity of homogeneous flow model for instability analysis," Nuclear Engineering and Design, Vol 95, 1986, p 65-77.
61. Auria, Sanctis, Marco, Lahey, Podowaski, "A linear model to study fluid dynamic instabilities in boiling channels due to density oscillations," Heat and Technology, Vol 5, 1987.
62. Di Marco P., Clause A., Lahey R.T, Drew D.A., "A nodal analysis of instabilities in boiling channels," Heat and Technology, Vol 8 , 1990.
63. Lee Sang Yong and Lee Dong Won, "Linear analysis of flow instabilities in an open two-phase natural-circulation loop," Nuclear Engineering and Design, Vol 128, 1991, p 317-330.
64. Hashimoto K., "Linear Nodal analysis of out of phase instability in boiling water reactor cores," Annals of Nuclear Energy, Vol 12, 1993, p 789-797.
65. Ambrosini W and Marco Ferreri, "Linear and nonlinear analysis of density wave instability phenomena," Heat and Technology, Vol 18, 2000, p 27-36.
66. Zboray R, Wilhelmus, Vanderahegen, HugoVandam, "Investigating the stability characteristics of natural-circulation boiling water reactors using root loci of a reduced order model," Nuclear technology, Vol 136, 2001, p 301-314.
67. Dijkman F.J.M., Slutter M.L.C., "One channel non-linear digital model for boiling water hydrodynamics," Nuclear Engineering and Design, Vol 16, 1971, p 237-248.

68. Gurugenci, Veziroglu, Kakac, "Simplified non-linear descriptions of two-phase flow instabilities in vertical boiling channel," *International Journal of Heat and Mass Transfer*, Vol 26, 671-679, 1983.
69. Chatoorgoon V., "SPORTS-A simple non-linear thermalhydraulic stability code," *Nuclear Engineering and Design*, Vol 93, 1986, p 51-67.
70. Dimarco P., Clause A., Lahey R.T., "An analysis of nonlinear instabilities in boiling systems," *Dynamics and Stability of Systems*, Vol 6, 1991.71.
71. Rizwan-Uddin, Dorning, "Nonlinear dynamics of two-phase flow in multiple parallel heated channels," *Two-phase Flow and Heat Transfer*, Vol 197, 1992, p 63-72.
72. Nigmatulin, Melikhov, Blinkov, Gakal, "The numerical analysis of boiling flow instability in parallel heated channels," *Nuclear Engineering and Design*, Vol 139, 1993, p 235-243.
73. Lin Y.N., Pan C., "Nonlinear analysis for a natural-circulation boiling channel," *Nuclear Engineering and Design*, Vol 152, 1994, p 349-360.
74. Harden D.G. and Boggs J.H., "Transient flow characteristics of a natural-circulation loop oriented om the critical region, *Proceedings of the 1964 Heat Transfer and Fluid Mechanics Institute*, Stanford University Press, 1964, p 38-50.
75. Walker B.J and Harder D.G., "The "Density Effect" model: prediction and verification of the flow oscillation threshold in a natural-circulation loop operating neat the critical point, *ASME Paper No. 64-WA/HT-23*, 1964.

76. Walker B.J and Harder D.G., "Heat driven pressure and flow transients in the supercritical thermodynamic region," ASME Paper No. 67-WA/HT-23, 1967.
77. Cornelius A.J and Parker J.D., "Heat transfer instabilities near the thermodynamic critical point," Proceedings of the 1965 Heat Transfer and Fluid Mechanics Institute, Stanford University Press, p 38-50, 1964.
78. Loperski S and Cho D, "Stability of a natural circulation loop with a fluid heated through the thermodynamic pseudocritical point," Proceedings of ICAPP'
79. Chatoorgoon V. "Stability of supercritical fluid flow in a single channel natural -circulation loop," International Journal of Heat and Mass Transfer, Vol 44, 2001, p 1963-1972.
80. Chatoorgoon V. and Leung L.W., "SPORTS user's guide," 1988, AECL, Thermalhydraulics Development Branch.
81. Lemmon E.W., Mc Linden M.O. and Huber M.L., "Reference fluid thermodynamic and transport properties-NIST Standard reference database 23, Version-7, 2002.
82. Chatoorgoon V, Voodi A, Fraser D., "The stability boundary for supercritical flow in natural convection loops Part I: Water studies," International Journal of Heat and Mass Transfer- to be published.
83. Chatoorgoon V, Voodi A, Preshit U., "The stability boundary for supercritical flow in natural convection loops Part II- carbon-dioxide and hydrogen studies" International Journal of Heat and Mass Transfer- to be published.

APPENDIX - A

A.1 SPORTS MAKE FILE FOR UNIX-VERSION

```
# sports.mak 2003-10-21
#-----#
# Make file to create sports.exe on Sun Unix (Solaris)
# Usage: % make -f sports.mak
#
# V2: Dependence on INCLUDED files is accounted for.
#   Separate compile rules for each file allows
#   use of separate compile options for each file if needed.
#
#-----#
# set up some variables needed later
#
FCFLAGS = -C -g -xtypemap=real:64,double:64,integer:64
#
#-----#
# List of object files to be linked
OBJECTS = sports.o \
arco.o \
assign6.o \
banner.o \
c2ji1.o \
chfpowr.o \
convhin.o \
CORE_ANC.o \
CORE_BWR.o \
CORE_CPP.o \
CORE_DE.o \
CORE_ECS.o \
CORE_FEQ.o \
CORE_MLT.o \
CORE_PH0.o \
CORE_STN.o \
FLASH2.o \
FLSH_SUB.o \
IDEALGAS.o \
MIX_HMX.o \
PROP_SUB.o \
REALGAS.o \
SAT_SUB.o \
SETUP.o \
SETUP2.o \
TRNS_ECS.o \
TRNS_TCX.o \
TRNS_VIS.o \
```

TRNSP.o \
UTILITY.o \
curve.o \
diametr.o \
dimmsc.o \
doloop.o \
fho.o \
flheat.o \
frctn.o \
fueltmp.o \
funio.o \
funxe.o \
g.o \
getall.o \
htcoefb.o \
htcoefc.o \
initcm.o \
input.o \
nkinit.o \
osv.o \
owtput.o \
pexchek.o \
phisq.o \
pmpcor.o \
pmphed.o \
pmpomg.o \
pmpthf.o \
powcorr.o \
poweqn.o \
reatb1.o \
reatb2.o \
reatb3.o \
reatio.o \
reativ.o \
reatxe.o \
rfalsi.o \
rhochek.o \
rhochekm.o \
rholoop.o \
rshos2.o \
savall.o \
slip.o \
solve.o \
steqn1.o \
stph3.o \
stphl.o \

```

stphnt.o \
stphrd.o \
stphsd.o \
stphsdd.o \
stphsh.o \
stphst.o \
stphv.o \
stphx.o \
stphy.o \
stphzz.o \
stphzzh.o \
stprop.o \
szsc.o \
treqn1.o \
treqn2.o \
velest.o \
vjsc.o \
wlheat.o \
ylhos.o \
#-----#
# Rules for making an executable.
# No optimization flags used.
#
sports.exe:    $(OBJECTS)
               f77 -g -C $(OBJECTS) -o sports.exe

#-----#
# Rule for creating all the object files from their dependent fortran files.

SPORTS_INCLUDES = array1.inc array2.inc constnt.inc curnode.inc\
                  delkix.inc dimension.inc factlim.inc flag.inc\
                  fueldat.inc neutkin.inc neutkn2.inc options.inc\
                  optpch.inc param1.inc parampch.inc parchl1.inc\
                  parchl2.inc pltpch.inc pltvar.inc pmpcnst.inc\
                  pmpdat.inc pmpval.inc resinf.inc rpltpch.inc\
                  rpltvar.inc rshos2c.inc slvcom.inc tinp.inc\
                  xenplt.inc ylabels.inc zstphm.inc
#
sports.o:      sports.F ${SPORTS_INCLUDES}
               f77 ${FCFLAGS} -c sports.F -o sports.o

ARCO_INCLUDES = array1.inc array2.inc constnt.inc factlim.inc flag.inc\
                options.inc param1.inc parampch.inc
#
arco.o:       arco.F ${ARCO_INCLUDES}
               f77 ${FCFLAGS} -c arco.F -o arco.o

```

```

ASSIGN6_INCLUDES = delkix.inc flag.inc options.inc optpch.inc\
    param1.inc parampch.inc pltpch.inc pltvar.inc\
    rpltpch.inc rpltvar.inc slvcom.inc xenplt.inc ylabels.inc
#
assign6.o:    assign6.F ${ASSIGN6_INCLUDES}
              f77 ${FCFLAGS} -c assign6.F -o assign6.o

BANNER_INCLUDES = param1.inc flag.inc
#
banner.o:    banner.F ${BANNER_INCLUDES}
            f77 ${FCFLAGS} -c banner.F -o banner.o

C2JI1_INCLUDES = array1.inc array2.inc constnt.inc flag.inc\
    neutkin.inc param1.inc parampch.inc
#
c2ji1.o:    c2ji1.F ${C2JI1_INCLUDES}
            f77 ${FCFLAGS} -c c2ji1.F -o c2ji1.o

CHFPOWR_INCLUDES = array1.inc array2.inc constnt.inc param1.inc\
    parampch.inc zstphs.inc
#
chfpowr.o:  chfpowr.F ${CHFPOWR_INCLUDES}
            f77 ${FCFLAGS} -c chfpowr.F -o chfpowr.o

CORE_ANC.o:  CORE_ANC.F
            f77 ${FCFLAGS} -c CORE_ANC.F -o CORE_ANC.o

CORE_BWR.o:  CORE_BWR.F
            f77 ${FCFLAGS} -c CORE_BWR.F -o CORE_BWR.o

CORE_CPP.o:  CORE_CPP.F
            f77 ${FCFLAGS} -c CORE_CPP.F -o CORE_CPP.o

CORE_DE.o:  CORE_DE.F
            f77 ${FCFLAGS} -c CORE_DE.F -o CORE_DE.o

CORE_ECS.o:  CORE_ECS.F
            f77 ${FCFLAGS} -c CORE_ECS.F -o CORE_ECS.o

CORE_FEQ.o:  CORE_FEQ.F
            f77 ${FCFLAGS} -c CORE_FEQ.F -o CORE_FEQ.o

CORE_MLT.o:  CORE_MLT.F
            f77 ${FCFLAGS} -c CORE_MLT.F -o CORE_MLT.o

```

CORE_PH0.o: CORE_PH0.F
f77 \${FCFLAGS} -c CORE_PH0.F -o CORE_PH0.o

CORE_STN.o: CORE_STN.F
f77 \${FCFLAGS} -c CORE_STN.F -o CORE_STN.o

FLASH2.o: FLASH2.F
f77 \${FCFLAGS} -c FLASH2.F -o FLASH2.o

FLSH_SUB.o: FLSH_SUB.F
f77 \${FCFLAGS} -c FLSH_SUB.F -o FLSH_SUB.o

IDEALGAS.o: IDEALGAS.F
f77 \${FCFLAGS} -c IDEALGAS.F -o IDEALGAS.o

MIX_HMX.o: MIX_HMX.F
f77 \${FCFLAGS} -c MIX_HMX.F -o MIX_HMX.o

PROP_SUB.o: PROP_SUB.F
f77 \${FCFLAGS} -c PROP_SUB.F -o PROP_SUB.o

REALGAS.o: REALGAS.F
f77 \${FCFLAGS} -c REALGAS.F -o REALGAS.o

SAT_SUB.o: SAT_SUB.F
f77 \${FCFLAGS} -c SAT_SUB.F -o SAT_SUB.o

SETUP.o: SETUP.F
f77 \${FCFLAGS} -c SETUP.F -o SETUP.o

SETUP2.o: SETUP2.F
f77 \${FCFLAGS} -c SETUP2.F -o SETUP2.o

TRNS_ECS.o: TRNS_ECS.F
f77 \${FCFLAGS} -c TRNS_ECS.F -o TRNS_ECS.o

TRNS_TCX.o: TRNS_TCX.F
f77 \${FCFLAGS} -c TRNS_TCX.F -o TRNS_TCX.o

TRNS_VIS.o: TRNS_VIS.F
f77 \${FCFLAGS} -c TRNS_VIS.F -o TRNS_VIS.o

TRNSP.o: TRNSP.F
f77 \${FCFLAGS} -c TRNSP.F -o TRNSP.o

UTILITY.o: UTILITY.F

```

f77 ${FCFLAGS} -c UTILITY.F -o UTILITY.o

CONVHIN_INCLUDES = array2.inc constnt.inc factlim.inc flag.inc\
    nprop.cmn param1.inc tinp.inc zstph3.inc zstph1.inc\
    zstphs.inc zstphv.inc
#
convhin.o:    convhin.F ${CONVHIN_INCLUDES}
    f77 ${FCFLAGS} -c convhin.F -o convhin.o

curve.o:     curve.F
    f77 ${FCFLAGS} -c curve.F -o curve.o

DIAMETR_INCLUDES = array1.inc param1.inc parampch.inc
#
diametr.o:   diametr.F ${DIAMETR_INCLUDES}
    f77 ${FCFLAGS} -c diametr.F -o diametr.o

DIMMSC_INCLUDES = array1.inc array2.inc constnt.inc flag.inc\
    neutkin.inc neutkn1.inc neutkni.inc options.inc\
    optpch.inc param1.inc parampch.inc parchl1.inc\
    parchl2.inc zstph1.inc zstphs.inc
#
dimmsc.o:   dimmsc.F ${DIMMSC_INCLUDES}
    f77 ${FCFLAGS} -c dimmsc.F -o dimmsc.o

doloop.o:   doloop.F
    f77 ${FCFLAGS} -c doloop.F -o doloop.o

FHO_INCLUDES = array1.inc constnt.inc csecpw.inc flag.inc neutkin.inc\
    neutkn1.inc neutkni.inc optpch.inc param1.inc\
    parampch.inc parchl1.inc parchl2.inc resinf.inc\
    zstph1.inc
#
fho.o:      fho.F ${FHO_INCLUDES}
    f77 ${FCFLAGS} -c fho.F -o fho.o

FLHEAT_INCLUDES = array1.inc array2.inc cdpow.inc constnt.inc\
    flag.inc neutkin.inc neutkn1.inc neutkn2.inc\
    neutkni.inc options.inc param1.inc parampch.inc\
    resinf.inc sdtone.inc
#
flheat.o:   flheat.F ${FLHEAT_INCLUDES}
    f77 ${FCFLAGS} -c flheat.F -o flheat.o

FRCTN_INCLUDES = array1.inc array2.inc constnt.inc factlim.inc\
    flag.inc param1.inc parampch.inc poly.inc\

```

```

#
frctn.o: frctn.F ${FRCTN_INCLUDES}
      f77 ${FCFLAGS} -c frctn.F -o frctn.o

FUELTMP_INCLUDES = array1.inc array2.inc constnt.inc csecpw.inc\
      flag.inc neutkin.inc neutkn1.inc neutkn2.inc\
      neutkni.inc optpch.inc param1.inc parampch.inc\
      parch11.inc parch12.inc resinf.inc zstphl.inc\
      zstphs.inc zstphv.inc
#
fueltmp.o:   fueltmp.F ${FUELTMP_INCLUDES}
      f77 ${FCFLAGS} -c fueltmp.F -o fueltmp.o

FUNIO_INCLUDES = constnt.inc delkix.inc flag.inc fueldat.inc\
      param1.inc xenplt.inc
#
funio.o:     funio.F ${FUNIO_INCLUDES}
      f77 ${FCFLAGS} -c funio.F -o funio.o

FUNXE_INCLUDES = constnt.inc delkix.inc flag.inc fueldat.inc\
      param1.inc xenplt.inc
#
funxe.o:     funxe.F ${FUNXE_INCLUDES}
      f77 ${FCFLAGS} -c funxe.F -o funxe.o

g.o:        g.F
      f77 ${FCFLAGS} -c g.F -o g.o

GETALL_INCLUDES = flag.inc param1.inc paramall.inc parampch.inc
#
getall.o:    getall.F ${GETALL_INCLUDES}
      f77 ${FCFLAGS} -c getall.F -o getall.o

HTCOEFB_INCLUDES = array1.inc array2.inc constnt.inc csecpw.inc\
      flag.inc neutkin.inc neutkn1.inc neutkni.inc\
      optpch.inc param1.inc parampch.inc parch11.inc\
      parch12.inc zstphl.inc zstphs.inc zstpht.inc\
      zstphv.inc
#
htcoefb.o:   htcoefb.F ${HTCOEFB_INCLUDES}
      f77 ${FCFLAGS} -c htcoefb.F -o htcoefb.o

HTCOEFC_INCLUDES = array2.inc flag.inc neutkn1.inc neutkni.inc\
      param1.inc zstphl.inc
#
htcoefc.o:   htcoefc.F ${HTCOEFC_INCLUDES}

```

```

f77 ${FCFLAGS} -c htcoefc.F -o htcoefc.o

initcm.o:    initcm.F
f77 ${FCFLAGS} -c initcm.F -o initcm.o

INPUT_INCLUDES = array1.inc constnt.inc ctabs.inc factlim.inc flag.inc\
    fueldat.inc mbuntyp.inc neutkin.inc neutkn1.inc\
    neutkn2.inc neutkni.inc options.inc optpch.inc\
    param1.inc parampch.inc parchl1.inc parchl2.inc\
    pmpcnst.inc pmpdat.inc pmptab.inc pmpval.inc poly.inc\
    resinf.inc tinp.inc velestc.inc wheat.inc
#
input.o:    input.F ${INPUT_INCLUDES}
f77 ${FCFLAGS} -c input.F -o input.o

NKINIT_INCLUDES = array1.inc array2.inc cdka.inc constnt.inc flag.inc\
    fueldat.inc neutkin.inc neutkn2.inc param1.inc\
    parampch.inc pltvar.inc resinf.inc
#
nkinit.o:    nkinit.F ${NKINIT_INCLUDES}
f77 ${FCFLAGS} -c nkinit.F -o nkinit.o

OSV_INCLUDES = array1.inc array2.inc constnt.inc flag.inc options.inc\
    param1.inc parampch.inc szscd.inc zstphl.inc zstphs.inc
#
osv.o:    osv.F ${OSV_INCLUDES}
f77 ${FCFLAGS} -c osv.F -o osv.o

OWTPUT_INCLUDES = array1.inc array2.inc cdpow.inc cmvoid.inc\
    constnt.inc curnode.inc flag.inc neutkin.inc\
    options.inc optpch.inc param1.inc parampch.inc\
    parchl1.inc parchl2.inc resinf.inc sdtone.inc wheat.inc
#
owtput.o:    owtput.F ${OWTPUT_INCLUDES}
f77 ${FCFLAGS} -c owtput.F -o owtput.o

PEXCHEK_INCLUDES = array1.inc array2.inc constnt.inc csecpw.inc\
    curnode.inc factlim.inc flag.inc mbuntyp.inc\
    neutkin.inc neutkn1.inc neutkn2.inc neutkni.inc\
    options.inc optpch.inc param1.inc parampch.inc\
    parchl1.inc parchl2.inc pmpcnst.inc pmpval.inc\
    resinf.inc tinp.inc
#
pexchek.o:    pexchek.F ${PEXCHEK_INCLUDES}
f77 ${FCFLAGS} -c pexchek.F -o pexchek.o

```

```
PHISQ_INCLUDES = array1.inc array2.inc constnt.inc flag.inc param1.inc\  
    parampch.inc
```

```
#
```

```
phisq.o:    phisq.F ${PHISQ_INCLUDES}  
    f77 ${FCFLAGS} -c phisq.F -o phisq.o
```

```
PMPCOR_INCLUDES = array1.inc array2.inc constnt.inc flag.inc\  
    options.inc param1.inc parampch.inc pmpcnst.inc pmpdat.inc
```

```
#
```

```
pmpcor.o:    pmpcor.F ${PMPCOR_INCLUDES}  
    f77 ${FCFLAGS} -c pmpcor.F -o pmpcor.o
```

```
PMPHED_INCLUDES = flag.inc param1.inc pmpdat.inc pmptab.inc
```

```
#
```

```
pmphed.o:    pmphed.F ${PMPHED_INCLUDES}  
    f77 ${FCFLAGS} -c pmphed.F -o pmphed.o
```

```
PMPOMG_INCLUDES = flag.inc param1.inc pmpdat.inc pmptab.inc
```

```
#
```

```
pmpomg.o:    pmpomg.F ${PMPOMG_INCLUDES}  
    f77 ${FCFLAGS} -c pmpomg.F -o pmpomg.o
```

```
PMPTHF_INCLUDES = flag.inc param1.inc pmpdat.inc pmptab.inc
```

```
#
```

```
pmpthf.o:    pmpthf.F ${PMPTHF_INCLUDES}  
    f77 ${FCFLAGS} -c pmpthf.F -o pmpthf.o
```

```
POWCORR_INCLUDES = array1.inc array2.inc cdka.inc cdpow.inc\  
    constnt.inc cpw.inc csecpw.inc factlim.inc flag.inc\  
    neutkn1.inc neutkn2.inc neutkni.inc\  
    options.inc param1.inc parampch.inc resinf.inc\  
    sdtone.inc
```

```
#
```

```
powcorr.o:    powcorr.F ${POWCORR_INCLUDES}  
    f77 ${FCFLAGS} -c powcorr.F -o powcorr.o
```

```
POWEQN_INCLUDES = constnt.inc resinf.inc
```

```
#
```

```
poweqn.o:    poweqn.F ${POWEQN_INCLUDES}  
    f77 ${FCFLAGS} -c poweqn.F -o poweqn.o
```

```
REATB1_INCLUDES = ctabs.inc flag.inc param1.inc
```

```
#
```

```
reatb1.o:    reatb1.F ${REATB1_INCLUDES}  
    f77 ${FCFLAGS} -c reatb1.F -o reatb1.o
```

```
REATB2_INCLUDES = ctabs.inc flag.inc param1.inc  
#
```

```
reatb2.o:      reatb2.F ${REATB2_INCLUDES}  
              f77 ${FCFLAGS} -c reatb2.F -o reatb2.o
```

```
REATB3_INCLUDES = ctabs.inc flag.inc param1.inc  
#
```

```
reatb3.o:      reatb3.F ${REATB3_INCLUDES}  
              f77 ${FCFLAGS} -c reatb3.F -o reatb3.o
```

```
REATIO_INCLUDES = cdpow.inc constnt.inc delkix.inc flag.inc\  
                  fueldat.inc options.inc param1.inc resinf.inc\  
                  sdtone.inc xenplt.inc
```

```
#  
reatio.o:      reatio.F ${REATIO_INCLUDES}  
              f77 ${FCFLAGS} -c reatio.F -o reatio.o
```

```
REATIV_INCLUDES = cdka.inc cdpow.inc constnt.inc flag.inc fueldat.inc\  
                  neutkin.inc param1.inc resinf.inc sdtone.inc
```

```
#  
reativ.o:      reativ.F ${REATIV_INCLUDES}  
              f77 ${FCFLAGS} -c reativ.F -o reativ.o
```

```
REATXE_INCLUDES = cdpow.inc constnt.inc delkix.inc flag.inc\  
                  fueldat.inc options.inc param1.inc resinf.inc\  
                  sdtone.inc xenplt.inc
```

```
#  
reatxe.o:      reatxe.F ${REATXE_INCLUDES}  
              f77 ${FCFLAGS} -c reatxe.F -o reatxe.o
```

```
rfalsi.o:      rfalsi.F  
              f77 ${FCFLAGS} -c rfalsi.F -o rfalsi.o
```

```
RHOCHK_INCLUDES = array1.inc array2.inc cdpow.inc constnt.inc\  
                  csecpw.inc curnode.inc factlim.inc flag.inc\  
                  neutkin.inc neutkn1.inc neutkn2.inc neutkni.inc\  
                  options.inc param1.inc parampch.inc resinf.inc\  
                  sdtone.inc wheat.inc zstphs.inc
```

```
#  
rhochk.o:      rhochk.F ${RHOCHK_INCLUDES}  
              f77 ${FCFLAGS} -c rhochk.F -o rhochk.o
```

```
RHOCHKM_INCLUDES = array1.inc array2.inc constnt.inc curnode.inc\  
                  factlim.inc flag.inc mbuntyp.inc options.inc\  
                  optpch.inc param1.inc parampch.inc parchl1.inc\  
                  parchl2.inc wheat.inc zstphs.inc
```

```

#
rhocheckm.o: rhocheckm.F ${RHOHECKM_INCLUDES}
               f77 ${FCFLAGS} -c rhocheckm.F -o rhocheckm.o

RHOLOOP_INCLUDES = array1.inc array2.inc cdpow.inc constnt.inc\
                   csecpw.inc curnode.inc factlim.inc flag.inc\
                   mbuntyp.inc neutkin.inc neutkn1.inc neutkn2.inc\
                   neutkni.inc options.inc optpch.inc param1.inc\
                   parampch.inc parchl1.inc parchl2.inc resinf.inc\
                   sdtone.inc wheat.inc zstphs.inc

#
rholoop.o:     rholoop.F ${RHOLOOP_INCLUDES}
               f77 ${FCFLAGS} -c rholoop.F -o rholoop.o

RSHOS2_INCLUDES = array1.inc array2.inc constnt.inc flag.inc\
                   neutkin.inc optpch.inc param1.inc parampch.inc\
                   rshos2c.inc szscd.inc zstphl.inc

#
rshos2.o:     rshos2.F ${RSHOS2_INCLUDES}
               f77 ${FCFLAGS} -c rshos2.F -o rshos2.o

SAVALL_INCLUDES = flag.inc param1.inc paramall.inc parampch.inc

#
savall.o:     savall.F ${SAVALL_INCLUDES}
               f77 ${FCFLAGS} -c savall.F -o savall.o

SLIP_INCLUDES = array1.inc array2.inc constnt.inc flag.inc param1.inc\
                parampch.inc

#
slip.o:      slip.F ${SLIP_INCLUDES}
           f77 ${FCFLAGS} -c slip.F -o slip.o

SOLVE_INCLUDES = array1.inc array2.inc cdka.inc cdpow.inc cmvoid.inc\
                 constnt.inc cpw.inc csecpw.inc curnode.inc delkix.inc\
                 factlim.inc flag.inc fueldat.inc neutkin.inc\
                 neutkn2.inc options.inc optpch.inc param1.inc\
                 parampch.inc parchl1.inc parchl2.inc pltpch.inc\
                 pltvar.inc pmpcnst.inc pmpval.inc resinf.inc\
                 sdtone.inc slvcom.inc tinp.inc wheat.inc xenplt.inc

#
solve.o:     solve.F ${SOLVE_INCLUDES}
           f77 ${FCFLAGS} -c solve.F -o solve.o

STEQN1_INCLUDES = array1.inc array2.inc constnt.inc flag.inc\
                  options.inc optpch.inc param1.inc parampch.inc\
                  pmpcnst.inc pmpval.inc zstphs.inc

```

```

#
steqn1.o:    steqn1.F ${STEQN1_INCLUDES}
             f77 ${FCFLAGS} -c steqn1.F -o steqn1.o

STPH3_INCLUDES = cstph3.inc cstpha.inc cstphd.inc cstphll.inc\
                cstphss.inc cstphvv.inc cstphx.inc
#
stph3.o:    stph3.F ${STPH3_INCLUDES}
            f77 ${FCFLAGS} -c stph3.F -o stph3.o

STPHL_INCLUDES = cstphd.inc cstphll.inc cstphx.inc
#
stphl.o:stphl.F ${STPHL_INCLUDES}
         f77 ${FCFLAGS} -c stphl.F -o stphl.o

STPHNT_INCLUDES = cstphss.inc
#
stphnt.o:    stphnt.F ${STPHNT_INCLUDES}
           f77 ${FCFLAGS} -c stphnt.F -o stphnt.o

STPHRD_INCLUDES = cstpha.inc cstphd.inc cstphm.inc cstphss.inc\
                 cstphx.inc
#
stphrd.o:    stphrd.F ${STPHRD_INCLUDES}
           f77 ${FCFLAGS} -c stphrd.F -o stphrd.o

STPHSDD_INCLUDES = cstphd.inc cstpht.inc cstphx.inc
#
stphsdd.o:    stphsdd.F ${STPHSDD_INCLUDES}
            f77 ${FCFLAGS} -c stphsdd.F -o stphsdd.o

STPHSH_INCLUDES = cstphd.inc cstphss.inc cstphx.inc
#
stphsh.o:    stphsh.F ${STPHSH_INCLUDES}
            f77 ${FCFLAGS} -c stphsh.F -o stphsh.o

STPHST_INCLUDES = cstphd.inc cstphss.inc cstphx.inc
#
stphst.o:    stphst.F ${STPHST_INCLUDES}
            f77 ${FCFLAGS} -c stphst.F -o stphst.o

STPHV_INCLUDES = cstphd.inc cstphvv.inc cstphx.inc
#
stphv.o:    stphv.F ${STPHV_INCLUDES}
            f77 ${FCFLAGS} -c stphv.F -o stphv.o

```

```

STPHX_INCLUDES = cstphd.inc cstphx.inc
#
stphx.o:      stphx.F ${STPHX_INCLUDES}
              f77 ${FCFLAGS} -c stphx.F -o stphx.o

STPHY_INCLUDES = cstphd.inc cstphx.inc
#
stphy.o:      stphy.F ${STPHY_INCLUDES}
              f77 ${FCFLAGS} -c stphy.F -o stphy.o

STPHZZ_INCLUDES = cstph3.inc cstphll.inc cstphm.inc cstphss.inc\
                  cstpht.inc cstphvv.inc zstph3.inc zstphl.inc\
                  zstphm.inc zstphs.inc zstpht.inc zstphv.inc
#
stphzz.o:      stphzz.F ${STPHZZ_INCLUDES}
              f77 ${FCFLAGS} -c stphzz.F -o stphzz.o

STPHZZH_INCLUDES = cstphl.inc cstphs.inc cstphv.inc flag.inc\
                  param1.inc zstph3.inc zstphl.inc zstphm.inc\
                  zstphs.inc zstphv.inc
#
stphzzh.o:     stphzzh.F ${STPHZZH_INCLUDES}
              f77 ${FCFLAGS} -c stphzzh.F -o stphzzh.o

STPROP_INCLUDES = array2.inc constnt.inc flag.inc nprop.cmn\
                  options.inc param1.inc resinf.inc zstph3.inc\
                  zstphl.inc zstphs.inc zstphv.inc
#
stprop.o:      stprop.F ${STPROP_INCLUDES}
              f77 ${FCFLAGS} -c stprop.F -o stprop.o

SZSC_INCLUDES = array1.inc array2.inc constnt.inc flag.inc neutkin.inc\
                  neutkn1.inc neutkni.inc options.inc optpch.inc\
                  param1.inc parampch.inc parchl1.inc parchl2.inc\
                  szscd.inc zstphl.inc zstphs.inc
#
szsc.o:        szsc.F ${SZSC_INCLUDES}
              f77 ${FCFLAGS} -c szsc.F -o szsc.o

TREQN1_INCLUDES = array1.inc array2.inc constnt.inc flag.inc\
                  optpch.inc param1.inc parampch.inc
#
treqn1.o:      treqn1.F ${TREQN1_INCLUDES}
              f77 ${FCFLAGS} -c treqn1.F -o treqn1.o

TREQN2_INCLUDES = array1.inc array2.inc constnt.inc flag.inc\

```

```

options.inc optpch.inc param1.inc parampch.inc\
pmpcnst.inc pmpval.inc zstphs.inc
#
treqn2.o:    treqn2.F ${TREQN2_INCLUDES}
            f77 ${FCFLAGS} -c treqn2.F -o treqn2.o

VELEST_INCLUDES = array1.inc array2.inc constnt.inc flag.inc\
options.inc optpch.inc param1.inc parampch.inc\
parchl1.inc parchl2.inc velestc.inc
#
velest.o:    velest.F ${VELEST_INCLUDES}
            f77 ${FCFLAGS} -c velest.F -o velest.o

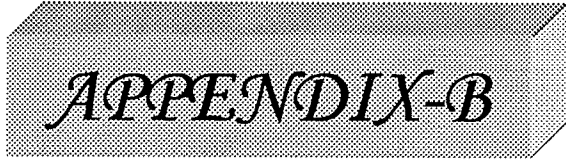
VJSC_INCLUDES = array1.inc array2.inc constnt.inc factlim.inc flag.inc\
neutkin.inc neutkn1.inc neutkni.inc options.inc\
optpch.inc param1.inc parampch.inc parchl2.inc\
zstphl.inc zstphs.inc
#
vjsc.o:      vjsc.F ${VJSC_INCLUDES}
            f77 ${FCFLAGS} -c vjsc.F -o vjsc.o

WLHEAT_INCLUDES = array1.inc array2.inc constnt.inc csecpw.inc\
flag.inc neutkn1.inc neutkn2.inc neutkni.inc\
options.inc param1.inc parampch.inc wheat.inc\
zstphl.inc zstphs.inc
#
wlheat.o:    wlheat.F ${WLHEAT_INCLUDES}
            f77 ${FCFLAGS} -c wlheat.F -o wlheat.o

YLHOS_INCLUDES = flag.inc param1.inc zstphl.inc zstphs.inc
#
ylhos.o:     ylhos.F ${YLHOS_INCLUDES}
            f77 ${FCFLAGS} -c ylhos.F -o ylhos.o

#-----#

```



APPENDIX-B

B.1 Sample Input Files

B.1.1 Sample Water Input File

```

/-----
/CASE TITLE
/-----
/TITLE      NAME
/          !
!
TITLE      Candu-X,
/-----
/OPTIONS DATA
/-----
/100          IOUT      IPLOT      IPLOT6      NSUBC      NOSV      NHEAT
ICHF
/          !          !          !          !          !          !
!
100          1          0          20          0          0          0
0
/100          ITR       NOPT      IFOPT      NEXP      NRES      IPLT
KOPT
/          !          !          !          !          !          !
!
100          0          0          0          0          0          1
0
/101          HC1       HC2       ITYPE      NCH
/          !          !          !          !
101          2.0       3.0       1          1
/-----
/GEOMETRIC DATA (HR geom)
/-----
/200          NREG      CHK
/          !          !
200          4          .04
/201(250)    RLEN      A          DE          ANGLE      NSECT
/          !          !          !          !          !
201          6.2       4.4E-3    .07485     0          62
201          10.0      4.4E-3    .07485     90.         100
201          6.2       4.4E-3    .07485     0.          62
201          10.0      4.4E-3    .07485     -90.        100
/299          IRPT     NCOD      TFA        TRK        TRUFF
/          !          !          !          !          !
299          16       3          0.0        0          0
299          1          3          .0          1          0
299          9          3          0          0          0
299          10         1          1.0        0          0
299          9          3          0.0        0.0        0
299          1          3          .0          0.5        0
299          16       3          0.0        0          0
299          100      3          0          0          0
299          1          3          0          0          0
299          25         3          0          0          0
299          10         3          -1.0       0          0
299          25         3          0          0          0
/299          60       40         -1.0       0          0
299          1          3          0          0          0
299          100      3          0          0          0
299          0          0          0          0          0
/-----
/BOUNDARY CONDITIONS
/-----

```

```

/300          POW          TIN          FLOW          PIN          PEX          ZIN
/            !            !            !            !            !            !
300          3500         340.0         4.7          25.E3         25.E3

```

```

/301          RHOF LG      TFLG      PRFLG      N2PH
/            !            !            !            !
301          0            0            5.0          2
/-----
/TRANSIENT DATA
/-----
/
/400          DT          FSDT          RAMP          DELKF/
REACTIR      SHDRTY      FPOW          SHDPOW          SDTDLY
/            !            !            !            !            !
!            !
400          .25          25           80.0          3500
/-----
/FUEL MODEL DATA
/-----
/500          NFPINS(TOT)  PINLEN      RADS          RADG          RADF
/            !            !            !            !            !
500          1            0.470 3.925E-02 3.925E-2 3.925E-2
/501          CPF          DENF          HG          THCF          THCS          RCTEMP          RFTEMP
/            !            !            !            !            !            !            !
501          450.0        5430.0       1.0E90       152          220.         40.         40.
/-----
/NEUTRON KINETIC DATA (SHIM PLATES INSERTED)
/-----

```

B.1.2 Sample Carbon-dioxide Input File

```

/-----
/CASE TITLE
/-----
/TITLE    NAME
/        !
!
TITLE    Candu-X,
/-----
/OPTIONS DATA
/-----
/100      IOUT      IPLOT      IPLOT6      NSUBC      NOSV      NHEAT
ICHF
/        !        !        !        !        !        !        !
!
100      1          0          20         0          0          0
0
/100      ITR       NOPT      IFOPT      NEXP      NRES      IPLT
KOPT
/        !        !        !        !        !        !        !
!
100      0          0          0          0          0          1
0
/101      HC1       HC2       ITYPE      NCH
/        !        !        !        !
101      2.0       3.0       1          1
/-----
/GEOMETRIC DATA (HR geom)
/-----
/200      NREG      CHK
/        !        !
200      4          .04
/201(250) RLEN      A          DE          ANGLE      NSECT
/        !        !        !        !        !
201      6.2       4.4E-3   .07485     0          62
201      10.0      4.4E-3   .07485     90.         100
201      6.2       4.4E-3   .07485     0.          62
201      10.0      4.4E-3   .07485     -90.        100
/299      IRPT      NCOD      TFA        TRK        TRUFF
/        !        !        !        !        !
299      16        3          0.0        0          0
299      1          3          .0          1          0
299      9          3          0          0          0
299      10         1          1.0        0          0
299      9          3          0.0        0.0        0
299      1          3          .0          0.5        0
299      16        3          0.0        0          0
299      100       3          0          0          0
299      1          3          0          0          0
299      25        3          0          0          0
299      10        40         -1.0       0          0
299      25        3          0          0          0
/299      60       40         -1.0       0          0
299      1          3          0          0          0
299      100       3          0          0          0
299      0          0          0          0          0
/-----
/BOUNDARY CONDITIONS
/-----
/300      POW      TIN      FLOW      PIN      PEX      ZIN
/        !        !        !        !        !        !        !
300      1500     25.0     12.0     8.E3     8.E3

```

```

/301      RHOFLG      TFLG      PRFLG      N2PH
/          !          !          !          !
301              0          0          5.0          2
/-----
/TRANSIENT DATA
/-----
/
/400      DT          FSDT          RAMP          DELKF/
REACTIR  SHDRTY          FPOW          SHDPOW          SDTDLY
/          !          !          !          !          !
!          !
400              .25          25          80.0          1500
/-----
/FUEL MODEL DATA
/-----
/500      NFPINS(TOT)  PINLEN          RADS          RADG          RADF
/          !          !          !          !          !
500              1          0.470 3.925E-02  3.925E-2  3.925E-2
/501      CPF          DENF          HG          THCF          THCS          RCTEMP          RFTEMP
/          !          !          !          !          !          !          !
501      450.0      5430.0      1.0E90          152          220.          40.          40.
/-----
/NEUTRON KINETIC DATA (SHIM PLATES INSERTED)
/-----

```

B.1.3 Sample Hydrogen Input File

```

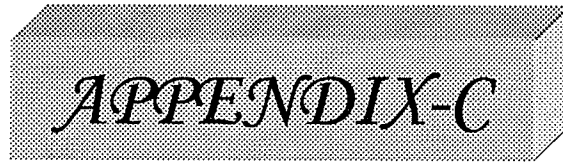
/-----
/CASE TITLE
/-----
/TITLE      NAME
/          !
!
TITLE      Candu-X,
/-----
/OPTIONS DATA
/-----
/100          IOUT      IPLOT      IPLOT6      NSUBC      NOSV      NHEAT
ICHF
/          !          !          !          !          !          !
!
100          1          0          20          0          0          0
0
/100          ITR       NOPT       IFOPT       NEXP       NRES       IPLT
KOPT
/          !          !          !          !          !          !
!
100          0          0          0          0          0          1
0
/101          HC1       HC2       ITYPE      NCH
/          !          !          !          !
101          2.0       3.0       1          1
/-----
/GEOMETRIC DATA (HR geom)
/-----
/200          NREG      CHK
/          !          !
200          4          .04
/201(250)    RLEN      A          DE          ANGLE      NSECT
/          !          !          !          !          !
201          6.2       4.4E-3    .07485     0          62
201          10.0      4.4E-3    .07485     90.        100
201          6.2       4.4E-3    .07485     0.         62
201          10.0      4.4E-3    .07485     -90.       100
/299          IRPT      NCOD      TFA        TRK        TRUFF
/          !          !          !          !          !
299          16       3          0.0        0          0
299          1          3          .0          1          0
299          9          3          0          0          0
299          10         1          1.0        0          0
299          9          3          0.0        0.0        0
299          1          3          .0          0.5        0
299          16       3          0.0        0          0
299          100      3          0          0          0
299          1          3          0          0          0
299          25       3          0          0          0
299          10       40         -1.0       0          0
299          25       3          0          0          0
/299          60       40         -1.0       0          0
299          1          3          0          0          0
299          100      3          0          0          0
299          0          0          0          0          0
/-----
/BOUNDARY CONDITIONS
/-----
/300          POW      TIN      FLOW      PIN      PEX      ZIN
/          !          !          !          !          !          !
300          500      -243.0    1.0       1.4E3    1.4E3

```

```

/301      RHOFLG      TFLG      PFLG      N2PH
/          !          !          !          !
301              0          0          5.0          2
/-----
/TRANSIENT DATA
/-----
/
/400      DT          FSDT      RAMP      DELKF/
REACTIR  SHDRTY      FPOW      SHDPOW      SDTDLY
/          !          !          !          !          !          !
!          !
400              .25          25          80.0          500
/-----
/FUEL MODEL DATA
/-----
/500      NFPINS(TOT)  PINLEN      RADS      RADG      RADF
/          !          !          !          !          !
500              1          0.470 3.925E-02 3.925E-2 3.925E-2
/501      CPF          DENF          HG          THCF      THCS      RCTEMP      RFTEMP
/          !          !          !          !          !          !          !
501      450.0      5430.0      1.0E90      152          220.          40.          40.
/-----
/NEUTRON KINETIC DATA (SHIM PLATES INSERTED)
/-----

```



APPENDIX-C

C.1 SUBROUTINE CONVHIN(PE,TEMPX,HE)

IMPLICIT DOUBLE PRECISION (a-h,o-z)

implicit integer (i-k,m,n)

C DOUBLE PRECISION TK

C

C=====

=====

C=====

=====

C <NAME>

C CONVHIN

C

C <DESCRIPTION>

C THIS SUBROUTINE CALCULATES THE INLET ENTHALPY CORRES-

C PONDING TO THE SPECIFIED INLET TEMPERATURE AND PRESSURE.

C

C=====

=====

C=====

=====

include "param1.inc"

include "flag.inc"

include "constnt.inc"

include "factlim.inc"

include "zstph3.inc"

include "zstphs.inc"

include "zstphl.inc"

include "zstphv.inc"

include "tinp.inc"

include "array2.inc"

include "nprop.cmn"

C

PARAMETER (ncmax=20)

INTEGER IWANT, IPCHK, IRIFLG, IWORK, IW, NRI, I2PHCK

> I2PH, ISCHK, ICCHK, IGFLG, IPFLG, ICFLG, ISFLG, ierr

c

dimension x(ncmax),xliq(ncmax),xvap(ncmax),f(ncmax),y(ncmax),

> z(ncmax)

character hrf*3, herr*255

character*255 hf(ncmax),hfmix

DIMENSION PROPR(NPROP), PROPSI(NPROP), RI(NRIMAX)

C

REAL PE, HE, HIN

common /prnterr/ iprnterr

m=1

hf(1)='CO2.FLD'

```

    hfmix='HMX.BNC'
    hrf='DEF'
    CALL SETUP (m,hf,hfmix,hrf,ierr,herr)
    if (ierr.ne.0) write (*,*) herr
TK = TIN + 273.15
    t=TK
PMPA = PE/1.0E3
    b= PMPA
    do 10 n=1,20
        z(n)=0
10 continue
    CALL TPFLSH(t,b,z,D,DI,Dv,x,y,q,e1,h1,s1,cv1,cp1,w1,ierr,herr)
    DOUT = D*44.0
RHO1 = DOUT
RO = DOUT
CALL TRNPRP(t,D,z,eta,tcx,ierr,herr)
CALL THERM(t,D,z,p2,e,h2,s,cv,cp,w,hjt)
PROPSI(6) = ((h2*1E+3)/44.0)
    PROPSI(9) = cp/44.0
HIN = PROPSI(6)
HE = HIN
H(1,1) = HE
RHO(1,JI2) = RHO1
RHOF(1,JI2)= RHO1
XMUF(1,1) = eta*1.0E-6
TEMPX = TIN
XQU(1,JI2) = 0.
XMUF(1,JI2) = eta*1E-6
XMUG(1,JI2) = eta*1E-6
AKLZ = tcx
CPLZ = PROPSI(9)
RETURN
END

```

C.2 SUBROUTINE STPROP(PRESS,HENTH,I,RHO1)

C

IMPLICIT DOUBLE PRECISION (a-h,o-z)
implicit integer (i-k,m,n)

C

C <NAME> : STPROP

C

C <DESCRIPTION> : THIS SUBROUTINE CALCULATES STEAM WATER
PROPERTIES

C USING A ROUTINE CALLED ' STPH ' DEVELOPED AT WNRE.

C

C (REFERENCE WRNE 467) OR USING HLWP (REFERENCE ARD-TD-207
)

C

C

C <CALLED FROM> : SOLVE, PEXCHEK, RHOCEKM, RHOCEK, ARCO

C

include "param1.inc"

include "flag.inc"

include "zstph3.inc"

include "zstphs.inc"

include "zstphv.inc"

include "zstphl.inc"

include "options.inc"

include "constnt.inc"

include "array2.inc"

include "resinf.inc"

include "nprop.cmn"

PARAMETER (ncmax=20)

dimension x(ncmax),xliq(ncmax),xvap(ncmax),f(ncmax), z(ncmax),

> y(ncmax)

character hrf*3, herr*255

character*255 hf(ncmax),hfmix

INTEGER IERR

INTEGER I

REAL PRESS, HENTH, RHO1

m=1

hf(1)='CO2.FLD'

C >sisres1\sisres1\NIST\fluids\CO2.FLD'

hfmix='HMX.BNC'

hrf='DEF'

CALL SETUP (m,hf,hfmix,hrf,ierr,herr)

if (ierr.ne.0) write (*,*) herr

TP = PRESS/1E+3

```

HS = ((HENTH*44.0)/1E+3)
do 10 n=1,20
  z(n)=0
10 continue
  CALL PHFLSH(TP,HS,z,TPOUT,D,DI,Dv,x,y,q,e1,s1,cv1,cp1,w1,ierr,herr)
  D1=D*44.0
  TEMP(I,JI2) = TPOUT - 273.15
  RHO1      = D1
  RHOF(I,JI2) = D1
  RHOG(I,JI2) = D1
  TK = TPOUT
  RO = D
  CALL TRNPRP(TK,RO,z,eta1,tcx1,ierr,herr)
  CALL THERM(TK,RO,z,c,e,h1,s,cv,cp,w,hjt)
  XQU(I,JI2) = 0.
  XMUF(I,JI2) = eta1*1.0E-6
  XMUG(I,JI2) = eta1*1.0E-6
  AKLZ      = tcx1
  CPLZ      = cp/44.0
40 CONTINUE
C
RETURN
END

```

APPENDIX-D

Table D1: Water: $h_t=14$ m, $T_{IN}=350^{\circ}\text{C}$

$T_{IN} (^{\circ}\text{C})$	$P_{in} (\text{MPa})$	B	η_2	$\rho_1 (\text{kg/m}^3)$	$h_1 (\text{J/kg})$	$g (\text{m/s}^2)$	D(m)	$A (\text{m}^2)$					
350	25	1.74E+23	3.277	625.45	1.62E+06	9.8	0.07485	0.0044					
θ	Φ	K_1	K_2	C_{k1}	C_{k2}	C_{k3}	$h_t (\text{m})$	ρ_{2b}	ξ	$Q_s (\text{W})$	Q_s^*	B^*	$(B^*/\Phi)^{1/\eta_2-1}$
0.80	0.40	1.0	0.5	7.1	14.7	11.3	14	250.05	9.67	4.80E+06	0.291	1.237	0.412
0.62	0.38	2.0	0.5	12.1	14.6	11.4	14	239.22	9.69	5.10E+06	0.318	1.237	0.431
0.51	0.37	3.0	0.5	17.1	14.5	11.5	14	229.85	9.71	5.40E+06	0.346	1.237	0.448
0.44	0.36	4.0	0.5	22.0	14.6	11.4	14	222.19	9.70	5.80E+06	0.380	1.237	0.463
0.38	0.34	5.0	0.5	27.0	14.5	11.5	14	214.83	9.72	6.20E+06	0.417	1.237	0.478
0.33	0.33	6.0	0.5	32.0	14.4	11.5	14	208.25	9.75	7.10E+06	0.487	1.237	0.493
0.30	0.32	7.0	0.5	37.0	14.5	11.5	14	202.67	9.73	7.30E+06	0.514	1.237	0.505
0.27	0.32	8.0	0.5	42.0	14.5	11.6	14	197.55	9.72	7.40E+06	0.537	1.237	0.517
0.25	0.31	9.0	0.5	47.0	14.6	11.7	14	192.79	9.71	7.45E+06	0.554	1.237	0.528
0.23	0.30	10.0	0.5	52.0	14.6	11.7	14	188.64	9.69	7.50E+06	0.572	1.237	0.538

Table D2: Water: $h_t=10$ m, $T_{IN}=350^{\circ}\text{C}$

0.94	0.41	1.0	1.0	7.0	14.8	8.7	10	256.73	8.13	5.50E+06	0.368	1.237	0.400
0.71	0.39	2.0	1.0	12.1	14.8	8.8	10	245.04	8.13	5.80E+06	0.405	1.237	0.420
0.57	0.38	3.0	1.0	17.0	14.8	8.9	10	235.43	8.13	6.60E+06	0.480	1.237	0.438
0.48	0.36	4.0	1.0	22.0	14.8	8.9	10	226.73	8.14	7.30E+06	0.558	1.237	0.454
0.41	0.35	5.0	1.0	27.0	14.8	9.0	10	219.30	8.13	7.40E+06	0.587	1.237	0.469
0.36	0.34	6.0	1.0	32.1	14.9	9.1	10	212.72	8.12	7.50E+06	0.616	1.237	0.483
0.32	0.33	7.0	1.0	37.1	14.9	9.1	10	206.85	8.10	7.60E+06	0.645	1.237	0.496
0.29	0.32	8.0	1.0	42.1	15.0	9.2	10	201.54	8.09	7.80E+06	0.685	1.237	0.508
0.27	0.32	9.0	1.0	47.0	15.2	9.2	10	197.37	8.04	8.00E+06	0.726	1.237	0.517
0.25	0.31	10.0	1.0	52.0	15.3	9.2	10	193.03	8.02	8.30E+06	0.779	1.237	0.528

Table D1: Water: $h_f=14$ m, $T_{IN}=350^{\circ}\text{C}$ (con...)

Conv flowrate (kg/s)	G_s (kg/m ² /s)	G_s^*	Peak Flowrate (kg/s)	G_m (kg/m ² /s)	G_m^*	Q_b (W)	Q_b^*	ρ_2 (kg/m ³)	R_s^*	T (^o C)	Time Step (s)	Time Period (s)
10.17	2311	0.382	10.874	2471.2	0.408	7.60E+06	0.430	348.7	0.558	384.06	0.25	7.0
9.88	2245	0.370	10.380	2359.0	0.389	7.40E+06	0.439	323.5	0.517	385.06	0.25	6.5
9.61	2184	0.360	9.958	2263.2	0.373	7.43E+06	0.459	299.7	0.479	385.24	0.25	7.0
9.39	2134	0.352	9.593	2180.1	0.359	7.50E+06	0.481	273.4	0.437	386.05	0.25	6.8
9.17	2083	0.343	9.271	2106.9	0.347	7.70E+06	0.511	248.9	0.398	387.15	0.25	6.0
8.98	2041	0.335	8.984	2041.6	0.335	7.80E+06	0.535	192.8	0.308	392.18	0.25	2.0
8.75	1988	0.327	8.726	1983.1	0.326	7.80E+06	0.550	214.3	0.343	393.66	0.25	1.9
8.49	1929	0.317	8.492	1929.9	0.317	7.80E+06	0.566	183.0	0.293	394.98	0.25	1.8
8.27	1881	0.310	8.279	1881.5	0.310	7.85E+06	0.584	177.4	0.284	396.38	0.25	1.8
8.08	1836	0.303	8.083	1837.0	0.303	7.85E+06	0.598	172.2	0.275	397.85	0.25	1.8

Table D2: Water: $h_f=10$ m, $T_{IN}=350^{\circ}\text{C}$ (con...)

9.20	2090	0.411	9.267	2106.0	0.414	6.20E+06	0.412	282.4	0.451	385.79	0.35	4.5
8.81	2003	0.394	8.855	2012.4	0.396	6.22E+06	0.433	256.2	0.410	386.76	0.35	3.5
8.46	1923	0.378	8.469	1924.8	0.378	6.24E+06	0.454	212.4	0.340	390.19	0.35	2.5
8.06	1832	0.360	8.153	1852.8	0.364	6.25E+06	0.472	177.7	0.284	396.39	0.35	3.0
7.77	1765	0.347	7.857	1785.6	0.351	6.26E+06	0.491	166.8	0.267	397.71	0.35	2.0
7.50	1704	0.336	7.628	1733.6	0.341	6.26E+06	0.505	156.9	0.251	403.61	0.35	1.7
7.26	1649	0.325	7.406	1683.2	0.332	6.26E+06	0.520	147.9	0.236	408.10	0.35	1.5
7.01	1594	0.315	7.206	1637.7	0.324	6.26E+06	0.535	136.9	0.219	415.49	0.35	1.5
6.79	1543	0.307	7.024	1596.2	0.318	6.26E+06	0.549	127.0	0.203	424.46	0.35	1.5
6.56	1491	0.297	6.856	1558.1	0.311	6.26E+06	0.562	115.6	0.185	438.69	0.35	1.5

Table D3: Water: $h_t=17$ m, $T_{IN}=350^{\circ}\text{C}$

T_{IN} ($^{\circ}\text{C}$)	P_{in} (MPa)	B	η_2	ρ_1 (kg/m ³)	h_1 (J/kg)	g (m/s ²)	D(m)	A(m ²)					
350	25	1.74E+23	3.28	625.45	1.62E+06	9.8	0.0749	0.0044					
θ	Φ	K_1	K_2	C_{k1}	C_{k2}	C_{k3}	h_t	ρ_{2b}	ξ	Q_s	Q_s^*	B^*	$(B^*/\Phi)^{1/\eta_2-1}$
0.92	0.41	0.5	0.5	4.5	16.1	13.1	17	255.67	10.16	5.50E+06	0.305	1.237	0.402
0.80	0.40	1.0	0.5	7.0	16.1	13.1	17	250.08	10.18	5.70E+06	0.321	1.237	0.411
0.64	0.38	2.0	0.5	12.0	16.1	13.1	17	240.57	10.17	6.20E+06	0.358	1.237	0.428
0.53	0.37	3.0	0.5	17.0	16.0	13.2	17	231.73	10.20	6.70E+06	0.398	1.237	0.445

Table D4: Water: $h_t=14$ m, $T_{IN}=340^{\circ}\text{C}$

T_{IN} ($^{\circ}\text{C}$)	P(MPa)	B	η_2	ρ_1 (kg/m ³)	h_1 (J/kg)	g (m/s ²)	D(m)	A(m ²)					
340	25	1.74E+23	3.28	6.55E+02	1.56E+06	9.8	0.0749	0.0044					
θ	Φ	K_1	K_2	C_{k1}	C_{k2}	C_{k3}	h_t	ρ_{2b}	ξ	Q_s	Q_s^*	B^*	$(B^*/\Phi)^{1/\eta_2-1}$
1.14	0.42	2.0	3.0	12.23	27.51	11.96	14	276.32	7.06	4.50E+06	0.344	1.354	0.427
0.70	0.39	5.0	3.0	27.19	27.51	12.04	14	256.15	7.06	5.00E+06	0.406	1.354	0.461
0.92	0.41	1.0	1.0	7.17	17.32	11.67	14	267.96	8.90	5.30E+06	0.349	1.354	0.441
0.72	0.39	2.0	1.0	12.16	17.05	11.58	14	257.24	8.97	5.50E+06	0.358	1.354	0.459
0.59	0.38	3.0	1.0	17.10	17.02	11.55	14	248.34	8.98	6.10E+06	0.403	1.354	0.475
0.50	0.37	4.0	1.0	22.04	16.84	11.52	14	239.97	9.03	7.40E+06	0.496	1.354	0.490
0.44	0.36	5.0	1.0	27.05	16.87	11.59	14	232.81	9.02	7.43E+06	0.514	1.354	0.504
0.39	0.35	6.0	1.0	32.06	16.96	11.66	14	226.57	8.99	7.45E+06	0.531	1.354	0.517
0.35	0.34	7.0	1.0	37.08	16.93	11.72	14	220.55	9.00	7.48E+06	0.548	1.354	0.529
0.32	0.33	8.0	1.0	42.09	16.98	11.78	14	215.31	8.99	7.50E+06	0.563	1.354	0.540
0.29	0.32	9.0	1.0	47.10	17.10	11.84	14	210.74	8.96	7.55E+06	0.581	1.354	0.550
0.27	0.31	10.0	1.0	52.11	17.02	11.89	14	205.90	8.98	7.60E+06	0.598	1.354	0.562
1.33	0.43	5	8	27.22	52.87	12.59	14	281.9	5.09	4.70E+06	0.483	1.354	0.419

Table D3: Water: $h_t=17$ m, $T_{IN}=350^{\circ}\text{C}$ (con...)

Conv flowrate	G_s	G_s^*	Peak Flowrate	G_m	G_m^*	Q_b	Q_b^*	ρ_2	R_s^*	T	Time Step	Time Period
(kg/s)	(kg/m ² /s)		(kg/s)	(kg/m ² /s)		(W)		(kg/m ³)		(^o C)	(s)	(s)
11.11	2524	0.397	11.644	2646.2	0.416	7.80E+06	0.413	335.3	0.536	335.26	0.35	7.0
10.95	2488	0.391	11.378	2585.7	0.406	7.90E+06	0.428	321.1	0.513	321.13	0.35	6.8
10.67	2426	0.381	10.906	2478.5	0.390	8.00E+06	0.452	290.4	0.464	290.40	0.35	6.2
10.38	2358	0.370	10.498	2385.9	0.374	8.00E+06	0.469	261.8	0.419	261.81	0.35	5.5

Table D4: Water: $h_t=14$ m, $T_{IN}=340^{\circ}\text{C}$ (con...)

Conv flowrate	G_s	G_s^*	Peak Flowrate	G_m	G_m^*	Q_b	Q_b^*	ρ_2	R_s^*	T	Time Step	Time Period
(kg/s)	(kg/m ² /s)		(kg/s)	(kg/m ² /s)		(W)		(kg/m ³)		(^o C)	(s)	(s)
8.39	1906.3	0.412	8.660	1968.2	0.425	6.00E+06	0.445	349.822	0.534	384.04	0.25	7.5
7.91	1798.2	0.389	8.006	1819.3	0.393	6.00E+06	0.481	297.867	0.455	385.31	0.25	6.5
9.75	2215.9	0.380	10.730	2438.5	0.418	7.60E+06	0.455	396.218	0.605	382.63	0.25	5.7
9.87	2244.1	0.382	10.288	2338.1	0.398	7.65E+06	0.477	137.852	0.210	384.32	0.25	2.7
9.72	2208.3	0.375	9.907	2251.6	0.383	7.70E+06	0.499	300	0.458	385.24	0.25	3.2
9.57	2175.5	0.368	9.573	2175.7	0.368	7.80E+06	0.523	233.512	0.356	388.15	0.25	2.4
9.28	2108.2	0.357	9.276	2108.1	0.357	7.80E+06	0.540	224.736	0.343	388.86	0.25	2.2
9.01	2047.6	0.347	9.010	2047.5	0.347	7.80E+06	0.556	216.761	0.331	389.63	0.25	2.1
8.77	1992.8	0.338	8.799	1999.6	0.339	7.80E+06	0.569	209.502	0.320	390.46	0.25	2.0
8.55	1942.8	0.330	8.547	1942.4	0.330	7.80E+06	0.586	206.156	0.315	390.84	0.25	2.0
8.35	1896.9	0.323	8.347	1896.9	0.323	7.80E+06	0.600	200.148	0.306	391.74	0.25	3.2
8.16	1853.9	0.315	8.161	1854.6	0.315	7.80E+06	0.614	190.973	0.292	393.31	0.25	7.5
6.24	1419.1	0.425	6.315	1435.2	0.430	4.50E+06	0.457	243.43	0.372	387.32	0.25	6.5

Table D5: Water: $h_t=14$ m, $T_{IN}=360^\circ\text{C}$

T_{IN} ($^\circ\text{C}$)	P(MPa)	B	η_2	$\rho_1(\text{kg/m}^3)$	$h_1(\text{J/kg})$	$g(\text{m/s}^2)$	D(m)	A(m^2)					
360	25	1.74E+23	3.28	5.89E+02	1.70E+06	9.8	0.0749	0.0044					
θ	Φ	K_1	K_2	C_{k1}	C_{k2}	C_{k3}	h_t	ρ_{2b}	ξ	Q_s	Q_s^*	B^*	$(B^*/\Phi)^{1/\eta_2}-1$
0.94	0.41	1.0	1.0	6.93	16.96	11.17	14	241.73	8.99	6.10E+06	0.373	1.133	1.363
0.73	0.39	2.0	1.0	11.94	16.90	11.27	14	231.95	9.01	6.80E+06	0.435	1.133	1.381
0.62	0.38	3.0	1.0	16.90	17.61	11.34	14	225.47	8.83	8.00E+06	0.544	1.133	1.393
0.51	0.37	4.0	1.0	21.97	17.08	11.43	14	216.71	8.96	8.05E+06	0.569	1.133	1.410
0.45	0.36	5.0	1.0	26.93	17.15	11.51	14	210.43	8.94	8.20E+06	0.600	1.133	1.422
0.40	0.35	6.0	1.0	31.94	17.22	11.58	14	204.75	8.93	8.30E+06	0.608	1.133	1.434
1.16	0.42	8	10	42.131	63.496	12.716	14	249.1449	4.6484	4.30E+06	0.519	1.133	1.351
1.06	0.42	9	10	47.14	63.52	12.77	14	246.1508	4.6475	4.40E+06	0.541	1.133	1.356

Table D5: Water: $h_t=14$ m, $T_{IN}=360^\circ\text{C}$ (con...)

Conv flowrate	G_s	G_s^*	Peak Flowrate	G_m	G_m^*	Q_b	Q_b^*	ρ_2	R_s^*	Time Step	Time Period
(kg/s)	($\text{kg/m}^2/\text{s}$)		(kg/s)	($\text{kg/m}^2/\text{s}$)		(W)		(kg/m^3)		(s)	(s)
9.62	2187.2	0.413	9.625	2187.4	0.413	6.30E+06	0.385	236.73	0.402	0.35	5.0
9.20	2091.4	0.394	9.229	2097.5	0.395	6.30E+06	0.402	202.17	0.343	0.35	4.0
8.65	1965.8	0.378	8.887	2019.8	0.388	6.30E+06	0.417	157.00	0.266	0.35	2.0
8.33	1892.9	0.358	8.588	1951.7	0.370	6.30E+06	0.432	147.95	0.251	0.35	2.0
8.04	1827.7	0.347	8.322	1891.3	0.359	6.30E+06	0.446	139.80	0.237	0.35	1.8
8.04	1827.7	0.347	8.083	1837.0	0.349	6.30E+06	0.459	132.40	0.225	0.35	1.7
4.88	1109.0	0.405	5.101	1159.3	0.423	3.30E+06	0.3809	166.202	0.28	0.35	2.2
4.79	1087.8	0.397	5.040	1145.4	0.418	3.30E+06	0.3855	158.218	0.27	0.35	2.2

Table D6: Water: 2 m, $h_t=14$ m, $T_{IN}=350^\circ\text{C}$

T_{IN} ($^\circ\text{C}$)	P(MPa)	B	η_2	$\rho_1(\text{kg/m}^3)$	$h_1(\text{J/kg})$	$g(\text{m/s}^2)$	D(m)	A(m^2)					
350	25	1.7E+23	3.277	625.45	1.62E+06	9.8	0.07	0.0044					
θ	Φ	K_1	K_2	C_{k1}	C_{k2}	C_{k3}	$h_t(\text{m})$	ρ_{2b}	ξ	$Q_s(\text{W})$	Q_s^*	B^*	$(B^*/\Phi)^{1/\eta_2}-1$
0.934	0.410	1	1	7.00	17.17	11.38	14	256.446	8.94	5.10E+06	0.317	1.237	0.401
0.738	0.395	2	1	11.94	17.21	11.38	14	246.764	8.93	5.50E+06	0.352	1.237	0.417
0.605	0.380	3	1	16.95	17.17	11.45	14	237.893	8.94	5.80E+06	0.382	1.237	0.433
0.515	0.368	4	1	21.90	17.19	11.51	14	230.31	8.93	6.10E+06	0.413	1.237	0.447
0.445	0.357	5	1	26.91	17.13	11.57	14	223.234	8.95	6.50E+06	0.453	1.237	0.461
0.397	0.348	6	1	31.85	17.24	11.57	14	217.489	8.92	6.80E+06	0.487	1.237	0.473
0.354	0.338	7	1	36.86	17.19	11.64	14	211.67	8.93	7.35E+06	0.542	1.237	0.485
0.323	0.331	8	1	41.81	17.28	11.71	14	206.818	8.91	7.60E+06	0.578	1.237	0.496
0.295	0.323	9	1	46.82	17.30	11.79	14	202.102	8.91	8.20E+06	0.645	1.237	0.506
0.272	0.316	10	1	51.83	17.35	11.86	14	197.851	8.89	8.30E+06	0.672	1.237	0.516

Table D7: Water: 2 m, $h_t=10$ m, $T_{IN}=350^\circ\text{C}$

0.930	0.410	0.5	0.5	4.58	12.40	8.75	10	256.281	8.89	4.30E+06	0.275	1.237	0.401
0.782	0.398	1	0.5	7.09	12.42	8.80	10	249.207	8.88	4.50E+06	0.296	1.237	0.413
0.599	0.380	2	0.5	12.04	12.48	8.80	10	237.455	8.86	4.65E+06	0.319	1.237	0.434
0.481	0.363	3	0.5	17.04	12.50	8.95	10	227.043	8.85	4.70E+06	0.336	1.237	0.454
0.406	0.349	4	0.5	22.00	12.55	8.93	10	218.587	8.84	5.10E+06	0.374	1.237	0.471
0.351	0.338	5	0.5	26.94	12.60	8.98	10	211.133	8.82	5.25E+06	0.397	1.237	0.486
0.308	0.327	6	0.5	31.95	12.61	9.04	10	204.286	8.82	5.35E+06	0.417	1.237	0.501
0.275	0.317	7	0.5	36.89	12.64	9.00	10	198.438	8.81	6.00E+06	0.477	1.237	0.515
0.248	0.308	8	0.5	41.90	12.65	9.05	10	192.904	8.80	6.10E+06	0.499	1.237	0.528
0.226	0.300	9	0.5	46.91	12.65	9.10	10	187.815	8.80	6.40E+06	0.537	1.237	0.540
0.208	0.293	10	0.5	51.85	12.70	9.14	10	183.478	8.78	6.80E+06	0.586	1.237	0.551

Table D6: Water: 2 m, $h_t=14$ m, $T_{IN}=350^{\circ}\text{C}$ (con...)

Conv Flowrate	G_s	G_s^*	Peak Flowrate	G_m	G_m^*	Q_b	Q_b^*	ρ_2	R_s^*	T	Time Step	Time Period
(kg/s)	(kg/m ² /s)		(kg/s)	(kg/m ² /s)		(W)		(kg/m ³)		(^o C)	(s)	(s)
9.90	2249.01	0.402	10.241	2327.39	0.416	6.80E+06	0.4089	324.05	0.518	384.66	0.35	6.8
9.63	2188.24	0.392	9.827	2233.23	0.400	6.82E+06	0.4274	295.10	0.472	385.38	0.35	6.2
9.35	2124.98	0.380	9.457	2149.12	0.384	6.84E+06	0.4454	272.24	0.435	386.11	0.35	6.1
9.09	2065.55	0.370	9.137	2076.47	0.372	6.85E+06	0.4617	250.91	0.401	387.06	0.35	6.1
8.84	2010.00	0.359	8.853	2012.05	0.359	6.86E+06	0.4771	227.23	0.363	388.05	0.35	4.5
8.60	1954.35	0.350	8.599	1954.27	0.350	6.87E+06	0.4920	208.98	0.334	390.54	0.35	4.2
8.34	1896.23	0.339	8.369	1901.93	0.340	6.88E+06	0.5062	182.95	0.293	395.2	0.35	3.6
8.10	1841.42	0.330	8.159	1854.16	0.333	6.90E+06	0.5208	167.25	0.267	399.46	0.35	3.3
7.83	1780.53	0.320	7.966	1810.42	0.325	6.70E+06	0.5179	148.00	0.237	408.02	0.35	3.2
7.60	1727.32	0.311	7.789	1770.03	0.318	6.70E+06	0.5297	135.89	0.217	416.22	0.35	3.0

Table D7: Water: 2 m, $h_t=10$ m, $T_{IN}=350^{\circ}\text{C}$ (con...)

9.62	2186.83	0.393	10.259	2331.48	0.419	7.20E+06	0.4322	351.29	0.562	384.1	0.25	6.5
9.36	2126.13	0.383	9.955	2262.39	0.407	7.20E+06	0.4454	343.45	0.549	384.2	0.25	6.1
8.97	2037.78	0.368	9.434	2144.06	0.387	7.20E+06	0.4700	322.84	0.516	384.7	0.25	6.0
8.60	1954.79	0.353	9.000	2045.36	0.369	7.20E+06	0.4926	307.25	0.491	385.06	0.25	5.5
8.40	1908.20	0.345	8.629	1961.04	0.355	7.20E+06	0.5138	278.04	0.445	385.91	0.25	5.5
8.14	1849.34	0.335	8.309	1888.32	0.342	7.20E+06	0.5336	261.55	0.418	386.56	0.25	5.3
7.89	1794.11	0.325	8.026	1824.22	0.331	6.85E+06	0.5256	248.36	0.397	387.21	0.25	5.4
7.74	1759.91	0.320	7.774	1766.64	0.321	6.80E+06	0.5387	213.75	0.342	349.95	0.25	4.0
7.53	1711.44	0.311	7.548	1715.32	0.312	6.60E+06	0.5385	203.19	0.325	391.34	0.25	4.0
7.34	1668.24	0.303	7.343	1668.69	0.303	6.60E+06	0.5535	186.06	0.297	394.63	0.25	4.2
7.15	1625.34	0.296	7.155	1626.41	0.296	6.60E+06	0.5680	167.18	0.267	399.52	0.25	6.5

Table D8: Water: 2 m, $h_t=17$ m, $T_{IN}=350^{\circ}\text{C}$

T_{IN} ($^{\circ}\text{C}$)	P(MPa)	B	η_2	$\rho_1(\text{kg/m}^3)$	$h_1(\text{J/kg})$	$g(\text{m/s}^2)$	D(m)	A(m^2)						
350	25	1.7E+23	3.277	625.45	1.62E+06	9.8	0.07	0.0044						
θ	Φ	K_1	K_2	C_{k1}	C_{k2}	C_{k3}	$h_t(\text{m})$	ρ_{2b}	ξ	$Q_s(\text{W})$	Q_s^*	B^*	$(B^*/\Phi)^{1/\eta_2-1}$	
0.937	0.410	1.0	1.0	6.99	19.05	13.35	17	256.5	9.35	4.60E+06	0.282	1.237	0.401	
0.748	0.395	2.0	1.0	12.00	18.99	13.39	17	247.3	9.37	4.80E+06	0.299	1.237	0.416	
0.624	0.383	3.0	1.0	17.01	19.03	13.48	17	239.3	9.36	5.00E+06	0.322	1.237	0.430	
0.535	0.371	4.0	1.0	21.95	18.95	13.45	17	232.2	9.38	5.50E+06	0.358	1.237	0.444	
0.469	0.361	5.0	1.0	26.96	18.97	13.51	17	225.8	9.37	5.70E+06	0.380	1.237	0.456	
0.418	0.352	6.0	1.0	31.90	19.00	13.57	17	220.1	9.36	5.90E+06	0.402	1.237	0.468	
0.375	0.343	7.0	1.0	36.84	18.94	13.61	17	214.6	9.38	6.30E+06	0.436	1.237	0.479	
0.343	0.336	8.0	1.0	41.85	19.01	13.61	17	209.9	9.36	6.60E+06	0.467	1.237	0.489	
0.314	0.328	9.0	1.0	46.86	19.01	13.67	17	205.4	9.36	6.75E+06	0.488	1.237	0.499	

Table D9: Water: 2 m, $h_t=14$ m, $T_{IN}=340^{\circ}\text{C}$

T_{IN} ($^{\circ}\text{C}$)	P(MPa)	B	η_2	$\rho_1(\text{kg/m}^3)$	$h_1(\text{J/kg})$	$g(\text{m/s}^2)$	D(m)	A(m^2)						
340	25	1.7E+23	3.277	6.55E+02	1.56E+06	9.8	0.07	0.0044						
θ	Φ	K_1	K_2	C_{k1}	C_{k2}	C_{k3}	$h_t(\text{m})$	ρ_{2b}	ξ	$Q_s(\text{W})$	Q_s^*	B^*	$(B^*/\Phi)^{1/\eta_2-1}$	
1.691	0.442	1.0	4.0	7.23	32.55	12.02	14	289.7	6.49	4.20E+06	0.329	1.354	0.407	
1.340	0.431	2.0	4.0	12.25	32.61	12.09	14	282.2	6.49	4.30E+06	0.347	1.354	0.418	
1.109	0.420	3.0	4.0	17.26	32.63	12.15	14	275.4	6.48	4.40E+06	0.364	1.354	0.429	
0.947	0.411	4.0	4.0	22.27	32.64	12.21	14	269.2	6.48	4.50E+06	0.381	1.354	0.439	

Table D8: Water: 2 m, $h_t=17$ m, $T_{IN}=350^{\circ}\text{C}$ (con...)

Conv Flowrate			Peak Flowrate			Q_b				T	Time Step	Time Period
(kg/s)	G_s	G_s^*	(kg/s)	G_m	G_m^*	(W)	Q_b^*	ρ_2	R_s^*	($^{\circ}\text{C}$)	(s)	(s)
10.06	2285.73	0.391	10.774	2448.47	0.419	7.40E+06	0.423	357.42	0.571	383.83	0.25	8.2
9.89	2247.83	0.384	10.367	2355.93	0.402	7.41E+06	0.440	329.45	0.527	384.52	0.25	7.4
9.57	2175.18	0.372	10.011	2275	0.389	7.42E+06	0.456	320.16	0.512	384.73	0.25	8.0
9.45	2148.39	0.366	9.695	2203.35	0.376	7.20E+06	0.457	289.00	0.462	385.51	0.25	6.8
9.24	2100.17	0.358	9.414	2139.35	0.365	7.25E+06	0.474	273.74	0.438	386.03	0.25	6.4
9.04	2054.94	0.351	9.159	2081.51	0.355	7.26E+06	0.488	258.42	0.413	386.66	0.25	6.1
8.90	2022.40	0.345	8.927	2028.83	0.346	7.27E+06	0.501	228.75	0.366	387.54	0.25	5.2
8.70	1976.79	0.338	8.715	1980.52	0.338	7.28E+06	0.514	219.11	0.350	389.36	0.25	5.2
8.52	1937.02	0.331	8.512	1934.43	0.330	7.28E+06	0.527	208.26	0.333	390.59	0.25	5.2

Table D9: Water: 2 m, $h_t=14$ m, $T_{IN}=340^{\circ}\text{C}$ (con...)

Conv Flowrate			Peak Flowrate			Q_b				T	Time Step	Time Period
(kg/s)	G_s	G_s^*	(kg/s)	G_m	G_m^*	(W)	Q_b^*	ρ_2	R_s^*	($^{\circ}\text{C}$)	(s)	(s)
8.19	1860.55	0.421	8.330	1893.18	0.445	5.60E+06	0.432	342.14	0.522	384.24	0.25	7.9
7.95	1806.13	0.330	8.109	1842.87	0.434	5.60E+06	0.443	339.83	0.519	384.29	0.25	7.7
7.76	1762.78	0.392	7.908	1797.14	0.423	5.40E+06	0.438	332.08	0.507	384.18	0.25	7.7
7.58	1723.43	0.421	7.725	1755.64	0.413	5.40E+06	0.449	324.87	0.496	384.64	0.25	8.0

$T_{IN}(^{\circ}C)$	P(MPa)	B	η_2	$\rho_1(kg/m^3)$	$h_1(J/kg)$	$g(m/s^2)$	D(m)	A(m ²)	Table D10: Water: 2 m, $h_t=14$ m, $T_{in}=360^{\circ}C$					
360	25	1.7E+23	3.277	5.89E+02	1.70E+06	9.8	0.07	0.0044						
θ	Φ	K_1	K_2	C_{k1}	C_{k2}	C_{k3}	h_t	ρ_{2b}	ξ	Q_s	Q_s^*	B^*	$(B^*/\Phi)^{1/\eta_2-1}$	
0.959	0.412	1.0	1.0	6.80	17.35	11.29	14	242.6	8.89	4.60E+06	0.289	1.13	0.362	
0.754	0.396	2.0	1.0	11.81	17.41	11.29	14	259.4	8.88	5.00E+06	0.323	1.13	0.378	
0.617	0.382	3.0	1.0	16.82	17.40	11.37	14	250.2	8.88	5.20E+06	0.347	1.13	0.394	
0.526	0.370	4.0	1.0	21.77	17.46	11.43	14	242.3	8.86	5.40E+06	0.372	1.13	0.407	
0.456	0.359	5.0	1.0	26.78	17.43	11.43	14	235.1	8.87	5.50E+06	0.389	1.13	0.420	
0.402	0.349	6.0	1.0	31.78	17.43	11.56	14	228.5	8.87	5.90E+06	0.430	1.13	0.433	
0.364	0.341	7.0	1.0	36.73	17.56	11.56	14	223.1	8.84	6.20E+06	0.464	1.13	0.443	
0.329	0.332	8.0	1.0	41.74	17.57	11.62	14	217.7	8.84	6.40E+06	0.491	1.13	0.454	
0.301	0.325	9.0	1.0	46.75	17.58	11.68	14	212.7	8.83	6.80E+06	0.537	1.13	0.464	
0.278	0.318	10.0	1.0	51.75	17.62	11.74	14	208.3	8.82	7.00E+06	0.567	1.13	0.474	
0.983	0.413	8.0	8.0	41.88	53.54	12.61	14	243.46	5.06	5.10E+06	0.599	1.13	0.360	
0.985	0.413	9.0	8.0	41.82	53.64	12.65	14	243.54	5.06	5.20E+06	0.619	1.13	0.360	
Table D10: Water: 2 m, $h_t=14$ m, $T_{IN}=360^{\circ}C$ (con...)														
C Flow	G_s	G_s^*	Pflow	G_m	G_m^*	Q_b	Q_b^*	ρ_2	R_s^*	Time Step (s)	Time Period (s)			
9.37	2130.2	0.407	9.63	2189.20	0.418	6.10E+06	0.373	297.72	0.51	0.25	6.8			
9.10	2069.0	0.396	9.24	2099.22	0.401	6.12E+06	0.390	270.69	0.46	0.25	6.2			
8.81	2002.6	0.383	8.89	2021.49	0.386	6.14E+06	0.406	253.49	0.43	0.25	6.0			
8.55	1942.6	0.372	8.59	1953.27	0.374	6.16E+06	0.422	237.45	0.40	0.25	5.6			
8.31	1889.5	0.361	8.13	1847.19	0.353	6.18E+06	0.448	218.70	0.37	0.25	5.0			
8.09	1837.4	0.351	8.09	1838.21	0.352	6.20E+06	0.451	204.87	0.35	0.25	4.7			
7.87	1788.9	0.343	7.87	1789.07	0.343	6.20E+06	0.464	188.55	0.32	0.25	4.5			
7.67	1742.6	0.335	7.65	1738.55	0.334	6.20E+06	0.477	176.69	0.30	0.25	4.5			
7.46	1694.8	0.326	7.49	1702.99	0.327	6.20E+06	0.487	159.59	0.27	0.25	4.5			
7.27	1651.9	0.318	7.33	1664.92	0.320	6.20E+06	0.498	149.64	0.25	0.25	4.0			
5.01	1139.3	0.382	5.44	1235.85	0.414	3.50E+06	0.3789	137.038	0.23	0.25	2.8			
4.94	1123.8	0.377	5.37	1219.28	0.409	3.50E+06	0.3841	134.907	0.23	0.25	2.9			

Table D11: Carbon-dioxide 1 m, $T_{IN}=25^{\circ}C$, $h_t=14$ m

T_{IN} ($^{\circ}C$)	P(MPa)	B	η_2	$\rho_1(kg/m^3)$	$h_1(J/kg)$	$g(m/s^2)$	D(m)	A(m^2)					
25	8	1.32E+18	2.797	777.4	263300	9.8	0.07485	0.0044					
θ	Φ	K_1	K_2	C_{k1}	C_{k2}	C_{k3}	$h_t(m)$	ρ_{2b}	ξ	$Q_s(W)$	Q_s^*	B^*	$(B^*/\Phi)^{1/\eta_2}-1$
1.16	0.42	2.0	3.0	11.8	26.1	10.8	14	328.61	7.25	1.50E+06	0.547	1.178	0.443
0.69	0.39	5.0	3.0	26.8	26.2	11.0	14	303.34	7.24	1.55E+06	0.614	1.178	0.484
0.94	0.41	1.0	1.0	6.7	16.0	10.4	14	319.00	9.26	1.40E+06	0.408	1.178	0.458
0.72	0.39	2.0	1.0	11.7	15.9	10.4	14	305.37	9.28	1.50E+06	0.454	1.178	0.481
0.58	0.38	3.0	1.0	16.7	15.9	10.5	14	293.63	9.30	1.60E+06	0.502	1.178	0.502
0.49	0.36	4.0	1.0	21.7	15.8	10.6	14	283.19	9.32	1.80E+06	0.587	1.178	0.521

Table D12: Carbon-dioxide 1 m, $T_{IN}=25^{\circ}C$, $h_t=10$ m

1.20	0.42	2.0	5.0	11.8	24.2	8.4	10	330.09	6.36	1.40E+06	0.585	1.178	0.440
0.96	0.41	1.0	1.0	6.7	14.2	8.0	10	320.13	8.31	1.10E+06	0.357	1.178	0.456
0.72	0.39	2.0	1.0	11.7	14.2	8.1	10	305.11	8.30	1.15E+06	0.393	1.178	0.481
0.57	0.38	3.0	1.0	16.8	14.2	8.2	10	292.42	8.30	1.20E+06	0.428	1.178	0.504
0.40	0.35	5.0	1.0	26.8	14.2	8.3	10	271.53	8.31	1.30E+06	0.495	1.178	0.544
0.35	0.34	6.0	1.0	31.8	14.2	8.3	10	262.91	8.31	1.35E+06	0.530	1.178	0.562
0.31	0.33	7.0	1.0	36.8	14.1	8.4	10	254.94	8.33	1.50E+06	0.606	1.178	0.580

Table D13: Carbon-dioxide 1 m, $T_{IN}=25^{\circ}C$, $h_t=17$ m

0.78	0.40	1.0	0.5	6.7	14.7	12.1	17	309.57	10.66	1.45E+06	0.384	1.178	0.474
0.60	0.38	2.0	0.5	11.8	14.5	12.3	17	295.28	10.73	1.50E+06	0.413	1.178	0.499
0.48	0.36	3.0	0.5	17.0	14.3	12.5	17	282.70	10.80	1.60E+06	0.454	1.178	0.522
0.42	0.35	4.0	0.5	21.9	14.4	12.4	17	273.97	10.75	1.66E+06	0.487	1.178	0.540
0.36	0.34	5.0	0.5	26.8	14.3	12.5	17	264.72	10.80	1.80E+06	0.543	1.178	0.559
1.38	0.43	1.0	3.0	6.9	27.2	12.8	17	336.15	7.82	1.40E+06	0.459	1.178	0.431

Table D11: Carbon-dioxide 1 m, $T_{IN}=25^{\circ}C$, $h_t=14$ m (cont...)

Conv Flowrate	G_s	G_s^*	Peak Flowrate	G_m	G_m^*	Q_b	Q_b^*	ρ_2	R_s^*	T	Time Step	Time Period
(kg/s)	(kg/m ² /s)		(kg/s)	(kg/m ² /s)		(W)		(kg/m ³)		(°C)	(s)	(s)
10.41	2364.9	0.420	10.493	2384.6	0.423	1.20E+06	0.434	268.3	0.345	40.76	0.25	4.3
9.59	2178.4	0.387	9.671	2197.8	0.391	1.20E+06	0.471	245.0	0.315	43.85	0.25	3.0
13.02	2959.6	0.411	13.161	2990.9	0.415	1.60E+06	0.462	358.8	0.461	35.68	0.25	5.7
12.54	2850.5	0.395	12.588	2860.7	0.396	1.60E+06	0.483	324.8	0.418	36.68	0.25	5.0
12.10	2749.3	0.380	12.097	2749.2	0.380	1.60E+06	0.502	293.5	0.378	38.31	0.25	4.5
11.65	2647.7	0.365	11.669	2652	0.366	1.60E+06	0.521	248.2	0.319	43.18	0.25	4.2

Table D12: Carbon-dioxide 1 m, $T_{IN}=25^{\circ}C$, $h_t=10$ m (cont...)

9.08	2064.3	0.417	9.253	2102.7	0.425	1.20E+06	0.493	249.5	0.321	43.27	0.25	3.6
11.69	2657.0	0.411	11.892	2702.6	0.418	1.60E+06	0.511	373.7	0.481	35.44	0.25	3.5
11.13	2528.9	0.392	11.304	2569.0	0.398	1.60E+06	0.538	357.9	0.460	35.74	0.25	3.6
10.65	2421.2	0.375	10.809	2456.5	0.381	1.60E+06	0.562	343.9	0.442	36.07	0.15	4.4
9.97	2266.4	0.351	10.018	2276.6	0.352	1.60E+06	0.607	298.7	0.384	38.06	0.15	5.1
9.68	2199.5	0.340	9.693	2202.8	0.341	1.60E+06	0.627	277.6	0.357	39.57	0.15	5.0
9.41	2138.1	0.330	9.403	2136.9	0.330	1.60E+06	0.646	239.8	0.308	44.72	0.15	4.5

Table D13: Carbon-dioxide 1 m, $T_{IN}=25^{\circ}C$, $h_t=17$ m (cont...)

14.35	3260.2	0.393	14.739	3349.6	0.404	2.00E+06	0.515	378.3	0.487	44.72	0.25	6.4
13.80	3136.2	0.376	14.080	3199.9	0.383	2.00E+06	0.539	354.9	0.457	45.72	0.25	6.3
13.38	3039.6	0.362	13.586	3087.6	0.368	2.00E+06	0.559	324.3	0.417	46.72	0.25	6.1
12.95	2942.8	0.352	13.024	2959.9	0.354	2.00E+06	0.583	302.7	0.389	47.72	0.25	5.8
12.59	2861.5	0.341	12.591	2861.5	0.341	2.00E+06	0.603	302.7	0.389	48.72	0.25	5.3
11.58	2632.7	0.433	11.585	2632.7	0.433	1.40E+06	0.459	302.7	0.389	49.72	0.25	5.0

Table D14: Carbon-dioxide 1 m, $T_{IN}=27^{\circ}C$, $h_t=14$ m

T_{IN} ($^{\circ}C$)	P(MPa)	B	η_2	ρ_1 (kg/m ³)	h_1 (J/kg)	g (m/s ²)	D(m)	A(m ²)					
27	8	1.32E+18	2.797	750.059	270611	9.8	0.07485	0.0044					
θ	Φ	K_1	K_2	C_{k1}	C_{k2}	C_{k3}	h_t (m)	ρ_{2b}	ξ	Q_s (W)	Q_s^*	B^*	$(B^*/\Phi)^{1/\eta_2-1}$
0.92	0.41	1.0	1.0	6.7	15.8	10.3	14	306.98	9.33	1.45E+06	0.422	1.131	0.438
0.69	0.39	2.0	1.0	11.8	15.5	10.7	14	292.26	9.42	1.50E+06	0.458	1.131	0.464
0.57	0.38	3.0	1.0	16.8	15.5	10.6	14	281.76	9.40	1.60E+06	0.506	1.131	0.483
0.15	0.26	1.0	3.0	6.9	2.6	10.9	14	197.31	23.02	1.30E+06	0.459	1.131	0.684
1.14	0.42	2.0	3.0	11.9	26.0	10.9	14	316.50	7.26	1.35E+06	0.491	1.131	0.423
0.93	0.41	3.0	3.0	16.8	25.9	10.9	14	307.53	7.27	1.40E+06	0.529	1.131	0.437

Table D14: Carbon-dioxide 1 m, $T_{IN}=27^{\circ}C$, $h_t=14$ m (cont...)

Conv Flowrate	G_s	G_s^*	Peak Flowrate	G_m	G_m^*	Q_b	Q_b^*	ρ_2	R_s^*	T	Time Step	Time Period
(kg/s)	(kg/m ² /s)		(kg/s)	(kg/m ² /s)		(W)		(kg/m ³)		($^{\circ}C$)	(s)	(s)
12.7033	2887.0	0.412	12.739	2895	0.414	1.60E+06	0.464	319.61	0.426	36.93	0.25	3.7
12.1085	2751.8	0.389	12.811	2911.5	0.412	1.60E+06	0.462	297.59	0.397	38.11	0.25	4.7
11.6814	2654.7	0.377	11.703	2659.6	0.377	1.60E+06	0.505	250.95	0.335	42.81	0.25	4.7
10.4738	2380.3	0.138	10.491	2384.2	0.138	1.20E+06	0.423	295.44	0.394	38.35	0.15	5.5
10.1616	2309.3	0.424	10.162	2309.4	0.424	1.20E+06	0.436	309.84	0.413	37.46	0.15	5.5
9.7866	2224.1	0.408	9.868	2242.5	0.411	1.20E+06	0.449	255.84	0.341	42.24	0.15	4.8

Table D15: Carbon-dioxide 2 m, $T_{IN} = 25^{\circ}C$, $h_t = 14$ m

T_{IN} ($^{\circ}C$)	P(MPa)	B	η_2	ρ_1 (kg/m ³)	h_1 (J/kg)	g(m/s ²)	D(m)	A(m ²)					
25	8	1.32E+18	2.8	777.4	2.6E+05	9.8	0.07485	0.0044					
θ	Φ	K_1	K_2	C_{k1}	C_{k2}	C_{k3}	h_t (m)	ρ_{2b}	ξ	Q_s (W)	Q_s^*	B^*	$(B^*/\Phi)^{1/\eta_2} - 1$
0.71	0.39	5.0	3.0	26.5	26.5	11.0	14	304.48	7.19	1.50E+06	0.594	1.178	0.482
0.97	0.41	1.0	1.0	6.4	16.4	10.4	14	320.69	9.16	1.30E+06	0.383	1.178	0.455
0.74	0.40	2.0	1.0	11.5	16.3	10.4	14	307.09	9.18	1.40E+06	0.426	1.178	0.478
0.60	0.38	3.0	1.0	16.5	16.3	10.5	14	295.49	9.19	1.45E+06	0.458	1.178	0.498
0.51	0.37	4.0	1.0	21.5	16.2	10.6	14	285.35	9.19	1.48E+06	0.483	1.178	0.517
0.44	0.36	5.0	1.0	26.5	16.2	10.1	14	277.35	9.19	1.50E+06	0.506	1.178	0.533
0.38	0.35	6.0	1.0	31.5	16.2	10.7	14	268.29	9.20	1.60E+06	0.554	1.178	0.551
0.34	0.34	7.0	1.0	36.4	16.2	10.8	14	261.09	9.20	1.80E+06	0.643	1.178	0.566
0.31	0.33	8.0	1.0	41.4	16.2	10.8	14	254.55	9.19	1.90E+06	0.701	1.178	0.581

Table D16: Carbon-dioxide 2 m, $T_{IN} = 25^{\circ}C$, $h_t = 10$ m

0.99	0.41	1.0	1.0	6.5	14.3	8.0	10	321.45	8.28	1.30E+06	0.418	1.178	0.454
0.73	0.39	2.0	1.0	11.5	14.3	8.1	10	306.29	8.27	1.35E+06	0.455	1.178	0.479
0.58	0.38	3.0	1.0	16.5	14.3	8.2	10	293.38	8.28	1.40E+06	0.492	1.178	0.502
0.48	0.36	4.0	1.0	21.5	14.3	8.2	10	282.40	8.27	1.45E+06	0.530	1.178	0.523
0.41	0.35	5.0	1.0	26.5	14.3	8.3	10	272.57	8.28	1.50E+06	0.568	1.178	0.542
0.36	0.34	6.0	1.0	31.5	14.4	8.3	10	264.36	8.26	1.55E+06	0.607	1.178	0.559
0.90	0.41	0.1	0.5	2.1	11.3	10.4	10	317.13	9.33	1.50E+06	0.420	1.178	0.461
0.86	0.41	0.2	0.5	2.6	11.3	10.4	10	314.86	9.33	1.51E+06	0.426	1.178	0.465
0.79	0.40	0.3	0.5	3.3	11.0	10.5	10	310.62	9.46	1.52E+06	0.430	1.178	0.472
0.77	0.40	0.4	0.5	3.8	11.0	10.5	10	308.85	9.45	1.52E+06	0.435	1.178	0.475
0.75	0.40	0.5	0.5	4.3	11.0	10.5	10	307.29	9.42	1.53E+06	0.439	1.178	0.478
0.73	0.39	0.6	0.5	4.8	11.0	10.4	10	306.00	9.42	1.53E+06	0.443	1.178	0.480
0.70	0.39	0.7	0.5	5.3	11.0	10.4	10	303.96	9.43	1.53E+06	0.445	1.178	0.483
0.68	0.39	0.8	0.5	5.8	11.0	10.5	10	302.06	9.42	1.53E+06	0.449	1.178	0.487
0.66	0.39	0.9	0.5	6.3	11.1	10.5	10	300.40	9.42	1.53E+06	0.454	1.178	0.490

Table D15: Carbon-dioxide 2 m, $T_{IN}=25^{\circ}C$, $h_t=14$ m (cont...)

Conv Flowrate	G_s	G_s^*	Peak Flowrate	G_m	G_m^*	Q_b	Q_b^*	ρ_2	R_s^*	Temp	Time Step	Time Period
(kg/s)	(kg/m ² /s)		(kg/s)	(kg/m ² /s)		(W)		(kg/m ³)		(^o C)	(s)	(s)
9.6	2179.88	0.390	9.675	2198.7	0.393	1.20E+06	0.471	245.13	0.315	43.82	0.25	6.0
12.9	2932.50	0.412	13.170	2993.0	0.420	1.60E+06	0.461	379.52	0.488	35.31	0.25	6.0
12.5	2834.00	0.397	12.597	2862.7	0.401	1.60E+06	0.482	344.79	0.444	36.01	0.25	6.5
12.0	2734.66	0.383	12.106	2751.2	0.385	1.60E+06	0.502	322.30	0.415	36.75	0.25	5.8
11.6	2645.81	0.370	11.677	2653.7	0.371	1.60E+06	0.520	301.41	0.388	37.78	0.25	5.3
11.3	2560.74	0.358	11.300	2568.0	0.359	1.60E+06	0.538	291.37	0.375	38.42	0.25	5.0
11.0	2491.02	0.348	10.961	2490.9	0.348	1.60E+06	0.554	264.06	0.340	40.96	0.25	5.0
10.6	2415.09	0.338	10.653	2421.0	0.339	1.60E+06	0.570	223.66	0.288	48.04	0.25	4.7
10.3	2340.46	0.328	10.374	2357.5	0.330	1.60E+06	0.586	202.89	0.261	54.35	0.25	3.7

Table D16: Carbon-dioxide 2 m, $T_{IN}=25^{\circ}C$, $h_t=10$ m (cont...)

11.8	2683.98	0.417	11.905	2705.6	0.420	1.60E+06	0.510	351.35	0.452	35.90	0.25	5.4
11.3	2561.95	0.398	11.315	2571.5	0.400	1.60E+06	0.537	324.55	0.417	36.74	0.25	5.0
10.8	2456.84	0.382	10.819	2458.8	0.382	1.60E+06	0.562	300.14	0.386	37.95	0.25	4.6
10.4	2361.55	0.367	10.393	2362.0	0.368	1.60E+06	0.585	288.06	0.371	38.77	0.25	4.5
10.0	2281.03	0.355	9.700	2204.4	0.343	1.60E+06	0.626	257.69	0.331	41.84	0.25	4.0
9.7	2205.28	0.344	9.409	2138.3	0.333	1.60E+06	0.646	239.28	0.308	44.81	0.25	3.7
13.6	3080.53	0.425	13.646	3101.2	0.428	1.80E+06	0.501	349.62	0.450	35.93	0.35	4.8
13.5	3060.42	0.422	13.547	3078.8	0.425	1.80E+06	0.505	345.40	0.444	36.04	0.35	4.8
13.4	3041.81	0.414	13.451	3057.0	0.416	1.80E+06	0.508	340.30	0.438	36.18	0.35	4.5
13.3	3018.36	0.411	13.358	3035.7	0.413	1.80E+06	0.512	340.98	0.439	36.16	0.35	4.8
13.2	2998.17	0.409	13.267	3015.0	0.412	1.80E+06	0.515	338.83	0.436	36.22	0.35	4.8
13.1	2978.49	0.407	13.178	2994.8	0.409	1.80E+06	0.519	336.74	0.433	36.29	0.35	4.6
13.0	2962.40	0.404	13.091	2975.0	0.406	1.80E+06	0.522	330.84	0.426	36.48	0.35	4.5
13.0	2943.27	0.402	13.006	2955.7	0.404	1.80E+06	0.526	328.63	0.423	36.40	0.35	4.6
12.8	2914.97	0.398	12.923	2936.9	0.401	1.80E+06	0.529	328.74	0.423	36.56	0.35	4.6

Table D17: Carbon-dioxide 2 m, $T_{IN}=25^{\circ}C$, $h_t=17$ m

T_{IN} ($^{\circ}C$)	P(MPa)	B	η_2	ρ_1 (kg/m ³)	h_1 (J/kg)	g (m/s ²)	D(m)	A(m ²)					
25	8	1.32E+18	2.8	777.4	2.6E+05	9.8	0.07485	0.0044					
θ	Φ	K_1	K_2	C_{k1}	C_{k2}	C_{k3}	h_t (m)	ρ_{2b}	ξ	Q_s (W)	Q_s^*	B^*	$(B^*/\Phi)^{1/\eta_2-1}$
0.79	0.40	1.0	0.5	6.6	14.7	12.1	17	309.99	10.65	1.51E+06	0.397	1.178	0.473
0.62	0.38	2.0	0.5	11.6	14.8	12.2	17	297.27	10.61	1.53E+06	0.419	1.178	0.495
0.50	0.37	3.0	0.5	16.8	14.6	12.4	17	284.38	10.70	1.53E+06	0.437	1.178	0.519
0.42	0.35	4.0	0.5	21.8	14.5	12.5	17	274.44	10.71	1.56E+06	0.460	1.178	0.539
0.37	0.34	5.0	0.5	26.7	14.6	12.5	17	266.13	10.69	1.65E+06	0.500	1.178	0.556

Table D18: Carbon-dioxide 2 m, $T_{IN}=27^{\circ}C$, $h_t=14$ m

T_{in} ($^{\circ}C$)	P(MPa)	B	η_2	P_1 (kg/m ³)	h_1 (J/kg)	g (m/s ²)	D(m)	A(m ²)					
27	8	1.32E+18	2.8	750.059	270611	9.8	0.07485	0.0044					
θ	Φ	K_1	K_2	C_{k1}	C_{k2}	C_{k3}	h_t (m)	ρ_{2b}	ξ	Q_s (W)	Q_s^*	B^*	$(B^*/\Phi)^{1/\eta_2-1}$
0.97	0.41	1.0	1.0	6.4	16.2	10.3	14	309.51	9.20	1.30E+06	0.379	1.131	0.434
0.75	0.40	2.0	1.0	11.4	16.3	10.4	14	296.61	9.19	1.40E+06	0.427	1.131	0.456
0.60	0.38	3.0	1.0	16.4	16.2	10.4	14	285.31	9.20	1.50E+06	0.474	1.131	0.476
0.51	0.37	4.0	1.0	21.4	16.2	10.5	14	275.42	9.20	1.55E+06	0.507	1.131	0.495
0.44	0.36	5.0	1.0	26.4	16.2	10.6	14	266.81	9.20	1.65E+06	0.559	1.131	0.512
0.80	0.40	1.0	0.5	6.5	13.4	10.2	14	300.14	10.11	1.45E+06	0.400	1.131	0.450
0.61	0.38	2.0	0.5	11.5	13.4	10.3	14	285.95	10.13	1.50E+06	0.431	1.131	0.475
0.50	0.37	3.0	0.5	16.6	13.3	10.4	14	273.98	10.14	1.55E+06	0.463	1.131	0.498
0.42	0.35	4.0	0.5	21.5	13.4	10.5	14	264.28	10.10	1.58E+06	0.491	1.131	0.517
0.36	0.34	5.0	0.5	26.5	13.5	10.6	14	255.44	10.09	1.60E+06	0.516	1.131	0.536
0.27	0.32	6.0	0.5	38.6	13.2	10.7	14	236.35	10.18	1.80E+06	0.599	1.131	0.579

Table D17: Carbon-dioxide 2 m, $T_{IN}=25^{\circ}C$, $h_t=17$ m (cont...)

Conv Flowrate	G_s	G_s^*	Peak Flowrate	G_m	G_m^*	Q_b	Q_b^*	ρ_2	R_s^*	T	Time Step	Time Period
(kg/s)	(kg/m ² /s)		(kg/s)	(kg/m ² /s)		(W)		(kg/m ³)		(^o C)	(s)	(s)
14.5	3286.89	0.397	14.752	3352.5	0.405	2.00E+06	0.515	364.73	0.469	35.52	0.25	6.4
13.8	3144.96	0.381	14.093	3202.7	0.388	2.00E+06	0.539	350.48	0.451	35.80	0.25	6.0
13.3	3019.56	0.363	13.527	3074.2	0.370	2.00E+06	0.562	340.56	0.438	36.45	0.25	6.0
12.9	2926.02	0.352	13.036	2962.6	0.356	2.00E+06	0.583	320.23	0.412	36.74	0.25	6.0
12.5	2847.89	0.343	12.602	2863.9	0.345	2.00E+06	0.603	294.41	0.379	38.11	0.25	5.0

Table D18: Carbon-dioxide 2 m, $T_{IN}=27^{\circ}C$, $h_t=14$ m (cont...)

Conv Flowrate	G_s	G_s^*	Peak Flowrate	G_m	G_m^*	Q_b	Q_b^*	ρ_2	R_s^*	Temp	Time Step	Time Period
(kg/s)	(kg/m ² /s)		(kg/s)	(kg/m ² /s)		(W)		(kg/m ³)		(^o C)	(s)	(s)
12.7	2881.7	0.418	12.749	2897.3	0.420	1.60E+06	0.464	329.40	0.439	36.54	0.25	6.0
12.1	2756.66	0.400	12.190	2770.3	0.402	1.60E+06	0.485	310.23	0.414	37.05	0.25	5.5
11.7	2659.21	0.385	11.711	2661.5	0.386	1.60E+06	0.505	285.79	0.381	38.90	0.25	5.5
11.3	2566.65	0.372	11.294	2566.7	0.372	1.60E+06	0.524	206.67	0.276	40.71	0.25	5.0
10.9	2480.95	0.360	10.925	2482.9	0.360	1.60E+06	0.541	240.95	0.321	44.42	0.25	4.6
13.4	3045.65	0.402	13.615	3094.1	0.408	1.80E+06	0.489	345.71	0.461	35.99	0.25	4.6
12.9	2921.27	0.384	12.948	2942.6	0.387	1.80E+06	0.514	312.89	0.417	37.18	0.25	5.6
12.4	2809.27	0.369	12.386	2814.8	0.370	1.80E+06	0.537	282.93	0.377	39.09	0.25	4.7
11.9	2701.01	0.356	11.902	2704.8	0.357	1.80E+06	0.559	271.87	0.362	40.11	0.25	4.8
11.5	2606.13	0.344	11.478	2608.4	0.345	1.80E+06	0.580	262.00	0.349	41.20	0.25	4.8
11.1	2522.83	0.330	11.102	2523.0	0.330	1.80E+06	0.599	223.26	0.298	48.12	0.25	4.6

Table D19: Hydrogen: 1 m, $T_{IN} = -243^{\circ}C$, $h_t = 14$ m

T_{IN} ($^{\circ}C$)	P(MPa)	B	η_2	ρ_1 (kg/m ³)	h_1 (J/kg)	g(m/s ²)	D(m)	A(m ²)						
-243	1.4	8.38E+10	1.7189	57.1422	1.4E+05	9.8	0.07	0.0044						
θ	Φ	K_1	K_2	C_{k1}	C_{k2}	C_{k3}	h_t (m)	ρ_{2b}	ξ	Q_s (W)	Q_s^*	B^*	$(B^*/\Phi)^{1/\eta_2}-1$	
0.87	0.41	1.00	1.00	7.27	16.49	11.62	14	23.18	9.12	1.70E+05	1.327	2.096	1.599	
0.69	0.39	2.00	1.00	12.16	16.48	11.70	14	22.28	9.12	1.75E+05	1.417	2.096	1.660	
0.57	0.38	3.00	1.00	17.24	16.53	11.78	14	21.48	9.11	1.80E+05	1.506	2.096	1.717	
0.49	0.36	4.00	1.00	22.19	16.59	11.78	14	20.81	9.09	1.90E+05	1.633	2.096	1.768	
0.43	0.35	5.00	1.00	27.13	16.58	11.77	14	20.20	9.10	2.00E+05	1.763	2.096	1.816	
0.37	0.34	6.00	1.00	32.21	16.51	11.84	14	19.60	9.12	2.10E+05	1.905	2.096	1.866	
0.34	0.33	7.00	1.00	37.16	16.60	11.91	14	19.12	9.09	2.15E+05	2.004	2.096	1.908	
0.31	0.33	8.00	1.00	42.17	16.63	11.97	14	18.66	9.08	2.15E+05	2.056	2.096	1.949	
0.28	0.32	9.00	1.00	47.18	16.63	12.02	14	18.22	9.08	2.15E+05	2.106	2.096	1.990	
0.26	0.31	10.00	1.00	52.19	16.69	12.08	14	17.84	9.07	2.15E+05	2.154	2.096	2.027	
0.74	0.39	1.00	0.50	7.25	13.91	11.50	14	22.57	9.93	1.70E+05	1.262	2.096	1.640	
0.58	0.38	2.00	0.50	12.27	13.89	11.60	14	21.57	9.94	1.75E+05	1.358	2.096	1.710	
0.48	0.36	3.00	0.50	17.22	13.95	11.67	14	20.76	9.92	1.85E+05	1.480	2.096	1.772	
0.41	0.35	4.00	0.50	22.23	13.95	11.68	14	20.03	9.92	1.95E+05	1.605	2.096	1.830	

Table D20: Hydrogen: 1 m, $T_{IN} = -243^{\circ}C$, $h_t = 10$ m

1.47	0.44	1.00	3.00	7.34	24.66	9.43	10	24.89	6.30	1.40E+05	1.450	2.096	1.494
1.14	0.42	2.00	3.00	12.29	24.69	9.42	10	24.10	6.30	1.50E+05	1.606	2.096	1.541
0.93	0.41	3.00	3.00	17.30	24.73	9.41	10	23.40	6.30	1.60E+05	1.766	2.096	1.585
0.78	0.40	4.00	3.00	22.25	24.74	9.48	10	22.76	6.29	1.65E+05	1.884	2.096	1.627
0.67	0.39	5.00	3.00	27.26	24.77	9.53	10	22.18	6.29	1.66E+05	1.946	2.096	1.667
0.59	0.38	6.00	3.00	32.27	24.79	9.59	10	21.65	6.29	1.67E+05	2.007	2.096	1.705
0.53	0.37	7.00	3.00	37.28	24.88	9.55	10	21.18	6.28	1.69E+05	2.054	2.096	1.739
0.48	0.36	8.00	3.00	42.29	24.90	9.59	10	20.73	6.27	1.69E+05	2.126	2.096	1.774
0.44	0.36	9.00	3.00	47.30	24.93	9.63	10	20.32	6.27	1.70E+05	2.178	2.096	1.806
0.40	0.35	10.00	3.00	52.31	24.95	9.67	10	19.93	6.27	1.70E+05	2.228	2.096	1.838

Table D19: Hydrogen: 1 m, $T_{IN} = -243^{\circ}C$, $h_t = 14$ m (con...)

Conv Flowrate	G_s	G_s^*	Peak Flowrate	G_m	G_m^*	Q_b	Q_b^*	ρ_2	R_s^*	Temp	Time Step	Time Period
(kg/s)	(kg/m ² /s)		(kg/s)	(kg/m ² /s)		(W)		(kg/m ³)		(^o C)	(s)	(s)
0.92	208.08	0.399	0.94	212.8762	0.408	2.10E+05	1.602	28.31	0.495	-239.54	0.25	5.9
0.88	200.66	0.385	0.90	204.2175	0.392	2.10E+05	1.670	26.67	0.467	-239.49	0.25	5.9
0.85	194.18	0.373	0.87	196.7178	0.378	2.10E+05	1.734	25.15	0.440	-239.42	0.25	5.9
0.83	188.93	0.364	0.84	190.1273	0.366	2.10E+05	1.794	23.15	0.405	-239.29	0.25	5.9
0.81	184.25	0.354	0.81	184.2639	0.354	2.10E+05	1.851	20.12	0.352	-238.93	0.25	4.5
0.79	179.03	0.344	0.79	178.9687	0.344	2.10E+05	1.906	18.92	0.331	-238.70	0.25	2.1
0.77	174.22	0.335	0.77	174.1962	0.335	2.10E+05	1.958	18.31	0.320	-238.51	0.25	2.2
0.75	169.84	0.327	0.75	169.8328	0.327	2.10E+05	2.008	17.75	0.311	-238.38	0.25	2.2
0.73	165.81	0.319	0.73	165.833	0.320	2.10E+05	2.057	17.23	0.302	-238.22	0.25	2.1
0.71	162.10	0.313	0.71	162.1286	0.313	2.10E+05	2.104	16.75	0.293	-238.04	0.25	2.1
0.96	218.81	0.386	1.00	226.7391	0.400	2.50E+05	1.791	18.31	0.320	-238.51	0.25	6.0
0.92	209.31	0.369	0.95	216.3987	0.381	2.50E+05	1.876	17.75	0.311	-238.38	0.25	6.0
0.89	203.05	0.358	0.91	207.3992	0.366	2.50E+05	1.958	17.23	0.302	-238.22	0.25	5.5
0.87	197.31	0.348	0.89	201.7631	0.356	2.50E+05	2.013	16.75	0.293	-238.04	0.25	5.0

Table D20: Hydrogen: 1 m, $T_{IN} = -243^{\circ}C$, $h_t = 10$ m (con...)

0.69	156.83	0.435	0.69	156.1743	0.434	1.70E+05	1.768	29.27	0.512	-239.97	0.25	5.4
0.67	151.75	0.422	0.66	151.0155	0.419	1.70E+05	1.828	27.27	0.477	-239.51	0.25	5.2
0.65	147.16	0.409	0.64	146.4021	0.407	1.70E+05	1.886	23.82	0.417	-239.35	0.25	5.2
0.63	142.29	0.396	0.62	141.3796	0.393	1.70E+05	1.953	23.32	0.408	-239.31	0.25	2.8
0.61	138.54	0.385	0.61	138.6297	0.386	1.60E+05	1.875	21.52	0.377	-239.14	0.25	2.0
0.59	135.14	0.376	0.60	135.3117	0.377	1.60E+05	1.921	19.83	0.347	-238.89	0.25	2.2
0.59	133.38	0.372	0.58	132.2891	0.369	1.60E+05	1.965	19.24	0.337	-238.73	0.25	2.1
0.57	129.12	0.360	0.57	129.4711	0.361	1.60E+05	2.007	18.70	0.327	-238.65	0.25	2.1
0.56	126.43	0.353	0.56	126.903	0.354	1.60E+05	2.048	18.70	0.327	-238.65	0.25	2.0
0.55	123.92	0.346	0.55	124.4713	0.348	1.60E+05	2.088	18.70	0.327	-238.65	0.25	2.0

Table D21: Hydrogen: 1 m, $T_{IN} = -243^{\circ}\text{C}$, $h_t = 17$ m

T_{IN} ($^{\circ}\text{C}$)	P(MPa)	B	η_2	$\rho_1(\text{kg/m}^3)$	$h_1(\text{J/kg})$	$g(\text{m/s}^2)$								
-243	1.4	8.38E+10	1.7189	57.1422	1.4E+05	9.8								
θ	Φ	K_1	K_2	C_{k1}	C_{k2}	C_{k3}	$h_t(\text{m})$	ρ_{2b}	ξ	$Q_s(\text{W})$	Q_s^*	B^*	$(B^*/\Phi)^{1/\eta_2-1}$	
0.87	0.41	1.00	1.00	7.20	18.19	13.60	17	23.19	9.57	1.70E+05	1.277	2.096	1.599	
0.71	0.39	2.00	1.00	12.20	18.19	13.60	17	22.36	9.57	1.80E+05	1.382	2.096	1.654	
0.59	0.38	3.00	1.00	17.15	18.14	13.59	17	21.63	9.58	1.90E+05	1.507	2.096	1.706	
0.51	0.37	4.00	1.00	22.16	18.17	13.69	17	20.98	9.58	1.95E+05	1.580	2.096	1.755	
0.44	0.36	5.00	1.00	27.11	18.11	13.81	17	20.37	9.59	2.00E+05	1.662	2.096	1.803	
0.40	0.35	6.00	1.00	32.12	18.17	13.76	17	19.86	9.58	2.05E+05	1.747	2.096	1.844	
0.36	0.34	7.00	1.00	37.13	18.20	13.83	17	19.37	9.57	2.10E+05	1.835	2.096	1.885	
0.33	0.33	8.00	1.00	42.14	18.70	13.90	17	19.05	9.44	2.20E+05	1.969	2.096	1.914	
0.30	0.32	9.00	1.00	47.14	18.26	13.96	17	18.52	9.55	2.20E+05	2.015	2.096	1.962	
0.28	0.32	10.00	1.00	52.16	18.28	14.02	17	18.14	9.55	2.20E+05	2.058	2.096	1.998	

Table D22: Hydrogen: 1 m, $T_{IN} = -245^{\circ}\text{C}$, $h_t = 14$ m

T_{IN} ($^{\circ}\text{C}$)	P(MPa)	B	η_2	$\rho_1(\text{kg/m}^3)$	$h_1(\text{J/kg})$	$g(\text{m/s}^2)$	D(m)	A(m^2)						
-245	1.4	8.38E+10	1.7189	61.6318	1.05E+05	9.8	0.07	0.0044	Time					
θ	Φ	K_1	K_2	C_{k1}	C_{k2}	C_{k3}	$h_t(\text{m})$	ρ_{2b}	ξ	$Q_s(\text{W})$	Q_s^*	B^*	$(B^*/\Phi)^{1/\eta_2-1}$	
1.84	0.45	1.00	5.00	7.51	36.90	12.58	14	27.48	6.10	1.60E+05	2.063	3.165	2.127	
1.48	0.44	2.00	5.00	12.45	36.94	12.57	14	26.85	6.09	1.62E+05	1.608	3.165	2.169	
1.23	0.43	3.00	5.00	17.46	36.95	12.63	14	26.26	6.09	1.63E+05	1.655	3.165	2.211	
1.05	0.42	4.00	5.00	22.47	37.01	12.68	14	25.72	6.09	1.64E+05	1.701	3.165	2.250	
0.92	0.41	5.00	5.00	27.48	37.03	12.73	14	25.21	6.09	1.65E+05	1.746	3.165	2.288	
0.82	0.40	6.00	5.00	32.49	36.98	12.58	14	24.76	6.09	1.66E+05	1.785	3.165	2.323	
0.74	0.39	7.00	5.00	37.43	37.11	12.83	14	24.32	6.08	1.66E+05	1.823	3.165	2.358	
0.67	0.39	8.00	5.00	42.41	37.12	12.87	14	23.91	6.08	1.66E+05	1.854	3.165	2.391	
0.62	0.38	9.00	5.00	47.45	37.13	12.91	14	23.52	6.08	1.66E+05	1.885	3.165	2.423	
0.57	0.38	10.00	5.00	52.45	37.20	12.89	14	23.17	6.07	1.66E+05	1.915	3.165	2.454	

Table D21: Hydrogen: 1 m, $T_{IN} = -243^{\circ}C$, $h_t = 17$ m (con...)

Conv Flowrate	G_s	G_s^*	Peak Flowrate	G_m	G_m^*	Q_b	Q_b^*	ρ_2	R_s^*	T	Time Step	Time Period
(kg/s)	(kg/m ² /s)		(kg/s)	(kg/m ² /s)		(W)		(kg/m ³)		(^o C)	(s)	(s)
0.95	216.28	0.395	0.99	224.01	0.410	2.50E+05	1.813	29.27	0.512	0.25	0.25	7.2
0.93	211.56	0.387	0.95	215.44	0.394	2.50E+05	1.885	27.27	0.477	0.25	0.25	6.5
0.90	204.75	0.374	0.92	207.97	0.380	2.50E+05	1.953	23.82	0.417	0.25	0.25	5.5
0.88	200.46	0.366	0.89	201.33	0.368	2.50E+05	2.017	23.32	0.408	0.25	0.25	5.4
0.86	195.49	0.357	0.86	195.49	0.357	2.40E+05	1.994	21.52	0.377	0.25	0.25	5.3
0.84	190.65	0.348	0.84	190.29	0.348	2.40E+05	2.049	19.83	0.347	0.25	0.25	2.4
0.82	185.85	0.340	0.82	185.54	0.339	2.10E+05	1.838	19.24	0.337	0.25	0.25	2.1
0.80	181.45	0.336	0.80	181.17	0.336	2.10E+05	1.883	18.70	0.327	0.25	0.25	2.2
0.78	177.38	0.325	0.78	177.15	0.325	2.10E+05	1.925	18.19	0.318	0.25	0.25	2.1
0.76	173.61	0.318	0.76	173.42	0.318	2.10E+05	1.967	17.72	0.310	0.25	0.25	2.0

Table D22: Hydrogen: 1 m, $T_{IN} = -245^{\circ}C$, $h_t = 14$ m (con...)

Conv Flowrate	G_s	G_s^*	Peak Flowrate	G_m	G_m^*	Q_b	Q_b^*	ρ_2	R_s^*	T	Time Step	Time Period
(kg/s)	(kg/m ² /s)		(kg/s)	(kg/m ² /s)		(W)		(kg/m ³)		(^o C)	(s)	(s)
0.74	167.34	0.445	0.74	167.49	0.446	1.70E+05	2.190	29.27	0.475	0.25	0.25	6.6
0.72	163.67	0.436	0.72	163.67	0.436	1.70E+05	2.241	27.27	0.443	0.25	0.25	3.3
0.70	160.01	0.426	0.70	160.02	0.426	1.70E+05	2.292	23.82	0.386	0.25	0.25	3.4
0.69	156.62	0.417	0.69	156.67	0.418	1.70E+05	2.341	23.32	0.378	0.25	0.25	3.2
0.68	153.52	0.409	0.68	154.47	0.412	1.70E+05	2.374	21.52	0.349	0.25	0.25	3.1
0.66	150.63	0.401	0.66	150.65	0.401	1.70E+05	2.434	19.83	0.322	0.25	0.25	3.0
0.65	147.95	0.395	0.65	147.95	0.395	1.70E+05	2.479	19.24	0.312	0.25	0.25	3.3
0.64	145.42	0.388	0.64	145.40	0.388	1.70E+05	2.522	18.70	0.303	0.25	0.25	3.2
0.63	143.05	0.382	0.63	143.02	0.382	1.70E+05	2.564	18.70	0.303	0.25	0.25	3.1
0.62	140.80	0.376	0.62	140.22	0.375	1.70E+05	2.615	18.70	0.303	0.25	0.25	3.0

Table D23: Hydrogen: 2 m, $T_{IN} = -243^{\circ}\text{C}$, $h_t = 14$ m

T_{IN} ($^{\circ}\text{C}$)	P(MPa)	B	η_2	$\rho_1(\text{kg/m}^3)$	$h_1(\text{J/kg})$	$g(\text{m/s}^2)$	D(m)	A(m^2)					
-243	1.4	8.38E+10	1.7189	57.1422	1.4E+05	9.8	0.07485	0.0044					
θ	Φ	K_1	K_2	C_{k1}	C_{k2}	C_{k3}	$h_t(\text{m})$	ρ_{2b}	ξ	$Q_s(\text{W})$	Q_s^*	B^*	$(B^*/\Phi)^{1/\eta_2-1}$
0.86	0.40	1.0	1.0	7.4	16.4	11.7	14	23.13	9.144	1.60E+05	1.262	2.096	1.603
0.69	0.39	2.0	1.0	12.3	16.5	11.7	14	22.25	9.124	1.70E+05	1.394	2.096	1.662
0.57	0.38	3.0	1.0	17.4	16.5	11.8	14	21.46	9.116	1.70E+05	1.433	2.096	1.719
0.48	0.36	4.0	1.0	22.3	16.6	11.9	14	20.78	9.105	1.75E+05	1.518	2.096	1.771
0.43	0.35	5.0	1.0	27.3	16.7	11.9	14	20.19	9.078	1.80E+05	1.604	2.096	1.817
0.38	0.34	6.0	1.0	32.3	16.6	11.9	14	19.61	9.097	1.90E+05	1.732	2.096	1.865
0.34	0.34	7.0	1.0	37.2	16.7	11.9	14	19.15	9.056	1.95E+05	1.826	2.096	1.905
0.31	0.33	8.0	1.0	42.2	16.7	12.0	14	18.68	9.061	2.00E+05	1.916	2.096	1.948
0.28	0.32	9.0	1.0	47.7	16.7	12.0	14	18.20	9.064	2.05E+05	2.009	2.096	1.992
0.26	0.31	10.0	1.0	52.2	16.7	12.1	14	17.85	9.059	2.10E+05	2.102	2.096	2.026

Table D24: Hydrogen: 2 m, $T_{IN} = -243^{\circ}\text{C}$, $h_t = 10$ m

0.87	0.41	1.0	1.0	7.4	14.4	9.1	10	23.19	8.253	1.50E+05	1.297	2.096	1.599
0.67	0.39	2.0	1.0	12.3	14.4	9.2	10	22.15	8.264	1.60E+05	1.435	2.096	1.669
0.54	0.37	3.0	1.0	17.3	14.4	9.2	10	21.29	8.238	1.63E+05	1.523	2.096	1.731
0.46	0.36	4.0	1.0	22.4	14.5	9.2	10	20.52	8.232	1.65E+05	1.600	2.096	1.790
0.40	0.35	5.0	1.0	27.3	14.5	9.3	10	19.85	8.232	1.68E+05	1.673	2.096	1.845
0.35	0.34	6.0	1.0	32.3	14.6	9.4	10	19.28	8.207	1.70E+05	1.747	2.096	1.894
0.31	0.33	7.0	1.0	37.3	14.6	9.3	10	18.76	8.184	1.75E+05	1.851	2.096	1.940
0.28	0.32	8.0	1.0	42.2	14.7	9.4	10	18.28	8.179	1.80E+05	1.949	2.096	1.985
0.26	0.31	9.0	1.0	47.2	14.7	9.4	10	17.83	8.173	1.85E+05	2.054	2.096	2.028
0.24	0.31	10.0	1.0	52.1	14.7	9.5	10	17.44	8.162	1.90E+05	2.160	2.096	2.068

Table D23: Hydrogen: 2 m, $T_{IN} = -243^{\circ}C$, $h_t = 14$ m (con...)

Conv Flowrate	G_s	G_s^*	Peak Flowrate	G_m	G_m^*	Q_b	Q_b^*	ρ_2	R_s^*	T	Time Step	Time Period
(kg/s)	(kg/m ² /s)		(kg/s)	(kg/m ² /s)		(W)		(kg/m ³)		(^o C)	(s)	(s)
0.91	206.00	0.394	0.94	212.88	0.407	2.10E+05	1.602	29.27	0.512	-239.97	0.25	7.14
0.87	198.07	0.380	0.90	204.37	0.392	2.10E+05	1.669	27.27	0.477	-239.51	0.25	6.7
0.85	192.75	0.370	0.87	196.88	0.378	2.10E+05	1.733	23.82	0.417	-239.35	0.25	6.5
0.82	187.24	0.360	0.84	190.27	0.366	2.10E+05	1.793	23.32	0.408	-239.31	0.25	6.0
0.80	182.27	0.351	0.81	184.39	0.355	2.10E+05	1.850	21.52	0.377	-239.14	0.25	5.5
0.78	178.16	0.343	0.79	178.88	0.344	2.10E+05	1.907	19.83	0.347	-238.89	0.25	5.6
0.76	173.49	0.335	0.77	174.33	0.337	2.10E+05	1.957	19.24	0.337	-238.73	0.25	5.4
0.75	169.52	0.327	0.75	169.96	0.328	2.10E+05	2.007	18.70	0.327	-238.65	0.25	4.6
0.73	165.78	0.320	0.73	165.95	0.320	2.10E+05	2.055	18.70	0.327	-238.65	0.25	4.8
0.71	162.25	0.313	0.71	162.24	0.313	2.10E+05	2.102	18.70	0.327	-238.65	0.25	4.8

Table D24: Hydrogen: 2 m, $T_{IN} = -243^{\circ}C$, $h_t = 10$ m (con...)

0.83	187.84	0.398	0.84	191.24	0.406	2.10E+05	1.784	29.27	0.512	-239.97	0.25	6.1
0.80	181.12	0.384	0.81	184.10	0.390	2.10E+05	1.853	27.27	0.477	-239.51	0.25	6.5
0.76	173.84	0.369	0.78	176.51	0.375	2.10E+05	1.932	23.82	0.417	-239.35	0.25	6.4
0.74	167.55	0.356	0.75	170.04	0.361	2.10E+05	2.006	23.32	0.408	-239.31	0.25	6.1
0.72	163.07	0.347	0.72	163.86	0.348	2.10E+05	2.082	21.52	0.377	-239.14	0.25	6.2
0.70	158.08	0.337	0.70	158.65	0.338	2.10E+05	2.150	19.83	0.347	-238.89	0.25	5.5
0.68	153.59	0.328	0.68	153.88	0.329	2.10E+05	2.217	19.24	0.337	-238.73	0.25	5.2
0.66	150.03	0.321	0.66	149.70	0.320	2.10E+05	2.279	18.70	0.327	-238.65	0.25	4.5
0.64	146.26	0.313	0.64	145.81	0.312	2.10E+05	2.339	18.70	0.327	-238.65	0.25	4.0
0.63	142.90	0.306	0.63	142.24	0.305	2.10E+05	2.398	18.70	0.327	-238.65	0.25	4.5

Table D25: Hydrogen: 2 m, $T_{IN} = -243^{\circ}\text{C}$, $h_t = 17$ m

$T_{IN} (^{\circ}\text{C})$	P(MPa)	B	η_2	$\rho_1(\text{kg/m}^3)$	$h_1(\text{J/kg})$	$g(\text{m/s}^2)$	D(m)	A(m ²)					
-243	1.4	8.38E+10	1.7189	57.14	1.4E+05	9.8	0.07485	0.0044					
θ	Φ	K_1	K_2	C_{k1}	C_{k2}	C_{k3}	$h_t(\text{m})$	ρ_{2b}	ξ	$Q_s(\text{W})$	Q_s^*	B^*	$(B^*/\Phi)^{1/\eta_2-1}$
1.78	0.44	1.0	5.0	7.3	38.2	14.2	17	25.39	6.61	1.60E+05	1.556	2.096	1.465
1.46	0.44	2.0	5.0	12.3	38.7	14.3	17	24.86	6.56	1.65E+05	1.642	2.096	1.496
1.23	0.43	3.0	5.0	17.2	38.8	14.3	17	24.35	6.55	1.70E+05	1.733	2.096	1.526
1.06	0.42	4.0	5.0	22.2	38.7	14.3	17	23.87	6.56	1.75E+05	1.832	2.096	1.556
0.83	0.40	5.0	5.0	32.2	38.8	14.5	17	23.00	6.56	1.80E+05	1.921	2.096	1.611
0.93	0.41	6.0	5.0	27.3	38.7	14.4	17	23.41	6.56	1.81E+05	1.968	2.096	1.585
0.75	0.40	7.0	5.0	37.2	38.7	14.5	17	22.60	6.56	1.82E+05	2.042	2.096	1.638
0.68	0.39	8.0	5.0	42.2	38.8	14.6	17	22.25	6.55	1.83E+05	2.079	2.096	1.663
0.63	0.38	9.0	5.0	47.2	38.8	14.6	17	21.89	6.55	1.84E+05	2.125	2.096	1.688
0.58	0.38	10.0	5.0	52.2	38.8	14.7	17	21.56	6.55	1.85E+05	2.170	2.096	1.711

Table D26: Hydrogen: 2 m, $T_{IN} = -245^{\circ}\text{C}$, $h_t = 14$ m

$T_{IN} (^{\circ}\text{C})$	P(MPa)	B	η_2	$\rho_1(\text{kg/m}^3)$	$h_1(\text{J/kg})$	$g(\text{m/s}^2)$	D(m)	A(m ²)					
-245	1.4	8.38E+10	1.7189	61.63	1.05E+05	9.8	0.07485	0.0044					
θ	Φ	K_1	K_2	C_{k1}	C_{k2}	C_{k3}	$h_t(\text{m})$	ρ_{2b}	ξ	$Q_s(\text{W})$	Q_s^*	B^*	$(B^*/\Phi)^{1/\eta_2-1}$
1.53	0.44	5.0	10.0	27.6	62.4	13.2	14	26.96	4.69	1.40E+05	2.418	3.165	2.162
1.36	0.43	6.0	10.0	32.6	62.4	13.2	14	26.60	4.69	1.42E+05	2.487	3.165	2.187
1.23	0.43	7.0	10.0	37.5	62.5	13.3	14	26.27	4.69	1.45E+05	2.573	3.165	2.210
1.12	0.42	8.0	10.0	42.5	62.5	13.3	14	25.94	4.69	1.47E+05	2.642	3.165	2.234
1.03	0.42	9.0	10.0	47.5	62.5	13.4	14	25.62	4.69	1.50E+05	2.730	3.165	2.257
0.95	0.41	10.0	10.0	52.5	62.5	13.4	14	25.33	4.69	1.50E+05	2.763	3.165	2.279
1.82	0.45	1.0	5.0	7.7	36.8	12.6	14	27.45	6.10	1.40E+05	1.813	3.165	3.129
1.49	0.44	2.0	5.0	12.7	36.9	12.1	14	26.88	6.10	1.50E+05	1.990	3.165	2.168
1.21	0.43	3.0	5.0	17.6	36.8	12.7	14	26.22	6.11	1.60E+05	2.159	3.165	2.214
1.05	0.42	4.0	5.0	22.6	37.0	12.7	14	25.70	6.09	1.65E+05	2.274	3.165	2.251
0.92	0.41	5.0	5.0	27.5	36.9	12.7	14	25.20	6.10	1.70E+05	2.387	3.165	2.289

Table D25: Hydrogen: 2 m, $T_{IN} = -243^{\circ}\text{C}$, $h_t = 17$ m (con...)

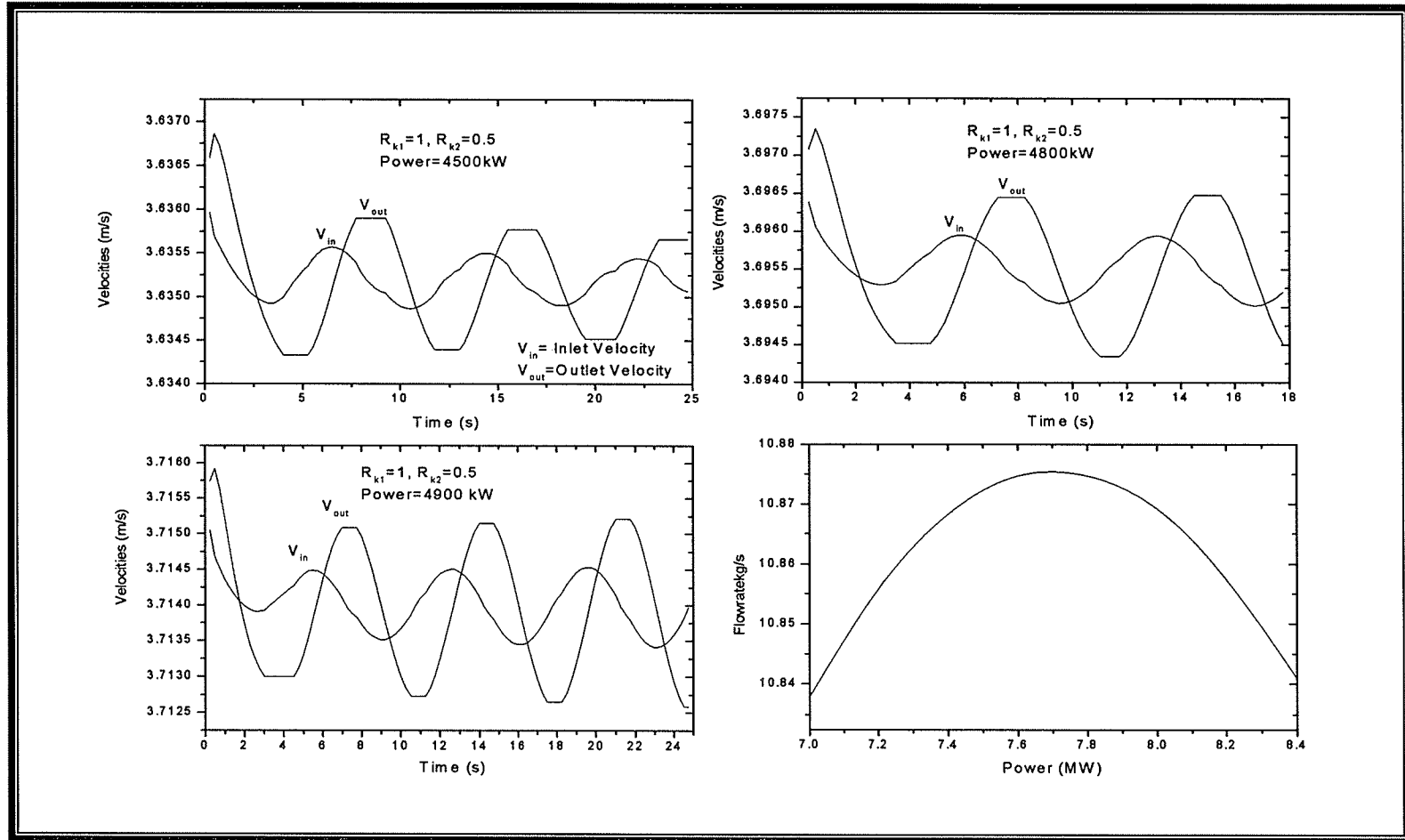
Conv Flowrate	G_s	G_s^*	Peak Flowrate	G_m	G_m^*	Q_b	Q_b^*	ρ_2	R_s^*	T	Time Step	Time Period
(kg/s)	(kg/m ² /s)		(kg/s)	(kg/m ² /s)		(W)		(kg/m ³)		(^o C)	(s)	(s)
0.73	167.00	0.442	0.73	166.56	0.441	1.70E+05	1.658	24.34	0.426	-239.72	0.25	6.5
0.72	163.21	0.435	0.72	162.74	0.434	1.70E+05	1.697	23.77	0.416	-239.33	0.25	7.0
0.70	159.30	0.425	0.69	157.83	0.421	1.70E+05	1.749	21.69	0.380	-239.14	0.25	5.3
0.68	155.15	0.414	0.68	155.63	0.415	1.70E+05	1.774	19.72	0.345	-239.85	0.25	5.8
0.67	152.17	0.406	0.67	153.08	0.409	1.70E+05	1.804	19.27	0.337	238.76	0.25	5.7
0.66	149.38	0.398	0.66	150.29	0.401	1.70E+05	1.837	18.85	0.330	-238.67	0.25	2.5
0.64	144.77	0.386	0.65	147.67	0.394	1.70E+05	1.870	17.08	0.299	-238.15	0.25	2.6
0.63	142.94	0.382	0.64	145.24	0.388	1.70E+05	1.901	16.72	0.293	-238.01	0.25	2.5
0.62	140.64	0.376	0.63	142.90	0.382	1.70E+05	1.932	18.70	0.327	-238.65	0.25	2.5
0.61	138.46	0.370	0.62	140.70	0.376	1.70E+05	1.963	18.70	0.327	-238.65	0.25	2.4

Table D26: Hydrogen: 2 m, $T_{IN} = -245^{\circ}\text{C}$, $h_t = 14$ m (con...)

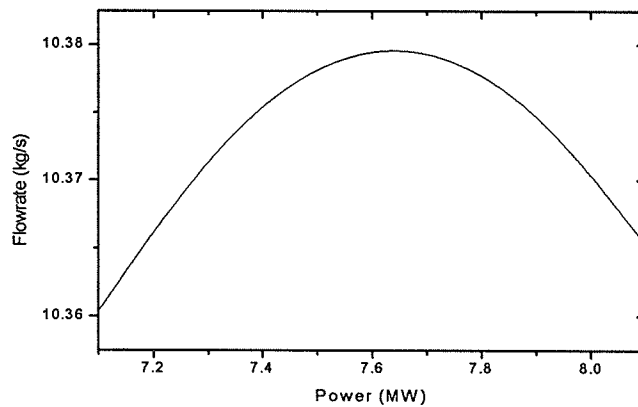
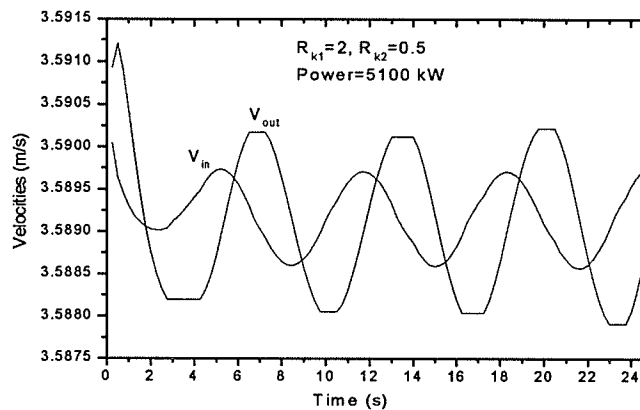
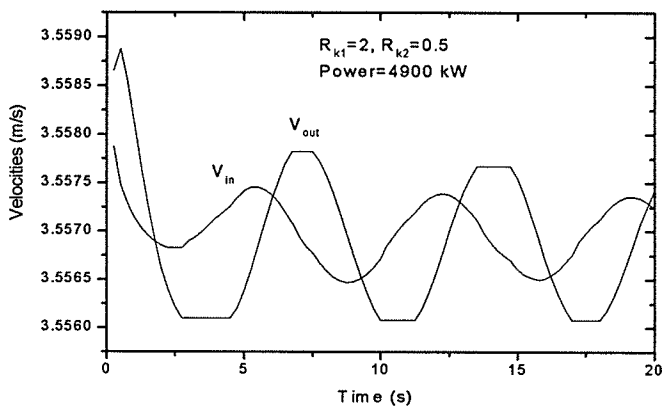
Conv Flowrate	G_s	G_s^*	Peak Flowrate	G_m	G_m^*	Q_b	Q_b^*	ρ_2	R_s^*	T	Time Step	Time Period
(kg/s)	(kg/m ² /s)		(kg/s)	(kg/m ² /s)		(W)		(kg/m ³)		(^o C)	(s)	(s)
0.55	124.89	0.432	0.56	126.36	0.437	1.30E+05	2.219	29.3	0.475	-239.97	0.25	7.2
0.54	123.18	0.426	0.55	124.65	0.431	1.30E+05	2.250	27.3	0.443	-239.51	0.25	7.1
0.53	121.56	0.421	0.54	123.04	0.426	1.30E+05	2.279	23.8	0.386	-239.35	0.25	6.8
0.53	120.01	0.416	0.53	121.49	0.421	1.30E+05	2.308	23.3	0.378	-239.31	0.25	6.6
0.52	118.52	0.410	0.53	120.02	0.416	1.30E+05	2.337	21.5	0.349	-239.14	0.25	6.2
0.52	117.10	0.406	0.52	118.61	0.411	1.30E+05	2.364	21.5	0.349	-239.14	0.25	4.3
0.73	166.55	0.443	0.74	167.72	0.446	1.70E+05	2.187	19.8	0.322	-238.89	0.25	3.9
0.72	162.64	0.432	0.72	163.74	0.435	1.70E+05	2.240	19.2	0.312	-238.73	0.25	3.8
0.70	159.84	0.425	0.70	160.08	0.425	1.70E+05	2.291	18.7	0.303	-238.65	0.25	3.8
0.69	156.51	0.417	0.69	156.74	0.417	1.70E+05	2.340	18.7	0.303	-238.65	0.25	3.8
0.68	153.62	0.409	0.68	153.63	0.409	1.70E+05	2.387	18.7	0.303	-238.65	0.25	3.8

APPENDIX-E

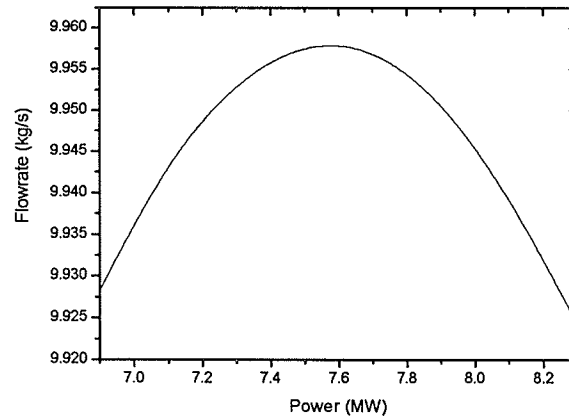
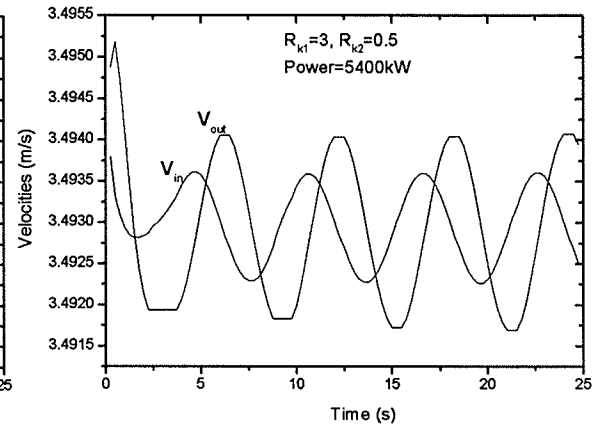
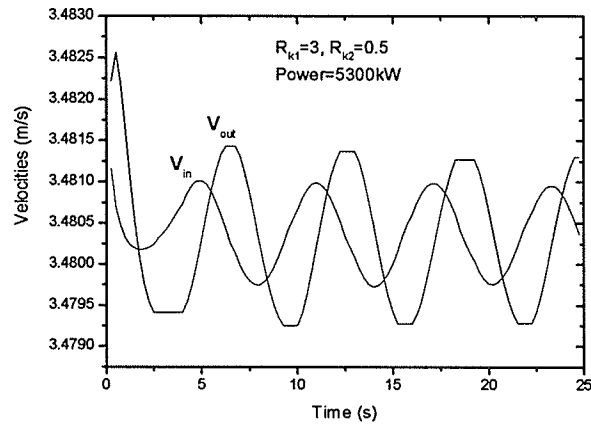
E-1: Water: $L_{TS}=1$ m, $T_{IN}=350$ C, $h_t=14$ m, $R_{k1}=1$, $R_{k2}=0.5$



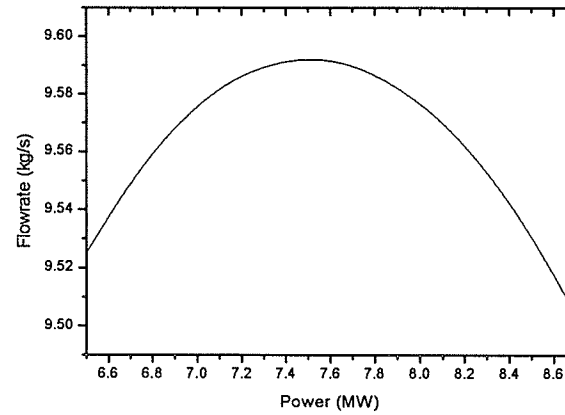
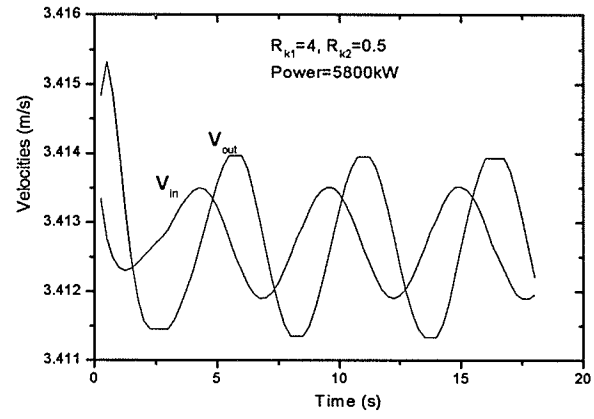
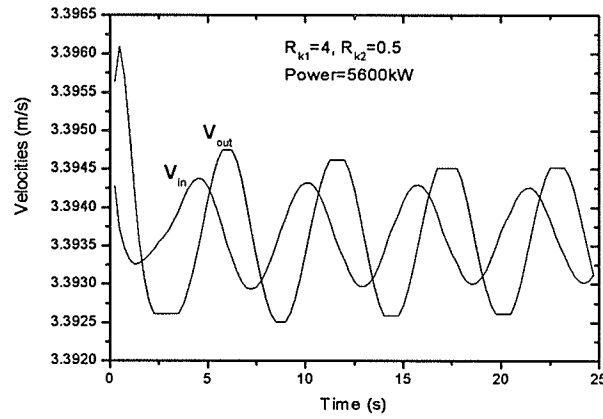
E-2: Water: $L_{TS}=1$ m, $T_{IN}=350$ C, $h_t=14$ m, $R_{k1}=2$, $R_{k2}=0.5$



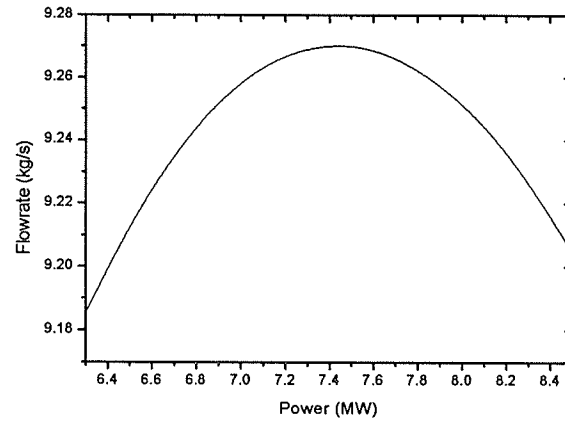
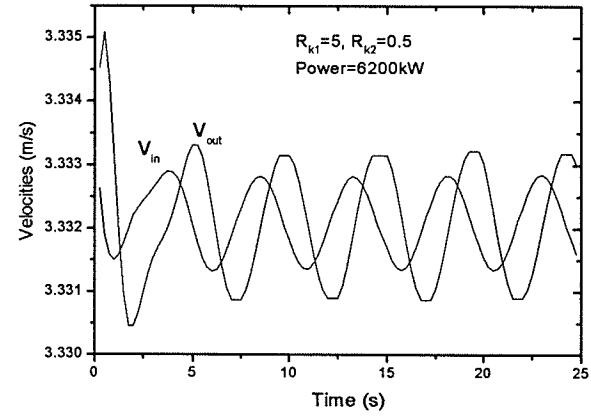
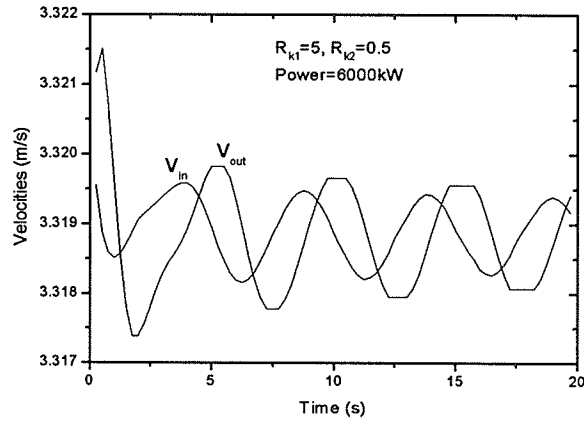
E-3: Water: $L_{TS}=1$ m, $T_{IN}=350$ C, $h_t=14$ m, $R_{k1}=3$, $R_{k2}=0.5$



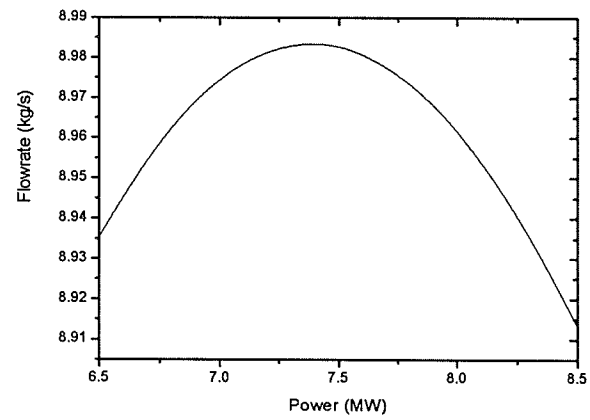
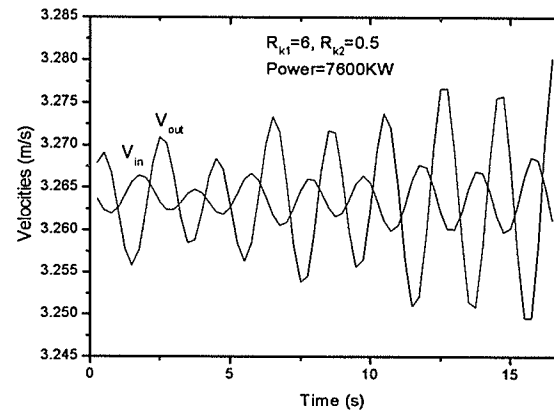
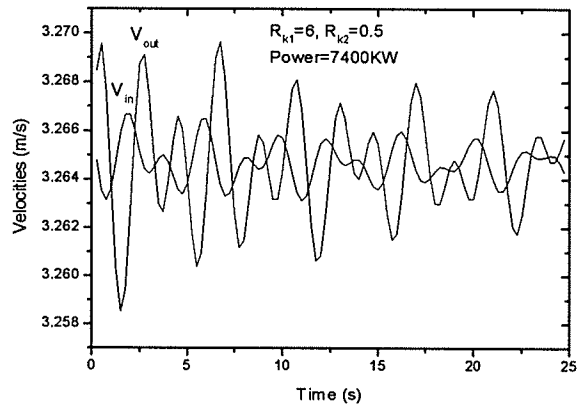
E-4: Water: $L_{TS}=1$ m, $T_{IN}=350$ C, $h_t=14$ m, $R_{k1}=4$, $R_{k2}=0.5$



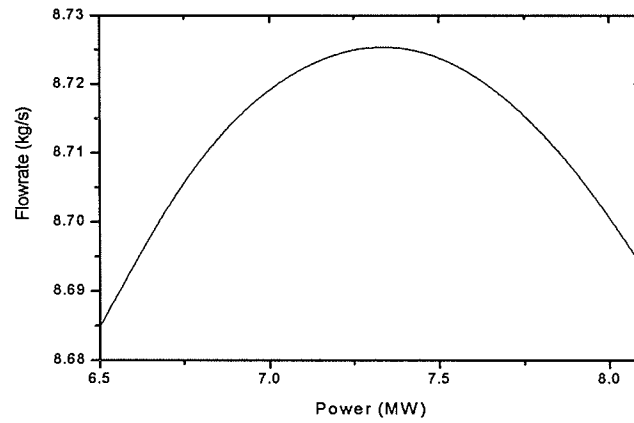
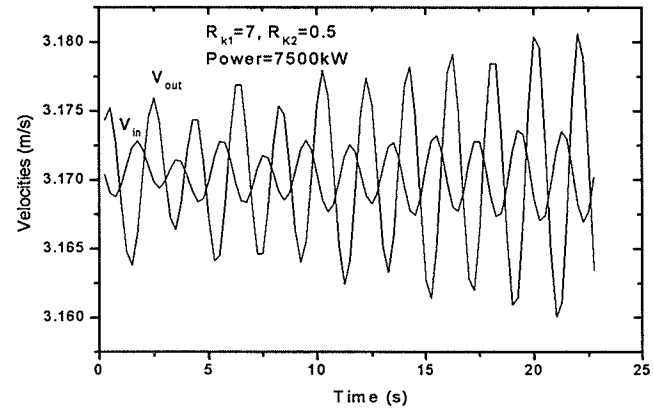
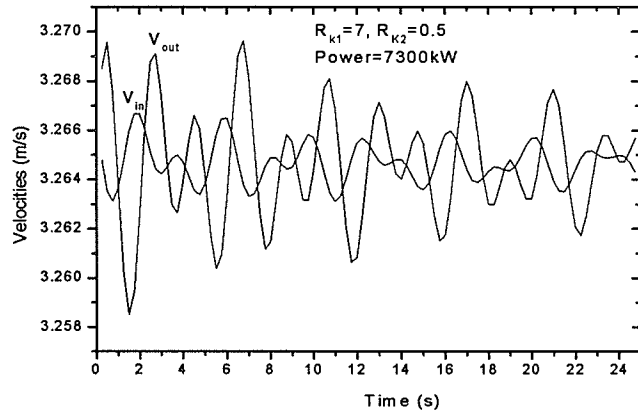
E-5: Water: $L_{TS}=1$ m, $T_{IN}=350$ C, $h_t=14$ m, $R_{k1}=5$, $R_{k2}=0.5$



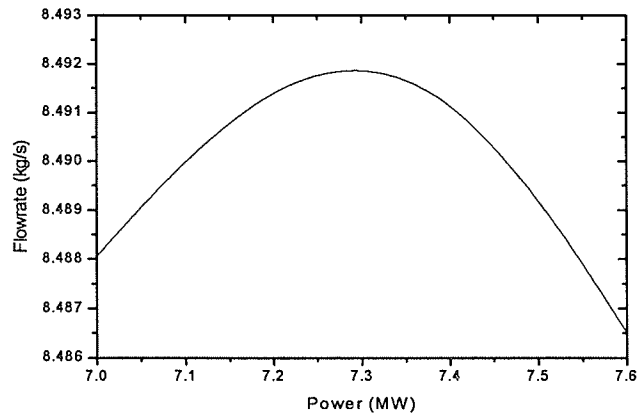
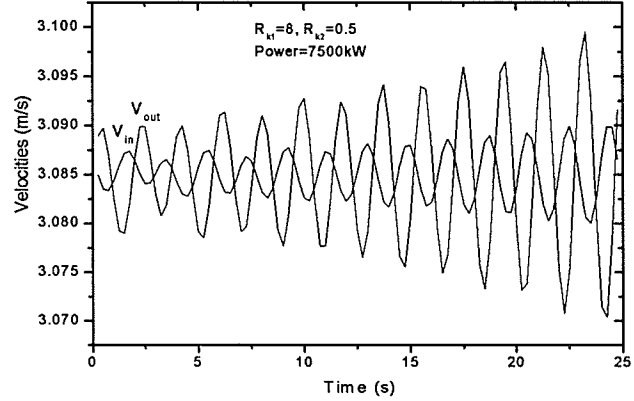
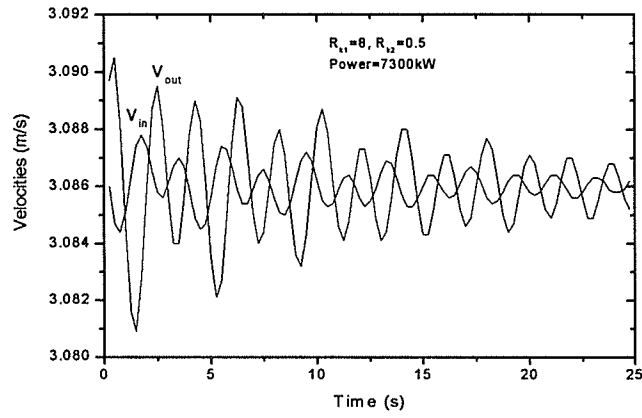
E-6: Water: $L_{TS}=1$ m, $T_{IN}=350$ C, $h_t=14$ m, $R_{k1}=6$, $R_{k2}=0.5$



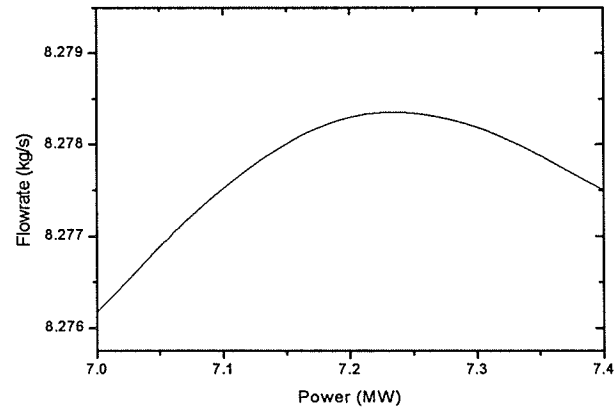
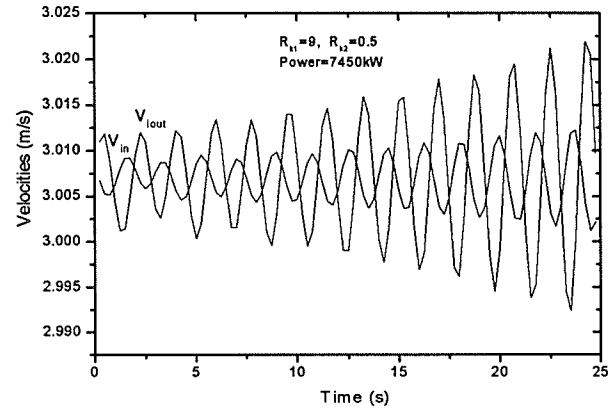
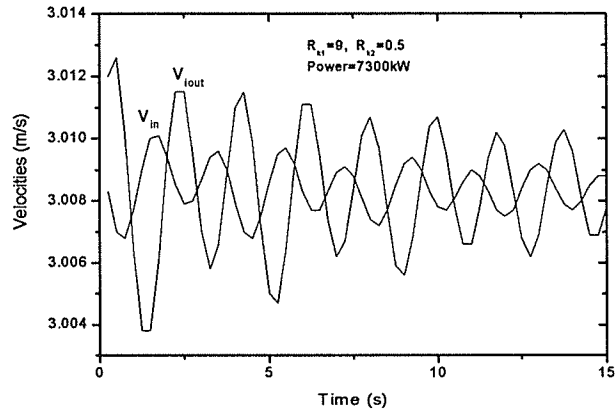
E-7: Water: $L_{TS}=1$ m, $T_{IN}=350$ C, $h_t=14$ m, $R_{k1}=7$, $R_{k2}=0.5$



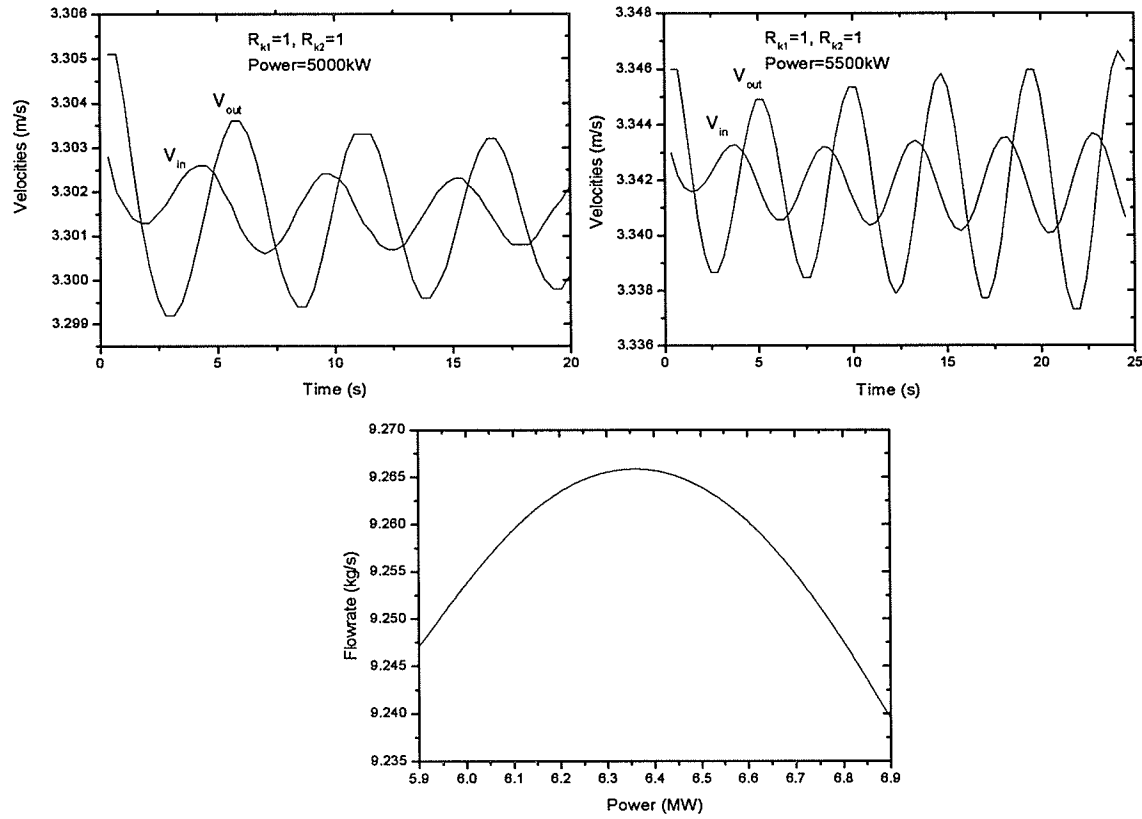
E-8: Water: $L_{TS}=1$ m, $T_{IN}=350$ C, $h_t=14$ m, $Rk_1=8$, $Rk_2=0.5$



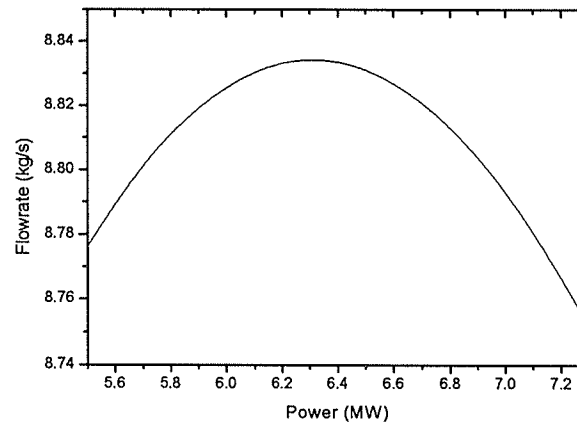
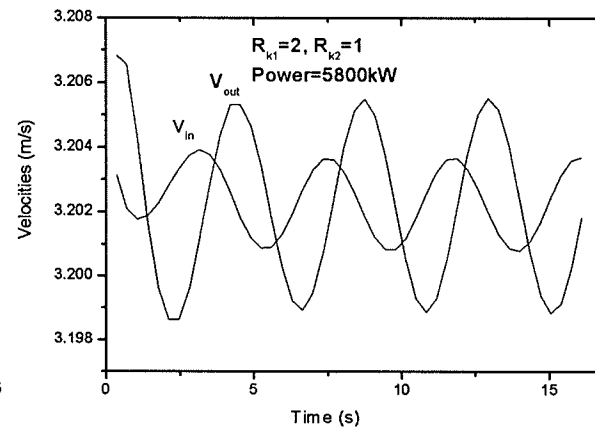
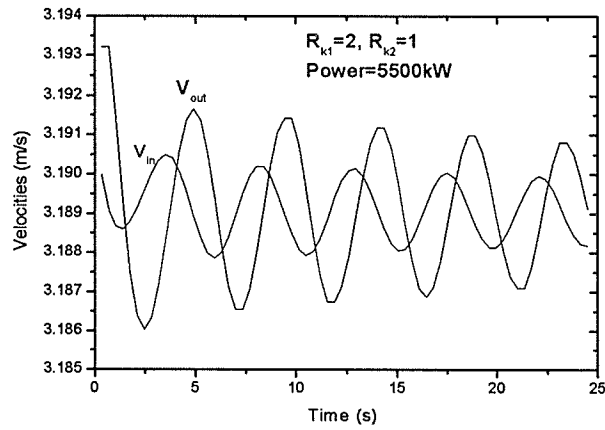
E-9: Water: $L_{TS}=1$ m, $T_{IN}=350$ C, $h_t=14$ m, $Rk_1=9$, $Rk_2=0.5$



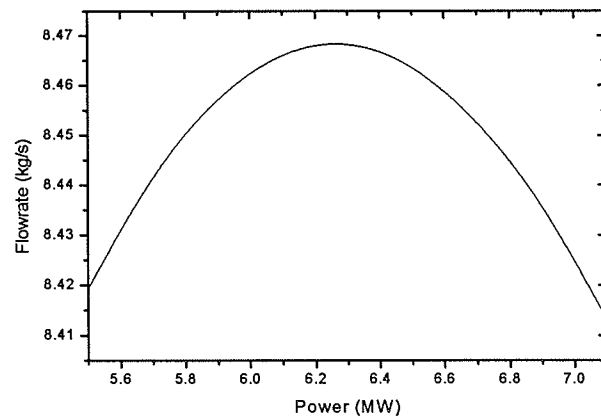
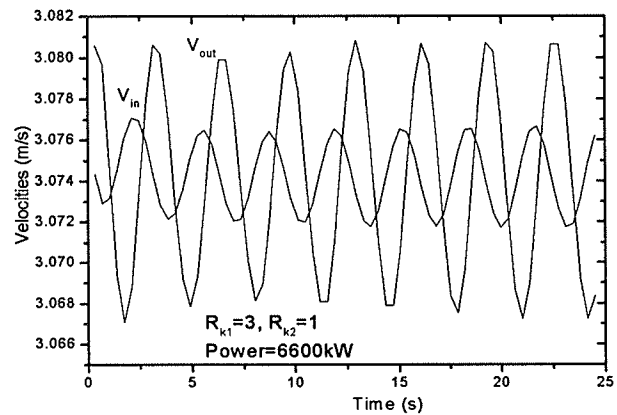
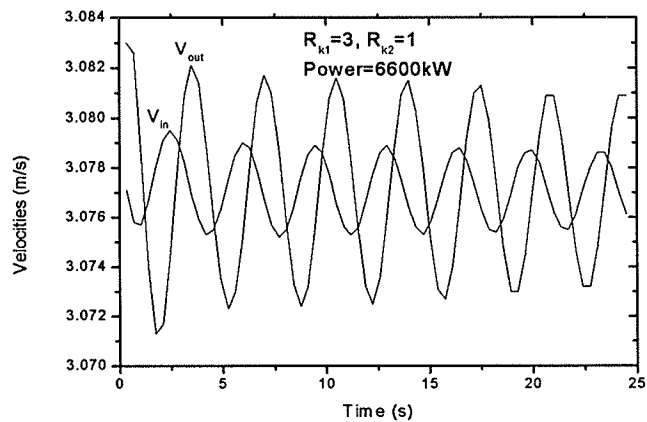
E-10: Water: $L_{TS}=1$ m, $T_{IN}=350$ C, $h_t=10$ m, $Rk_1=1$, $Rk_2=1$



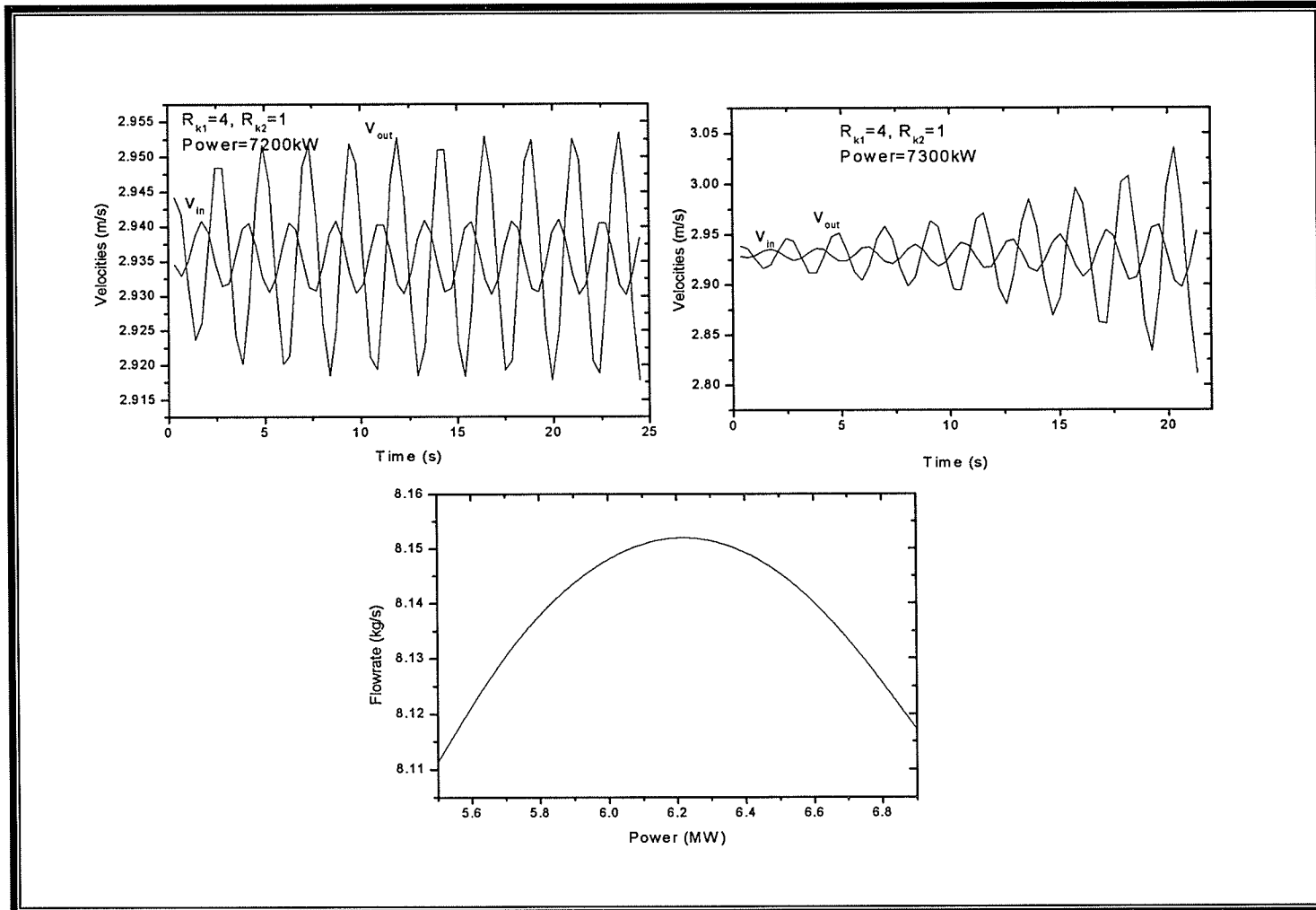
E-11: Water: $L_{TS}=1$ m, $T_{IN}=350$ C, $h_t=10$ m, $R_{k1}=2$, $R_{k2}=1$



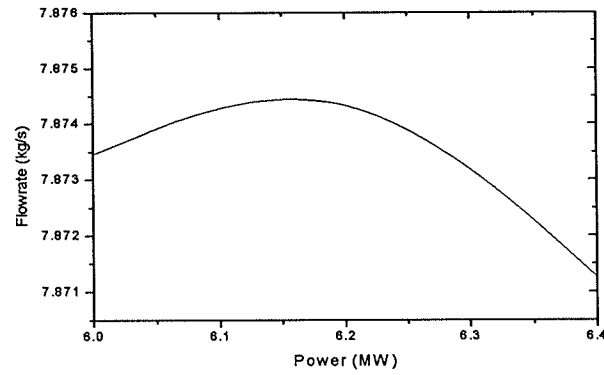
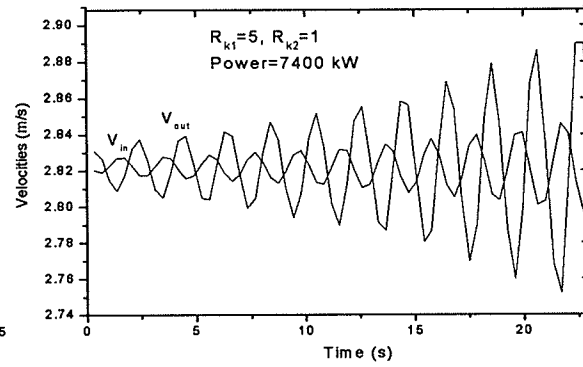
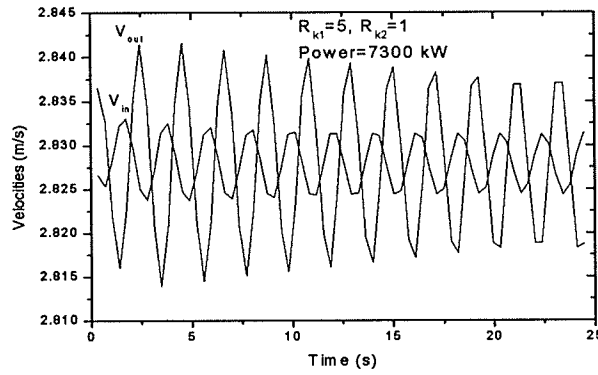
E-12: Water: $L_{TS}=1$ m, $T_{IN}=350$ C, $h_t=10$ m, $R_{k1}=3$, $R_{k2}=1$



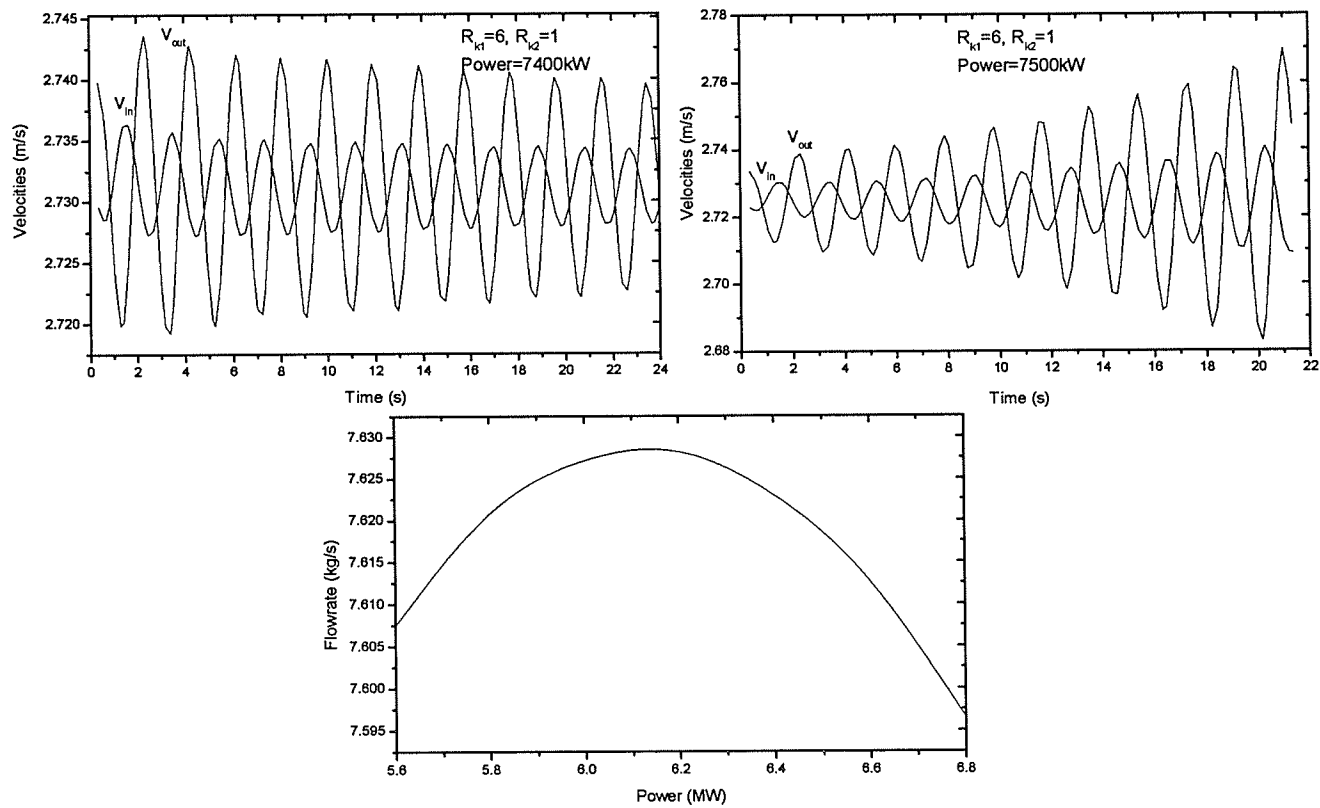
E-13: Water: $L_{TS}=1$ m, $T_{IN}=350$ C, $h_t=10$ m, $R_{k1}=4$, $R_{k2}=1$



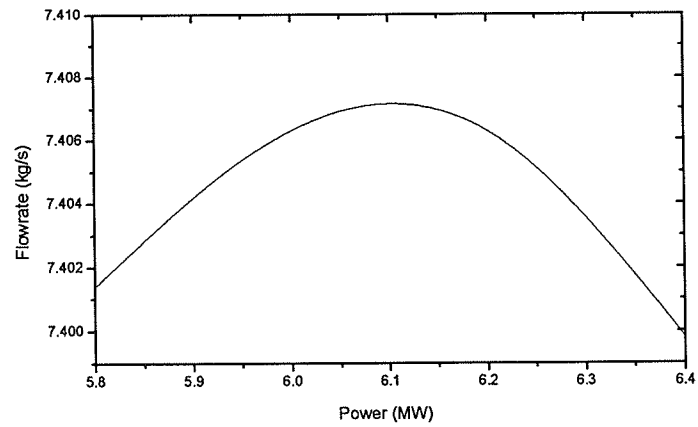
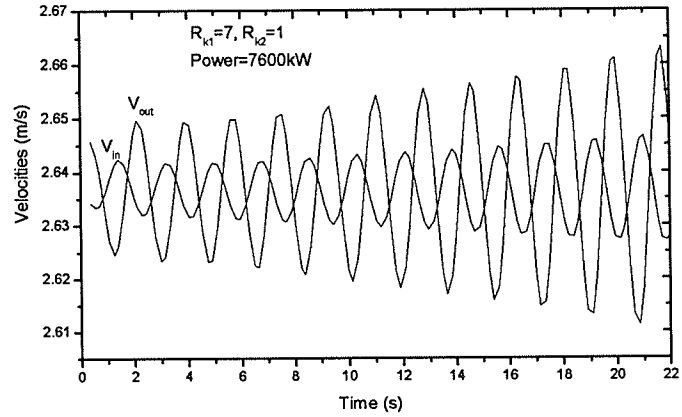
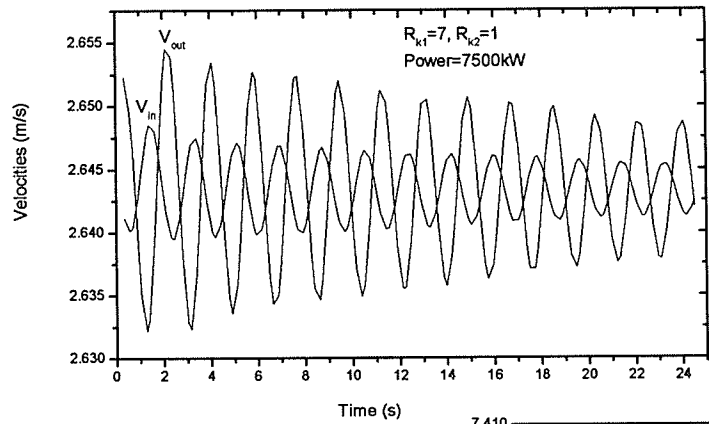
E-14: Water: $L_{TS}=1$ m, $T_{IN}=350$ C, $h_t=10$ m, $Rk_1=5$, $Rk_2=1$



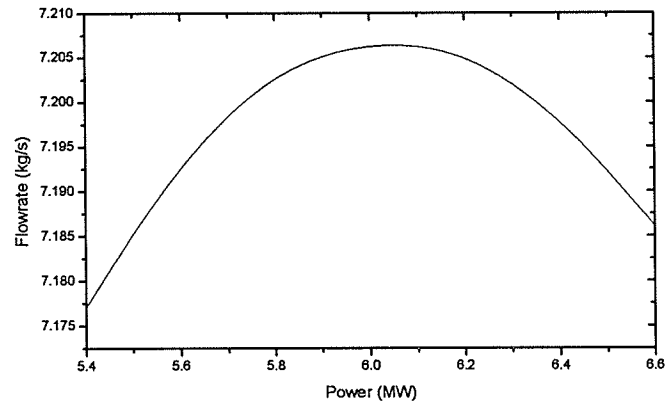
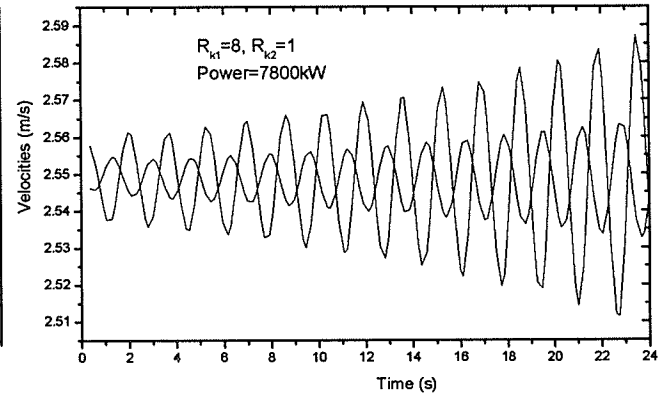
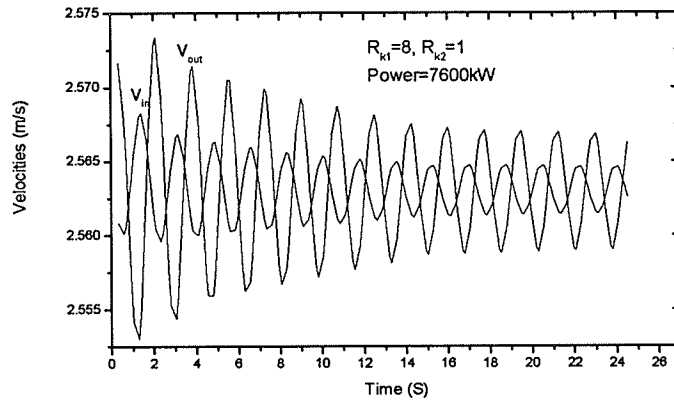
E-15 Water: $L_{TS}=1$ m, $T_{IN}=350$ C, $h_t=10$ m, $Rk_1=6$, $Rk_2=1$



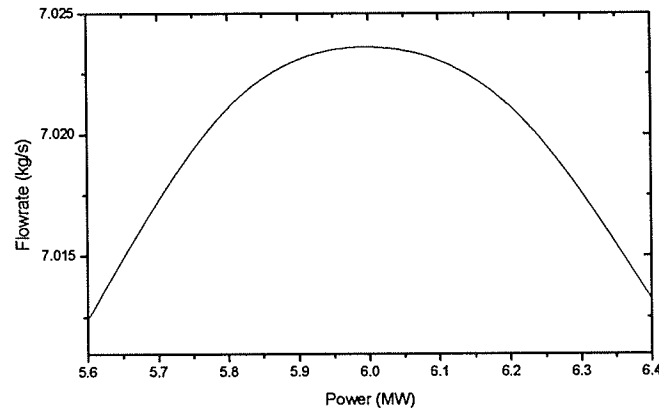
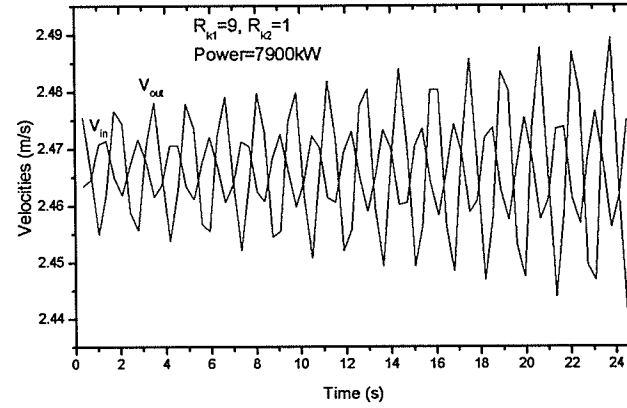
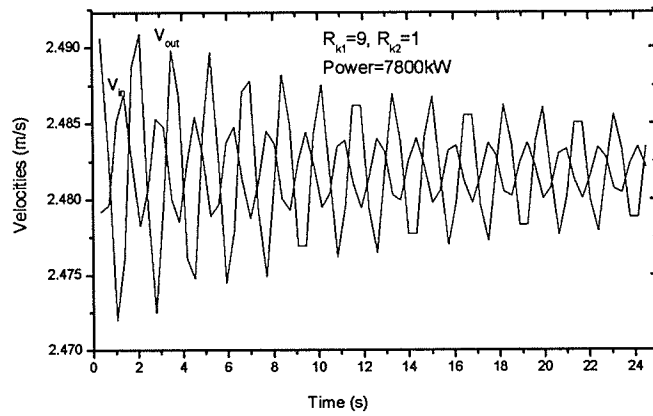
E-16 Water: $L_{TS}=1$ m, $T_{IN}=350$ C, $h_t=10$ m, $R_{k1}=7$, $R_{k2}=1$



E-17 Water: $L_{TS}=1$ m, $T_{IN}=350$ C, $h_t=10$ m, $R_{k1}=8$, $R_{k2}=1$



E-18 Water: $L_{TS}=1$ m, $T_{IN}=350$ C, $h_t=10$ m, $Rk_1=9$, $Rk_2=1$



E-19 Water: $L_{TS}=1$ m, $T_{IN}=350$ C, $h_t=10$ m, $Rk_1=10$, $Rk_2=1$

